USGS
science for a changing world

Prepared in cooperation with the city of Sioux Falls

Groundwater-Flow Model and Analysis of Groundwater and Surface-Water Interactions for the Big Sioux Aquifer, Sioux Falls, South Dakota

Scientific Investigations Report 2019–5117

U.S. Department of the Interior
U.S. Geological Survey

Cover. The Big Sioux River in Sioux Park, Sioux Falls, South Dakota, facing south, October 17, 2019. Outcrops of Sioux Quartzite are visible in the foreground. Photograph by Josh Valder, U.S. Geological Survey (USGS).

Back cover. Left: The Big Sioux River in Sioux Park, Sioux Falls, South Dakota, facing southwest, October 17, 2019. Photograph by Josh Valder, USGS. Upper right: The Big Sioux River Diversion north of Sioux Falls, South Dakota, facing south from north bank, March 20, 2019. Photograph by Josh Valder, USGS. Middle right: The Big Sioux River near Dell Rapids, South Dakota, May 4, 2017. Photograph by Josh Valder, USGS. Bottom right: The Big Sioux River in Sioux Park, Sioux Falls, South Dakota, June 2, 2019. Photograph by Kyle Davis, USGS.

Groundwater-Flow Model and Analysis of Groundwater and Surface-Water Interactions for the Big Sioux Aquifer, Sioux Falls, South Dakota

By Kyle W. Davis, William G. Eldridge, Joshua F. Valder, and Kristen J. Valseth

Prepared in cooperation with the city of Sioux Falls

Scientific Investigations Report 2019–5117

U.S. Department of the Interior
U.S. Geological Survey

U.S. Department of the Interior
DAVID BERNHARDT, Secretary

U.S. Geological Survey
James F. Reilly II, Director

U.S. Geological Survey, Reston, Virginia: 2019

Suggested citation:
Davis, K.W., Eldridge, W.G., Valder, J.F., and Valseth, K.J., 2019, Groundwater-flow model and analysis of groundwater and surface-water interactions for the Big Sioux aquifer, Sioux Falls, South Dakota: U.S. Geological Survey Scientific Investigations Report 2019–5117, 86 p., https://doi.org/10.3133/sir20195117.

Associated data for this publication:
Eldridge, W.G., and Davis, K.W., 2019, MODFLOW–6 model of the Big Sioux aquifer, Sioux Falls, South Dakota: U.S. Geological Survey data release, https://doi.org/10.5066/P9O59RO0.

ISSN 2328-0328 (online)

Acknowledgments

The authors thank the city of Sioux Falls for their continued support of past and ongoing studies that provided valuable data and resources for this report.

The authors also acknowledge Jason Bellino and Brian Clark (U.S. Geological Survey) for reviewing this report and Jeremy White for offering technical guidance for the numerical groundwater-flow model design and calibration. The authors also acknowledge U.S. Geological Survey personnel who assisted with the collection, processing, and analysis of geophysical data.

Contents

Figures

Tables

Conversion Factors

U.S. customary units to International System of Units

Multiply	By	To obtain
	Length	
inch (in.)	2.54	centimeter (cm)
inch (in.)	25.4	millimeter (mm)
foot (ft)	0.3048	meter (m)
	Area	
square mile (mi^2)	259.0	hectare (ha)
square mile (mi^2)	2.590	square kilometer (km^2)
	Volume	
gallon (gal)	3.785	liter (L)
gallon (gal)	0.003785	cubic meter (m^3)
gallon (gal)	3.785	cubic decimeter (dm^3)
million gallons (Mgal)	3,785	cubic meter (m^3)
cubic foot (ft^3)	28.32	cubic decimeter (dm^3)
cubic foot (ft^3)	0.02832	cubic meter (m^3)
acre-foot (acre-ft)	1,233	cubic meter (m^3)
acre-foot (acre-ft)	0.001233	cubic hectometer (hm^3)
	Flow rate	
cubic foot per second (ft^3/s)	0.02832	cubic meter per second (m^3/s)
cubic foot per day (ft^3/d)	0.02832	cubic meter per day (m^3/d)
gallon per minute (gal/min)	0.06309	liter per second (L/s)
million gallons per day (Mgal/d)	0.04381	cubic meter per second (m^3/s)
inch per year (in/yr)	25.4	millimeter per year (mm/yr)
	Hydraulic conductivity	
foot per day (ft/d)	0.3048	meter per day (m/d)
	Transmissivity and Conductance	
foot squared per day (ft^2/d)	0.09290	meter squared per day (m^2/d)

Temperature in degrees Fahrenheit (°F) may be converted to degrees Celsius (°C) as

$$°C = (°F - 32) / 1.8.$$

International System of Units to U.S. customary units

Multiply	By	To obtain
	Length	
centimeter (cm)	0.3937	inch (in.)
meter (m)	3.281	foot (ft)
	Resistivity	
ohm-meter (ohm-m)	39.37	ohm-inch (ohm-in)

Temperature in degrees Celsius (°C) may be converted to degrees Fahrenheit (°F) as

$$°F = (1.8 \times °C) + 32.$$

Datum

Vertical coordinate information is referenced to the North American Vertical Datum of 1988 (NAVD 88).

Horizontal coordinate information is referenced to the North American Datum of 1983 (NAD 83).

Altitude, as used in this report, refers to distance above the vertical datum.

Supplemental Information

Specific conductance is given in microsiemens per centimeter at 25 degrees Celsius (µS/cm at 25 °C).

Abbreviations

AEM	airborne electromagnetic
ASCII	American Standard Code for Information Interchange
cps	counts per second
DEM	digital elevation model
DIS	Discretization (Package)
DRN	Drain (Package)
ETg	evapotranspiration from groundwater
EVT	Evapotranspiration (Package)
GIS	geographic information systems
gSSURGO	Gridded Soil Survey Geographic
IC	Initial Conditions (Package)
MSI	Mount Sopris Instruments
NMR	nuclear magnetic resonance
NPF	Node Property Flow (Package)
PEST	Parameter ESTimation [software]
PET	potential evapotranspiration
R^2	coefficient of determination
RCH	Recharge (Package)
RIV	River (Package)
SDDENR–WR	South Dakota Department of Environment and Natural Resources-Water Rights
SDR	Schlumberger-Doll Research
SFR	Streamflow Routing (Package)

SOE	sum of square echoes
STO	Storage (Package)
SWB	Soil-Water-Balance (model)
USGS	U.S. Geological Survey
PVC	polyvinyl chloride
WEL	Well (Package)

Groundwater-Flow Model and Analysis of Groundwater and Surface-Water Interactions for the Big Sioux Aquifer, Sioux Falls, South Dakota

By Kyle W. Davis, William G. Eldridge, Joshua F. Valder, and Kristen J. Valseth

Abstract

The city of Sioux Falls, in southeastern South Dakota, is the largest city in South Dakota. The U.S. Geological Survey (USGS), in cooperation with the city of Sioux Falls, completed a groundwater-flow model to use for improving the understanding of groundwater-flow processes, estimating hydrogeologic properties, and analyzing groundwater and surface-water interactions for the Big Sioux aquifer in the model area.

The model area includes the Big Sioux aquifer and the underlying hydrogeologic units from Dell Rapids, South Dakota, to the confluence of the Big Sioux River and the outlet of the Sioux Falls Diversion Channel in eastern Sioux Falls, S. Dak. The Big Sioux aquifer is the primary aquifer in the model area and the focus of the groundwater-flow model. The Big Sioux River is the largest stream in the model area and is in hydraulic connection with the Big Sioux aquifer.

A conceptual model for the area was constructed and includes a characterization of the hydrogeologic framework, analysis and construction of potentiometric surfaces, and summary of estimated water budget components in the model area. The primary hydrogeologic units in the model area consist of (1) the Big Sioux aquifer, (2) a glacial till confining unit, and (3) bedrock aquifers (Split Rock Creek and Sioux Quartzite aquifers). Sources of groundwater recharge included infiltration of precipitation, stream seepage, and groundwater exchanges among the hydraulically connected Big Sioux aquifer, glacial till confining unit, and bedrock aquifers. Groundwater losses included evapotranspiration, groundwater discharge to streams, and groundwater withdrawal to supply water-use needs.

A numerical groundwater-flow model (numerical model) was constructed and was used to simulate all aspects of the conceptual model for predevelopment (steady-state) and time-varying (transient) monthly conditions for 1950–2017. The numerical model was constructed using the USGS modular hydrologic simulation program, MODFLOW–6, and was calibrated using the Parameter ESTimation software, PEST++.

The transient numerical model was calibrated for steady-state and transient monthly conditions for 1950–2017. Calibration targets were observations of hydraulic head, changes in hydraulic head, monthly mean streamflow (as a rate), and cumulative monthly stream discharge (as a volume). Parameters adjusted during model calibration were horizontal and vertical hydraulic conductivity, specific storage, specific yield, recharge and evapotranspiration multipliers, and streambed hydraulic conductivity. Horizontal and vertical hydraulic conductivity were estimated at pilot points distributed within the model area; specific storage and specific yield were assigned to uniform values in each layer in the model area; recharge and evapotranspiration multipliers were assigned uniformly for every stress period in the numerical model; and streambed hydraulic conductivity values were assigned uniformly between stream confluences.

The final calibrated parameter values of horizontal and vertical hydraulic conductivity, specific yield, specific storage, streambed hydraulic conductivity, recharge, and evapotranspiration were considered reasonable for the hydrogeologic materials and conditions in the model area for 1950–2017.

Overall, simulated hydraulic head altitudes had a linear regression coefficient of determination (R^2) of 0.48. Hydraulic head altitude residuals for the glacial till confining unit and bedrock aquifers were typically greater in magnitude when compared to residuals in the Big Sioux aquifer, but simulated hydraulic head altitudes in the Big Sioux aquifer compared favorably with mean observed hydraulic head altitudes and had a linear regression R^2 of 0.93.

Simulated streamflow hydrographs matched the general trends of observed increases and decreases in streamflow for USGS streamgages 06482000 (Big Sioux River at Sioux Falls, S. Dak.) and 06482020 (Big Sioux River at North Cliff Avenue at Sioux Falls, S. Dak.), but larger streamflows were overestimated at the first streamgage and underestimated at the second streamgage. The numerical model reasonably estimated cumulative monthly stream discharge for the first 10–15 years of available streamflow records at both USGS streamgages. After the first 10–15 years of available streamflow record,

cumulative monthly stream discharge was closely estimated for USGS streamgage 06482000 and underestimated at USGS streamgage 06482020.

Composite sensitivities without regularization were calculated by PEST++ for the calibrated numerical model parameters and were averaged by parameter group. The parameter group with the highest mean composite sensitivity was the recharge multiplier parameter group.

Model simplifications, assumptions, and limitations were necessary for construction of the conceptual and numerical models and for calibration efficiency. Spatial simplification of hydraulic properties could cause the numerical model to misrepresent reactions to changes in localized stresses, such as additional demands for groundwater withdrawal. The numerical model was temporally discretized into monthly periods and required scaling daily rates into representative monthly rates for model input and calibration targets. Based on the comparison between the observed and simulated groundwater levels, monthly mean streamflow and cumulative monthly stream discharge, and general groundwater distribution and flow, the numerical model favorably simulated the flow in the Big Sioux aquifer.

Eventual capture was calculated in the model area using a steady-state numerical groundwater-flow model. The eventual capture map shows areas of higher streamflow capture adjacent to the Big Sioux River north of the city of Sioux Falls and along the lower part of the Sioux Falls Diversion Channel, and areas of lower streamflow capture along aquifer boundaries and near the southern Sioux Quartzite barrier.

The timing of capture was determined using a transient numerical groundwater-flow model to determine the likely captured water sources for 30 years of groundwater withdrawal at three hypothetical wells using three continuous withdrawal rates (112.5, 450.0, and 900.0 gallons per minute). Supply for all three hypothetical wells became capture-dominated after only a short period of continuous withdrawal. Capture stabilized after about 10–15 years for well A, and after 20–25 years for well B, and after about 10–15 years for well C.

The groundwater-flow model is a suitable tool to use for improving the understanding of groundwater-flow processes, estimating hydrogeologic properties, and analyzing groundwater and surface-water interactions for the Big Sioux aquifer near Sioux Falls, S. Dak. The numerical model can be used to simulate hydrologic scenarios, advance understanding of groundwater budgets, compute system response to stress, and determine likely sources of water supplied to wells.

Introduction

The population of the city of Sioux Falls (fig. 1) increased by 14 percent from 2010 through 2016 (U.S. Census Bureau, 2018) and prompted the city to begin planning for additional municipal water resources. The city of Sioux Falls, in southeastern South Dakota near the Minnesota border (fig. 1), is the largest city in South Dakota with a population of more than 174,000 as of July 2017 (U.S. Census Bureau, 2018). The U.S. Geological Survey (USGS), in cooperation with the city of Sioux Falls, completed a groundwater-flow model to use for improving the understanding of groundwater-flow processes, estimating hydrogeologic properties, and analyzing groundwater and surface-water interactions for the Big Sioux aquifer in the model area (fig. 1). The model can be used to simulate hydrologic scenarios, advance understanding of groundwater budgets, compute system response to stress, and determine likely sources of water supplied to wells.

Purpose and Scope

The purpose of this report is to describe a groundwater-flow model of the Big Sioux aquifer in a model area (fig. 1) in southeastern South Dakota and to provide an analysis of groundwater and surface-water interactions. The groundwater-flow model described in this report includes conceptual and numerical models of groundwater flow of the Big Sioux aquifer and underlying hydrogeologic units in the model area from Dell Rapids, S. Dak., to the confluence of the Big Sioux River and the outlet of the Sioux Falls Diversion Channel in eastern Sioux Falls, S. Dak. (fig. 1). The conceptual model includes the development of a hydrogeologic framework, an overview of groundwater flow, and descriptions of water budget components in the model area. The numerical model is a three-dimensional, numerical groundwater-flow model, constructed using the USGS modular hydrologic simulation program, MODFLOW–6 (Langevin and others, 2017). The hydrogeologic framework and conceptual model provide the basis for the vertical, spatial, and temporal boundaries of the numerical model. The purpose of the numerical model and its intended uses include the following: (1) simulating hydrologic scenarios of interest to groundwater managers; (2) advancing understanding of groundwater budgets and their components such as recharge, discharge, and aquifer storage; (3) computing historical and projected system response to natural and anthropogenic stresses; and (4) determining likely sources of water supplied to wells in the model area.

Location and Description of Model Area

The model area is in the south-central part of the Big Sioux River Basin. The Big Sioux River Basin comprises an area of about 9,000 square miles (mi^2) in eastern South Dakota, southwestern Minnesota, and northwestern Iowa (fig. 1). The model area includes about 121 mi^2 of the Big Sioux River Basin with an extent about equivalent to the drainage basin between USGS streamgages 06481000 (Big Sioux River near Dell Rapids, S. Dak.) and 06482020 (Big Sioux River at North Cliff Avenue at Sioux Falls, S. Dak.) in southeastern South Dakota (fig. 1). The portion of the Big Sioux River Basin upstream from the confluence of Skunk

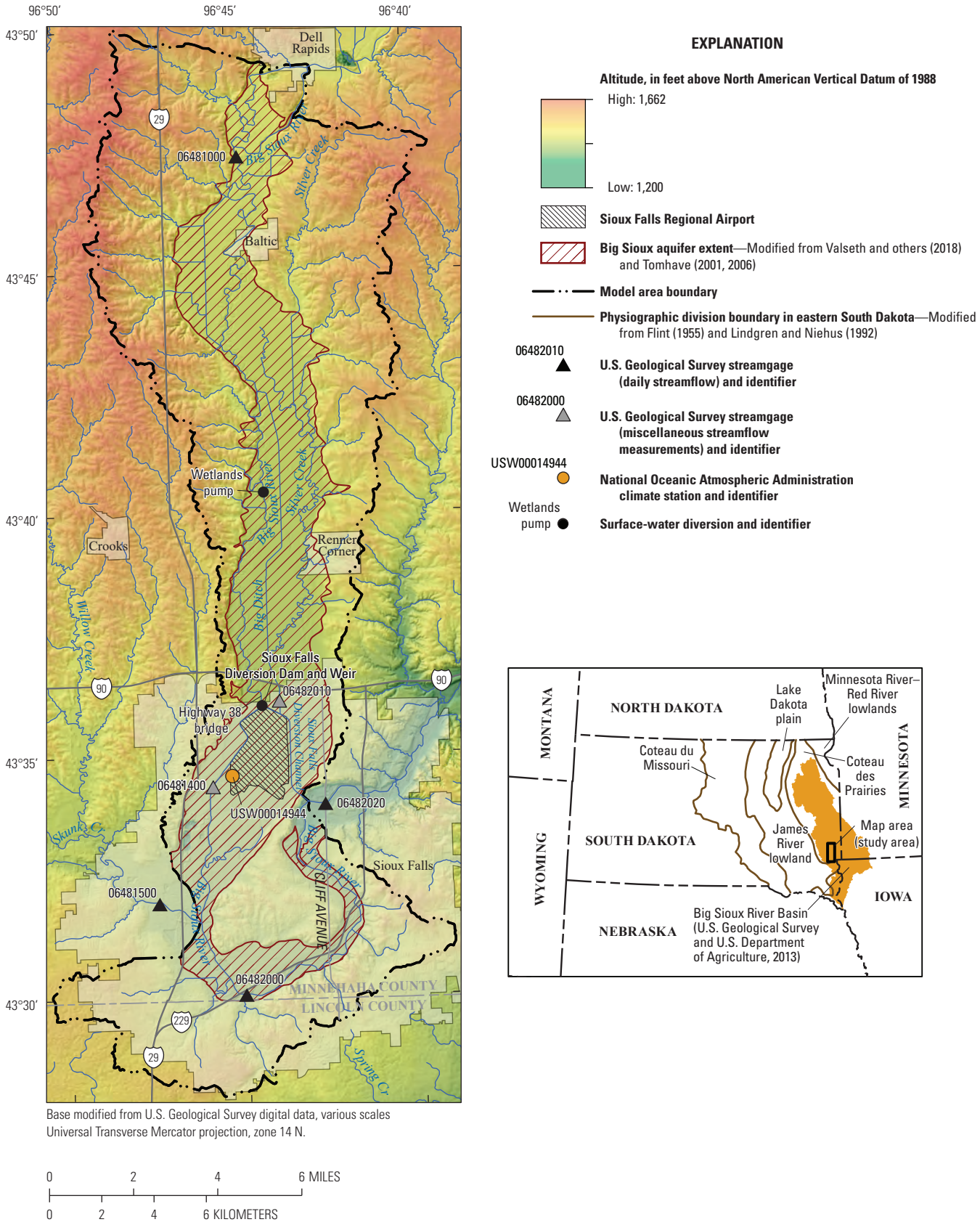

Base modified from U.S. Geological Survey digital data, various scales
Universal Transverse Mercator projection, zone 14 N.

Figure 1. Location of model area, U.S. Geological Survey streamgages, National Oceanic and Atmospheric Administration climate station, and the Sioux Falls Regional Airport.

Creek (fig. 1) and the Big Sioux River was not included in the model area.

The model area includes the Big Sioux aquifer and the underlying hydrogeologic units from Dell Rapids, S. Dak., to the confluence of the Big Sioux River and the outlet of the Sioux Falls Diversion Channel in eastern Sioux Falls, S. Dak. The Big Sioux aquifer, a major glacial-drift aquifer, extends most of the length of the basin along the Big Sioux River and its tributaries (fig. 1).

The groundwater-flow model extent was determined primarily based on the drainage basin of the Big Sioux River and USGS streamgages where continuous streamflow information was available. The northern and western extents of the model, where the model boundary crossed surface-water features, were determined based on the locations of USGS streamgages 06481000 (Big Sioux River near Dell Rapids, S. Dak.) and 06481500 (Skunk Creek at Sioux Falls, S. Dak.; fig. 1). The eastern extent of the model, where the model boundary crosses the Big Sioux River, was determined based on the location of USGS streamgage 06482020 (Big Sioux River at North Cliff Avenue at Sioux Falls, S. Dak.; fig. 1). The southern model extent was based on the southern boundary of the Big Sioux River Basin upstream from USGS streamgage 06482020.

The Big Sioux aquifer is the primary aquifer in the model area and the focus of the groundwater-flow model. In the model area, the Big Sioux aquifer extends from Dell Rapids in the north, to the center of the city of Sioux Falls in the south. The aquifer narrows substantially in the north at the western edge of Dell Rapids and again in the south at the confluence of Skunk Creek and the Big Sioux River just south of the Sioux Falls Regional Airport (fig. 1; Koch, 1982). In the model area, the Big Sioux aquifer generally is underlain by glacial till deposits, but in some areas, the aquifer is underlain by Sioux Quartzite. Before 2012, the Big Sioux aquifer was the primary water supply for the city of Sioux Falls. However, in July 2012, the city began receiving water from the Lewis and Clark Regional Water system, which provides water from wells near the Missouri River to 13 community water systems in southeastern South Dakota, Iowa, and Minnesota (Lewis and Clark Regional Water System, 2018).

Physiography, Climate, Streamflow, and Land Use

The model area is almost entirely in the Coteau des Prairies physiographic division (fig. 1; Flint, 1955; Lindgren and Niehus, 1992). The Coteau des Prairies is a highland plateau between the Minnesota River–Red River lowlands and the James River lowland (fig. 1) with scarp-like edges formed by glacial ice moraines. The wedge-shaped bedrock plateau likely separated two glacial lobes, and the Big Sioux River formed when glacial meltwater flowed southward between the two lobes and along the plateau (Koch, 1982). The Coteau des Prairies consists of bedrock formations overlain with unconsolidated Quaternary-age glacial drift. In the model area, the bedrock is Proterozoic-aged Sioux Quartzite and the glacial drift includes till and the silts, sands, and gravels of the Big Sioux aquifer.

The region that includes the model area is characterized by hilly topography, generated by at least two periods of glacial advance and retreat, and the topography varies from smooth rolling plains to very rough knobby hills (Rothrock and Otton, 1947). The altitude of land surface in the model area ranges from about 1,662 feet (ft) in the northern part of the model area to about 1,200 ft in the southern part (U.S. Geological Survey, 2017). The climate of the model area is classified as subhumid continental (Lebeda Consulting, 2016). The annual precipitation for 1950–2017 at National Oceanic and Atmospheric Administration climate station USW00014944 (fig. 1; Sioux Falls Foss Field, S. Dak.) ranged from 11.4 to 38.3 inches (in.) for 1976 and 2010, respectively (fig. 2; National Oceanic and Atmospheric Administration, 2018). Annual mean temperature for 1950–2017 ranged from 42.2 degrees Fahrenheit for 1950 and 1951 to 50.5 degrees Fahrenheit for 2012 (fig. 2; National Oceanic and Atmospheric Administration, 2018).

The Big Sioux River is the major perennial river in the model area between USGS streamgages 06481000 and 06482020 (fig. 1). Skunk and Silver Creeks (fig. 1) are secondary streams that flow into the Big Sioux River between Dell Rapids and the city of Sioux Falls, and both creeks are prominent surface-water features in the model area. Skunk Creek, a perennial stream, flows into the Big Sioux River south of the Sioux Falls Regional Airport near USGS streamgage 06481500 (fig. 1). Silver Creek, also a perennial stream, flows into the Big Sioux River near USGS streamgage 06482010, downstream from the inlet of the Sioux Falls Diversion Channel north of the Sioux Falls Regional Airport. Smaller unnamed tributaries also provide seasonal flows to the Big Sioux River, typically in the spring and early summer. Surface-water diversions existed at the following two locations in the model area: the Sioux Falls Diversion Dam and Weir, north of the Sioux Falls Regional Airport, and at a transfer pump (wetlands pump), north of the city of Sioux Falls (fig. 1).

Intermittent or continuous daily streamflow data were available for four of the USGS streamgages in the model area, which included the Big Sioux River near Dell Rapids, S. Dak. (06481000), Skunk Creek at Sioux Falls, S. Dak. (06481500), Big Sioux River at Sioux Falls, S. Dak. (06482000), and Big Sioux River at North Cliff Avenue at Sioux Falls, S. Dak. (06482020; fig. 1; U.S. Geological Survey, 2018). All streamflow statistics presented in this section are for the period of record for each streamgage (fig. 3). Streamflow throughout this report is defined as a rate of surface-water flow (for example, cubic feet per second [ft^3/s]), and stream discharge is defined as a volume of surface-water (for example, cubic feet [ft^3]). Mean monthly streamflow is defined as the mean streamflow for all of a specific month for a designated period (for example, all Aprils during 1950–2017), and monthly mean

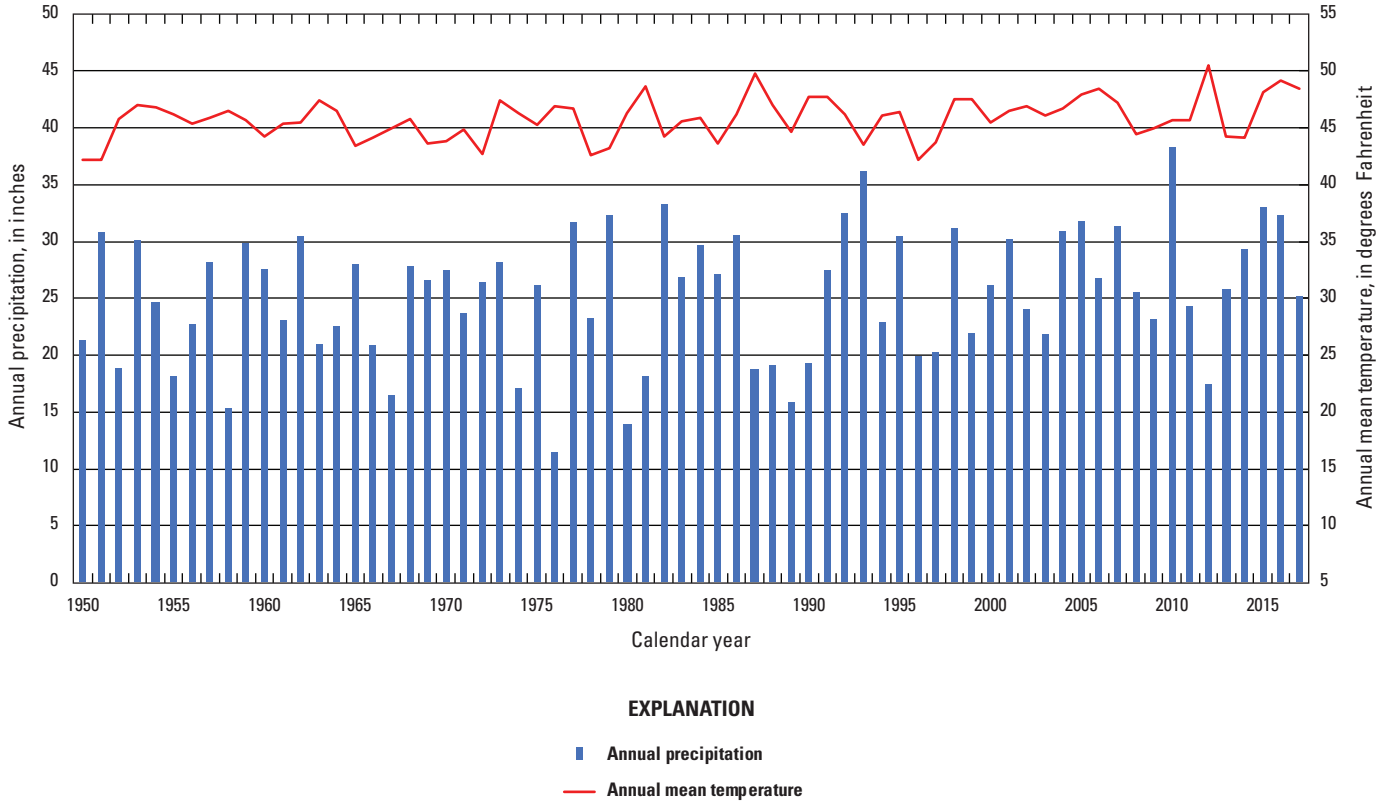

Figure 2. Annual precipitation and annual mean temperature for 1950–2017 at National Oceanic and Atmospheric Administration climate station USW00014944 (Sioux Falls Foss Field, South Dakota). (Data from National Oceanic and Atmospheric Administration, 2018.)

streamflow is defined as the mean streamflow during a single month (for example, April 1997).

Data from USGS streamgages 06481000 and 06481500 were used to determine surface-water inflows for the Big Sioux River in the model area. Mean monthly streamflow at USGS streamgage 06481000 ranged from 70 ft^3/s in January to 1,435 ft^3/s in April and at USGS streamgage 06481500 from 13 ft^3/s in January to 291 ft^3/s in April (U.S. Geological Survey, 2018; fig. 3). Data from USGS streamgage 06482020 were used to determine surface-water outflow for the Big Sioux River in the model area with mean monthly streamflow ranging from 131 ft^3/s in January to 1,933 ft^3/s in April (U.S. Geological Survey, 2018; fig. 3). Mean monthly streamflow in the Big Sioux River at USGS streamgage 06482000, in the southern part of the model area, ranged from 39 ft^3/s in January to 888 ft^3/s in April (U.S. Geological Survey, 2018; fig. 3).

Maximum monthly mean streamflow at USGS streamgage 06481000 from October 1948 through October 2017 was 8,439 ft^3/s in April 1997, and the cumulative monthly stream discharge was about 11.8 million ft^3 (88.3 million gallons; fig. 4). Maximum monthly mean streamflow for USGS streamgage 06481500 from October 1948 through October 2017 was 2,915 ft^3/s in July 1993, and the cumulative monthly stream discharge was about 2.5 million ft^3 (18.9 million gallons; U.S. Geological Survey, 2018; fig. 4).

General trends in streamflow correlated well with monthly trends in precipitation and temperature for the model area (fig. 3; table 1). The lowest mean monthly streamflow was recorded in January and the highest mean monthly streamflow was recorded in April (fig. 3). Low streamflow in January corresponded with low monthly precipitation and temperature, and high streamflow in April corresponded with periods of high precipitation and snowmelt with temperatures above freezing (table 1). Although the highest mean monthly precipitation was in June, the highest streamflow was generally observed in April, which could indicate that snowmelt contributes more substantially to maximum and high streamflow than spring and summer precipitation.

The 2011 National Land Cover Database was the primary source of land cover classification in the model area (Homer and others, 2015). The primary land uses in the model area were cultivated crops (37.0 percent); hay/pasture (20.1 percent); and developed, open space (17.1 percent) (fig. 5; table 2). Remaining land uses totaled about 25.8 percent in the model area (table 2). Within the Sioux Falls city limits and in Dell Rapids, Baltic, and Renner Corner, S. Dak. (fig. 1), primary land uses were developed, open space (32.8 percent);

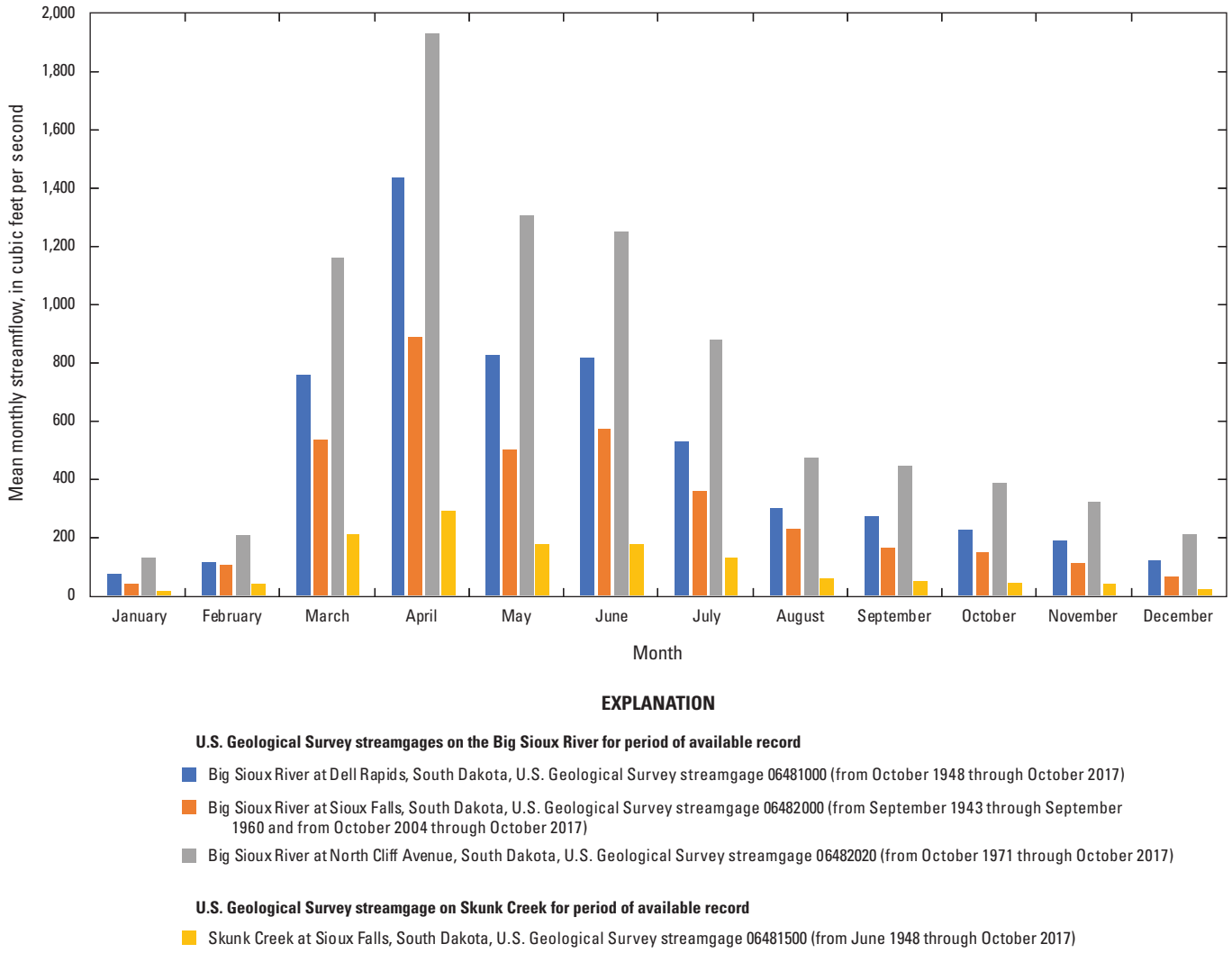

Figure 3. Mean monthly streamflow at U.S. Geological Survey streamgages in the model area. (Data from U.S. Geological Survey, 2018.)

developed, low intensity (24.4 percent); developed, medium intensity (18.7 percent); developed, high intensity (8.1 percent); and cultivated crops (6.5 percent) (table 2). Other land uses within the Sioux Falls, Baltic, Dell Rapids, and Renner Corner city limits totaled about 9.5 percent in the model area (fig. 5; table 2). About 87 percent of the deciduous forest land cover in the model area was within 600 ft of the Big Sioux River and its tributaries (fig. 5).

Hydrogeologic Setting

Surface water and aquifers in glacial drift and fractures in quartzite are the primary sources of water in the model area (Koch, 1982). The Big Sioux River is the largest stream in the model area and the only large stream system that drains the Coteau des Prairies (fig. 1). Most of the tributaries to the Big Sioux River flow from the east. Precipitation or surface-water inflows from the north are the primary supplies to surface water and groundwater in the glacial drift in the model area. The volume of water from precipitation is greater than the volume of surface-water runoff and water added to surface and groundwater storage, meaning that a large volume of precipitation is returned to the atmosphere by evapotranspiration (Koch, 1982).

Water in the Big Sioux River is in hydraulic connection with the Big Sioux aquifer, which is a water-table aquifer contained in alluvium-mantled valley train glacial outwash consisting of silt, fine to coarse sand, and gravel (Koch, 1982; fig. 6). The aquifer mostly overlies a low permeability clayey glacial till that represents a regional confining layer in the model area. In some areas north of Sioux Falls, the Big Sioux aquifer unconformably overlies the Cretaceous-aged, valley-fill sediments of the Split Rock Creek Formation (not shown; Pence, 1996). The regional confining layer outside the extent of the Big Sioux aquifer consists of various glacial tills and is exposed at the land surface (fig. 6). The Big Sioux aquifer is

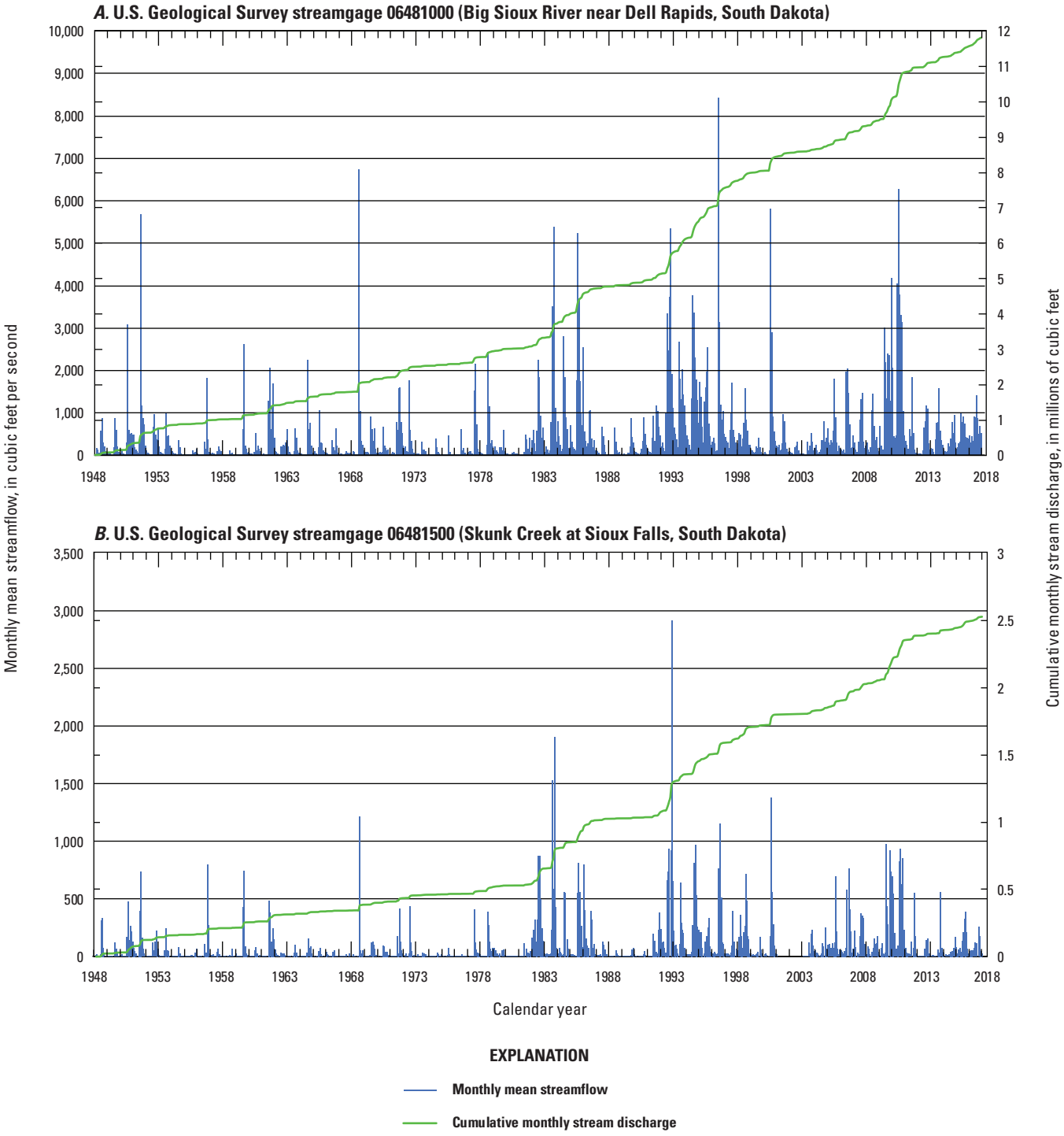

Figure 4. Monthly mean streamflow and cumulative monthly stream discharge for 1948–2017 at U.S. Geological Survey streamgages in the model area. (Data from U.S. Geological Survey, 2018.)

Table 1. Monthly precipitation and mean monthly temperature, January 1932 through December 2017, at National Oceanic and Atmospheric Administration weather station USW00014944 (Sioux Falls Foss Field, South Dakota). (Data from National Oceanic and Atmospheric Administration, 2018.)

[in., inch; °F, degrees Fahrenheit]

Month	Monthly precipitation (in.)	Mean monthly temperature (°F)
January	0.6	15.4
February	0.8	20.3
March	1.6	32.3
April	2.6	46.7
May	3.4	58.6
June	4.0	68.4
July	2.9	74.1
August	3.3	71.5
September	2.7	61.9
October	1.8	49.5
November	1.1	33.3
December	0.7	20.3

bounded on the north and on the south by outcrops or subcrops of the low permeability Sioux Quartzite (fig. 6; Koch, 1982; Lindgren and Niehus, 1992). The Sioux Quartzite in these areas creates a barrier to groundwater flow in the Big Sioux aquifer.

Overview of Groundwater Flow

Groundwater in the model area exists primarily in glacial drift aquifers, including the Big Sioux aquifer, and fractures in the quartzite (Koch, 1982). Groundwater flow in the Big Sioux aquifer in the model area normally is constrained between Sioux Quartzite barriers near Dell Rapids and the city of Sioux Falls because the Big Sioux aquifer thins vertically where Sioux Quartzite is close to the land surface in those areas (fig. 6). Groundwater levels in the Big Sioux aquifer respond to seasonal changes in recharge from precipitation and streamflow in the Big Sioux River. As a result, water levels typically rise during spring and early summer when recharge from percolation of snowmelt and spring runoff is greater than discharge from evapotranspiration, river seepage, and groundwater withdrawal. Water levels typically decline from midsummer to fall or midwinter when groundwater discharge is greater than recharge (Koch, 1982).

Previous Investigations

Previous numerical groundwater simulations for the model area include Jorgensen and Ackroyd (1973), Koch (1982), and HDR Engineering (1990). Jorgensen and Ackroyd (1973) constructed two-dimensional electric analog and numerical models to measure storage depletion in the Big Sioux aquifer near the city of Sioux Falls from groundwater withdrawals at rates of 9 to 10 million gallons per day (Mgal/d) for 1 year. Koch (1982) developed a single-layer digital numerical groundwater-flow model to test three withdrawal scenarios under various climate and streamflow conditions. HDR Engineering (1990) used a single-layer numerical model to investigate undeveloped parts of the Big Sioux aquifer and recommended location and types of production wells for expanding the municipal supply system for the city of Sioux Falls. Numerical model simulations of the Big Sioux aquifer adjacent to the north and south of the model area were completed by Hansen (1988) and Niehus and Thompson (1998), respectively. Putnam (1998) completed numerical model simulations of the Split Rock Creek aquifer and included parts of the Big Sioux aquifer in the uppermost layer of the model.

The hydrogeologic properties of the Big Sioux aquifer, and adjacent aquifers, were investigated in several studies dating back to the early 20th century. Rothrock and Newcomb (1926) mapped and characterized the sand and gravel deposits of Minnehaha County, S. Dak. (fig. 1). Rothrock and Otton (1947) described the geology and hydrology of the Sioux Falls area and estimated the amount of groundwater available for the city. Flint (1955) provided a general description of the glacial deposits in eastern South Dakota to prepare for proposed dam construction in the region and summarized other studies dating back to 1840 that described regional glacial depositions. Ellis and others (1969) mapped the geology and hydrology of the Big Sioux River Basin in eastern South Dakota and included water budgets for the basin, aquifer test results for several wells in the basin, and a potentiometric surface of outwash deposits in the Big Sioux River Basin. Stach and others (1981) used well drillers' logs and geologic maps from the 1950s to the early 1980s to define the extent and geochemical characteristics of the Big Sioux aquifer and to map the aquifer's potentiometric surface. Lindgren and Niehus (1992) investigated the water resources of Minnehaha County, S. Dak., that included information for the Big Sioux aquifer, such as aquifer characterization, water budget estimates, and a potentiometric map. Tomhave (1994) detailed the geology of Minnehaha County, S. Dak., and provided a cursory evaluation of the water resources in the county.

Recent map editions defining the Big Sioux aquifer boundaries in the model area were completed by Tomhave (2001, 2006). Older and smaller-scaled geologic maps depicting the extent of glacial outwash and Sioux Quartzite outcrops in the model area and surrounding region include maps by Steece (1959a, 1959b) and Tipton (1959a, 1959b). Ellis and others (1969) mapped the hydrology of a part of the Big Sioux River Basin that included the Sioux Falls area and charted basin geology, aquifer test results, potentiometric surfaces, and water quality. At a larger extent, but including the model area, Bayless and others (2017) estimated and mapped glacial deposit thickness, total thickness of coarse-grained

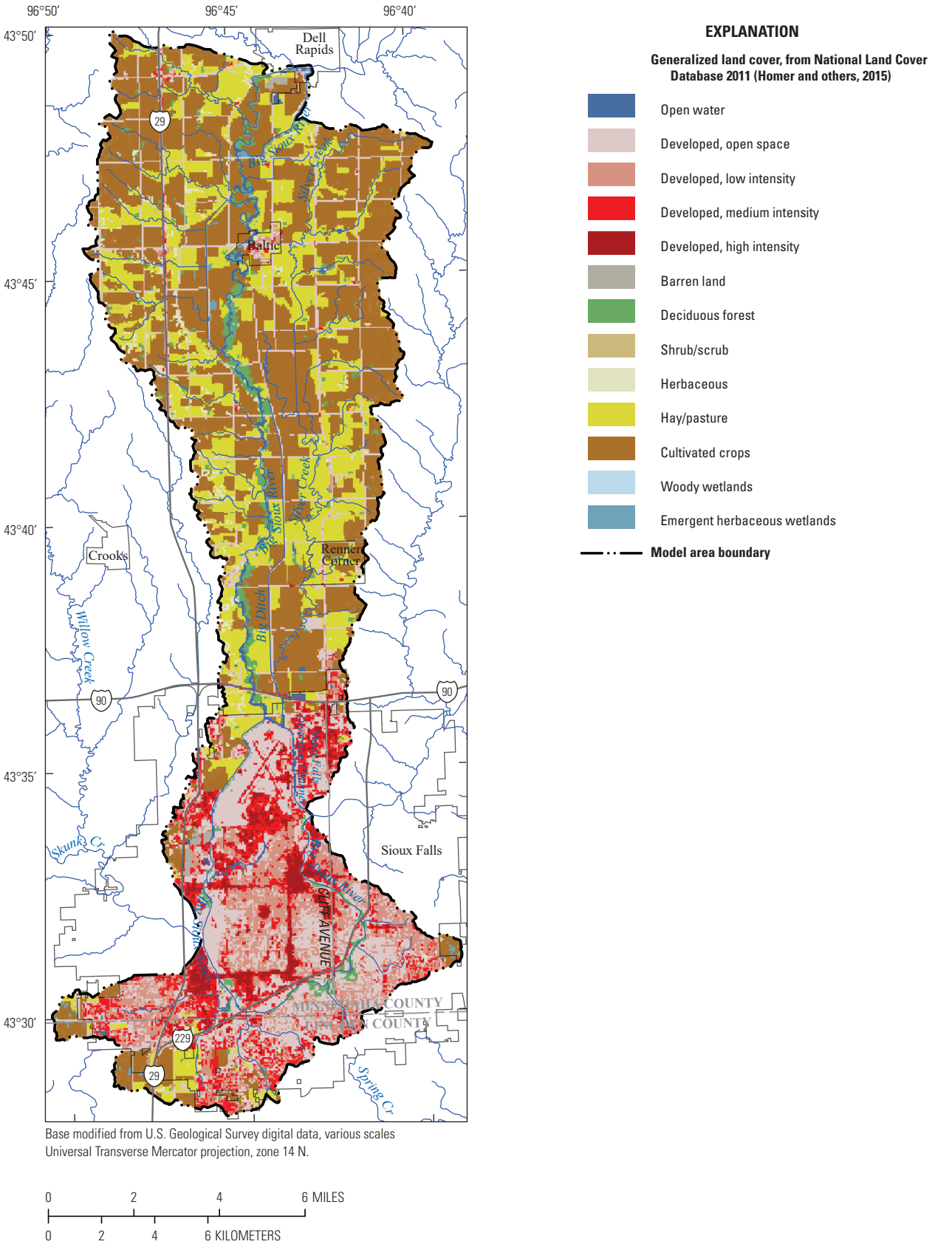

Figure 5. Generalized land cover in the model area.

Table 2. Summary of land cover in model area and in city and town boundaries.

[mi², square mile; <, less than; --, not applicable]

Land cover classification	Total land area in the model area		Total land area within city limits[a]	
	(mi²)	(percent)	(mi²)	(percent)
Cultivated crops	44.7	37.0	2.8	6.5
Hay/pasture	24.2	20.1	2.1	4.8
Developed, open space	20.6	17.1	14.2	32.8
Developed, low intensity	11.1	9.2	10.6	24.4
Developed, medium intensity	8.5	7.0	8.1	18.7
Herbaceous	2.2	1.8	0.4	0.9
Deciduous forest	3.2	2.7	0.7	1.7
Developed, high intensity	3.5	2.9	3.5	8.1
Open water	1.2	1.0	0.5	1.1
Emergent herbaceous wetlands	0.9	0.8	0.2	0.4
Barren land	0.3	0.3	0.2	0.5
Shrub/scrub	<0.1	<0.1	--	--
Woody wetlands	<0.1	<0.1	<0.1	<0.1
Evergreen forest	<0.1	<0.1	--	--
Total[b]	**120.6**	**100.0**	**43.4**	**100.0**

[a]City limits include parts of Sioux Falls, Baltic, Dell Rapids, and Renner Corner, South Dakota.

[b]Values may not sum to total because of rounding.

deposits, specific capacity-based transmissivity and hydraulic conductivity, and texture-based horizontal and vertical hydraulic conductivity and transmissivity for the glaciated United States. Valseth and others (2018) used results from an airborne electromagnetic (AEM) survey to define and map the extent and thickness of parts of the Big Sioux aquifer north of Sioux Falls.

Methods Overview

Several geophysical, data collection, and numerical methods were used to develop the conceptual and numerical models of groundwater flow for the model area. Ground-based and AEM geophysical surveys were completed to determine aquifer geometries and to improve knowledge of variations in aquifer hydrogeologic properties (Valseth and others, 2018). Borehole geophysical methods including nuclear magnetic resonance (NMR), gamma detection, and conductance were used to estimate hydrogeologic properties of the Big Sioux aquifer and are described in appendix 1. Additionally, falling-head slug tests were completed at 15 observation wells to measure hydraulic conductivity in the Big Sioux aquifer (Eldridge and Medler, 2019). Potentiometric surfaces were developed from hydraulic head measurements collected during 2017 (U.S. Geological Survey, 2018). A Soil-Water-Balance (SWB) model (Westenbroek and others, 2010) was the only numerical method using the conceptual model and was used to generate spatially and temporarily varying estimates of recharge and evapotranspiration in the model area, described in appendix 2.

MODFLOW–6 (Langevin and others, 2017) was used to simulate all aspects of the conceptual model and groundwater flow for the hydrogeologic units in the model area. MODFLOW–6 incorporates the Newton-Raphson formulations and accompanying upstream weighting schemes implemented by previous MODFLOW versions, including MODFLOW–NWT (Niswonger and others, 2011) and provides a robust representation of dry or nearly dry cells by smoothly reducing the conductance between a dry cell and an adjoining wetted cell to zero. The Newton-Raphson approach keeps a dry cell active and allows inflow to the cell from adjacent cells and from external sources while not allowing water to flow out of the cell (Niswonger and others, 2011).

The numerical model was calibrated using the Parameter ESTimation (PEST) software PEST++ (version 4.1.12; Welter and others, 2015) by optimizing selected hydraulic properties (parameters) to provide the best comparison of numerical model results and observed hydrologic data. The PEST++ software (Welter and others, 2015) was developed based on the theory and processes of the original PEST software (Doherty, 2018), with specific emphasis on handling highly

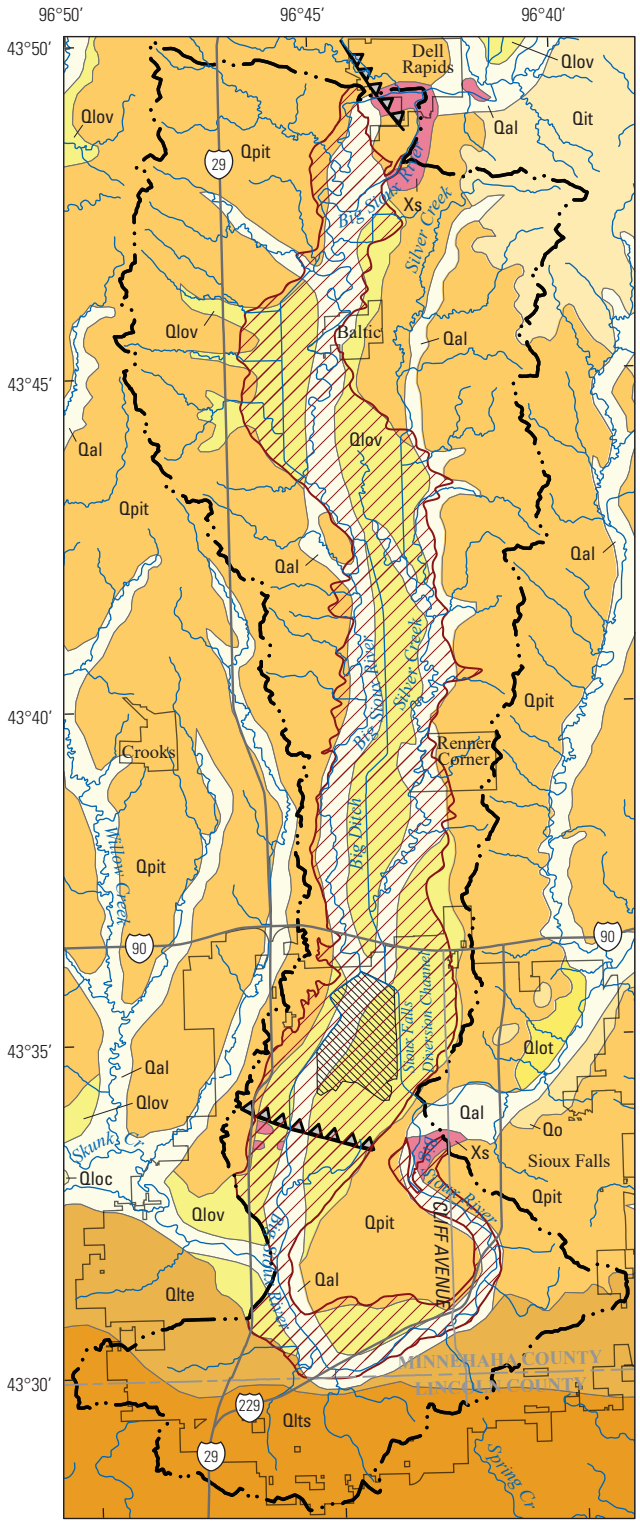

Base modified from U.S. Geological Survey digital data, various scales
Universal Transverse Mercator projection, zone 14 N.

0 2 4 6 MILES
0 2 4 6 KILOMETERS

EXPLANATION

Generalized surface geology—Modified from Stoeser and others (2005)

Quaternary-age sedimentary deposits

- Qal — Alluvium
- Qlot — Outwash, terrace
- Qlov — Outwash, valley train
- Qloc — Outwash, collapsed
- Qit — Till, ground moraine
- Qlts — Till, stagnation moraine
- Qlte — Till, end moraine
- Qpit — Clayey till, ground moraine
- Qo — Outwash, undifferentiated

Proterozoic-age sedimentary deposits

- Xs — Sioux Quartzite

Sioux Falls Regional Airport

Big Sioux aquifer extent—Modified from Valseth and others (2018) and Tomhave (2001, 2006)

Model area boundary

Sioux Quartzite barrier—Modified from Ellis and others (1969) and Koch (1982)

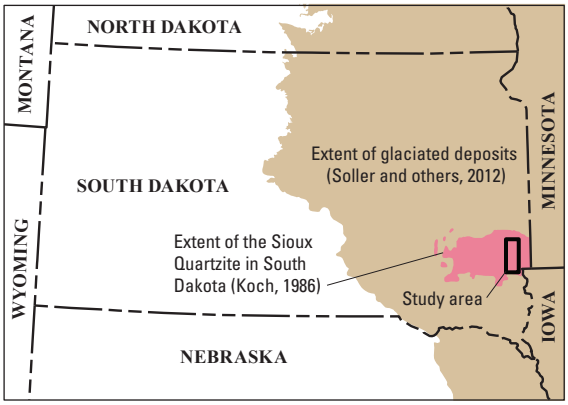

Figure 6. Generalized surface geology in the model area.

parameterized inverse problems (Doherty and Hunt, 2010). The PEST++ software is a model-independent calibration tool that applies statistical nonlinear parameter estimation techniques to optimize model input parameters. The PEST++ software systematically adjusts model input parameters based on the comparison between observed (measured or estimated) values and model-computed (simulated) variables, such as hydraulic head or streamflow, until the best simulated fit to the observed data is mathematically determined. The PEST++ software also was used to complete an assessment of numerical model parameter sensitivities.

Eventual capture and timing-of-capture analyses were completed using the calibrated MODFLOW–6 numerical model to provide insight into the timing and magnitude of the likely sources of water supplied to wells in the model area. Automated Python (Rossum and Drake, 2011) scripts were used to compare MODFLOW–6 calculated groundwater budget terms from a numerical model without hypothetical withdrawal to groundwater budget terms from a numerical model with hypothetical groundwater withdrawals. The groundwater budget comparisons were used to determine the timing, magnitude, and extent of capture from all available sources that could be incurred from hypothetical wells completed in the Big Sioux aquifer in the model area. The automated scripts and numerical model input and output files are available in the accompanying USGS data release (Eldridge and Davis, 2019).

Groundwater-Flow Model

This section provides information and descriptions of the groundwater-flow model for the Big Sioux aquifer in southeastern South Dakota and includes conceptual and numerical models of groundwater flow in the model area. A conceptual model for the area was constructed and includes a characterization of the hydrogeologic framework, analysis and construction of potentiometric surfaces, and summary of estimated water budget components in the model area. Information from the conceptual model was used to create a numerical model of groundwater flow for the Big Sioux aquifer and underlying hydrogeologic units in the model area. The numerical model was used to simulate groundwater flow and all aspects of the groundwater budget in the model area for predevelopment (steady-state) and time-varying (transient) monthly conditions for 1950–2017. The numerical model was calibrated using automated parameter estimation techniques that adjust selected hydraulic properties (parameters) with the goal of minimizing the differences between hydraulic observations of interest (including hydraulic head measurements, monthly mean streamflow, and cumulative monthly stream discharge) and model-simulated values.

Conceptual Model

A simple conceptual model was developed for the model area, shown in figure 7, and illustrates the hydrogeologic framework and sources and sinks of groundwater in the model area. In the model area, three aquifers and one confining unit were conceptualized as three hydrogeologic units (figs. 7 and 8). Sources of groundwater recharge included infiltration of precipitation, stream seepage, and groundwater exchanges among the hydraulically connected Big Sioux aquifer, glacial till confining unit, and bedrock aquifers. Groundwater losses included evapotranspiration, groundwater discharge to streams, and groundwater withdrawal to supply water-use needs. The groundwater-flow model included the 121 mi^2 area between USGS streamgages 06481000 and 06482020, and the model boundaries were coincident with the drainage area of the Big Sioux River in the area (fig. 1). Groundwater-flow exchanges exist among the aquifers, the streams and aquifers, and the aquifers and wells. Additionally, the system receives groundwater recharge from precipitation and loses groundwater to evapotranspiration.

Hydrogeologic Framework

The exposed geologic formations in the model area are the Quaternary-aged alluvium, glacial outwash, glacial till, and Proterozoic-aged Sioux Quartzite (fig. 6), and the primary hydrogeologic units in the model area are the Big Sioux aquifer, glacial till confining unit, and bedrock aquifers (fig. 8). This section of this report provides descriptions of the hydrogeologic units within the model area including the horizontal and vertical aquifer extents as well as estimates of hydraulic properties for each of the hydrogeologic units.

Hydrogeologic Units

The primary hydrogeologic units in the model area evaluated in this study consist of (1) the Big Sioux aquifer, an alluvium-mantled glacial outwash aquifer; (2) a confining unit, which primarily consists of glacial till; and (3) the bedrock aquifers, which consist of the Split Rock Creek aquifer and the Sioux Quartzite aquifer (Lindgren and Niehus, 1992; Hansen, 1988). The three hydrogeologic units in the model area were conceptualized and represented as three layers in the groundwater-flow model (model layering and application of the conceptual model is described in the "Numerical Model" section of this report). The three hydrogeologic units were selected for this study based on previous investigations, lithologic logs from well drillers' reports, and geophysical surveys completed in the model area. Previous reports by Hansen (1988), Koch (1986), Rothrock and Otton (1947), and Flint (1955) documented the geologic history and formation of the Big Sioux aquifer in the model area. Lindgren and Niehus (1992) provided complete descriptions of all available water resources in Minnehaha County, S. Dak., including the hydrogeologic units described in this report. In addition, Valseth and

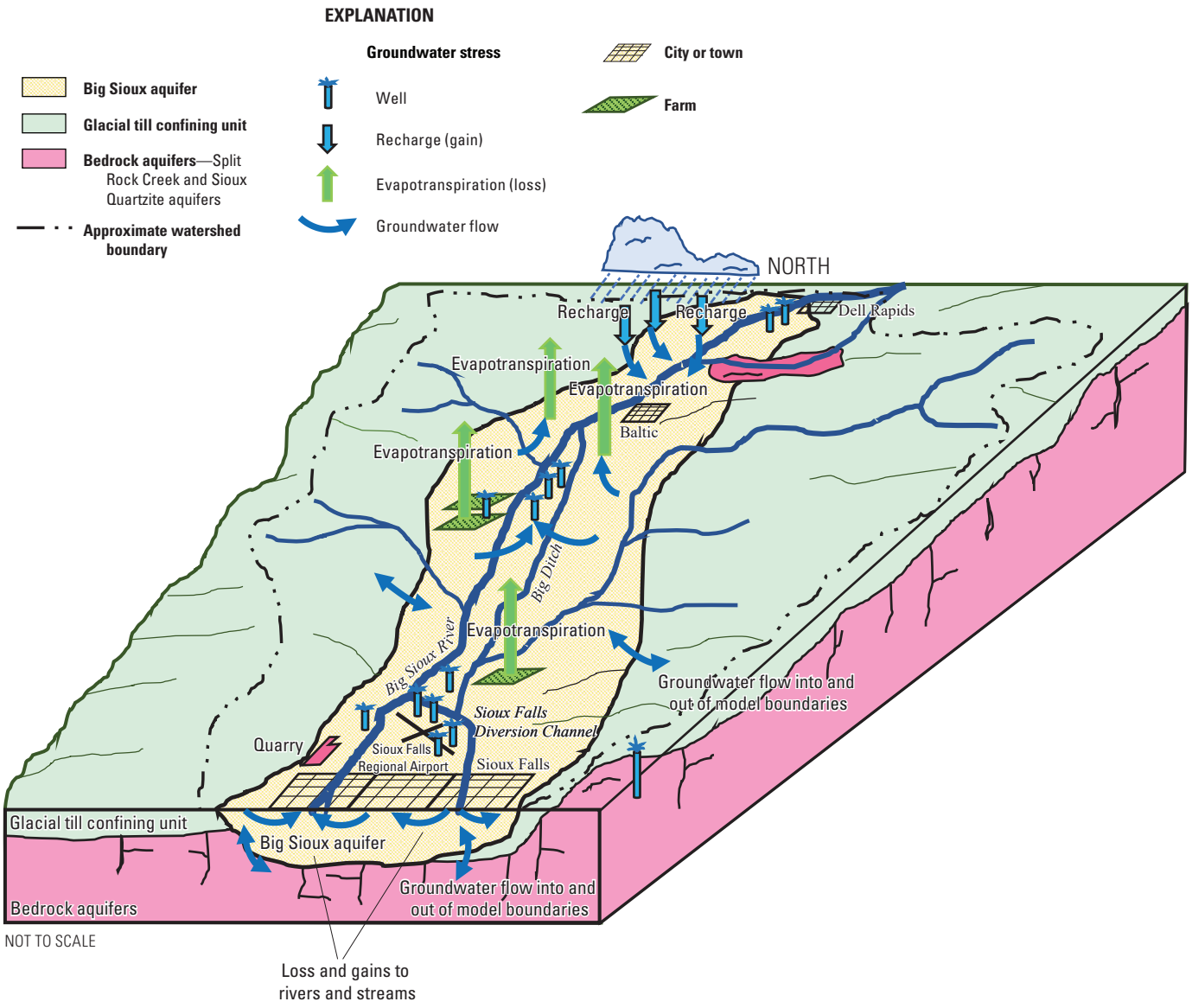

Figure 7. Conceptual model of the Big Sioux aquifer and underlying hydrogeologic units as viewed from south to north.

others (2018) described the horizontal and vertical delineation of three hydrogeologic units using ground-based electromagnetic (resistivity) and AEM survey geophysical techniques.

Big Sioux Aquifer

The Big Sioux aquifer, the primary aquifer in the model area, is the uppermost hydrogeologic unit (fig. 7) where the aquifer underlies the Big Sioux River floodplain (not shown). The section of the Big Sioux aquifer of interest for this study has a spatial extent of about 42 mi^2 between Dell Rapids and Sioux Falls in southeastern South Dakota (fig. 1) and is bounded (horizontally and vertically) by a glacial till confining unit and bedrock in the model area (figs. 6 and 7). The Big Sioux aquifer is a water-table aquifer contained in alluvium-mantled valley train glacial outwash (Koch, 1982) and consists of fine to coarse, poorly sorted sand and fine to coarse pebble gravel with thin (3- to 5-ft thick) interbedded clay and till layers in some areas (Lindgren and Niehus, 1992; fig. 8). Alluvial sediments of black to brownish-black organic-rich silts, clay, and fine sands were deposited in the model area by the primary river, the Big Sioux River, and from the smaller tributaries that contribute to the Big Sioux River streamflow (Tomhave, 1994).

The horizontal extent of the aquifer was determined based on previously published aquifer boundaries from Valseth and others (2018) and Tomhave (2001, 2006), and the depth of the Big Sioux aquifer was determined by incorporating information from geophysical surveys (Valseth and others,

[Modified from Tomhave, 1994; Putnam, 1998; Koch, 1982; Lindgren Niehus, 1992; --, not applicable]

Era	System	Series	North American stage	Lithologic unit	Hydrogeologic unit	Thickness, in feet	Description and origin
Cenozoic	Quaternary	Holocene	--	Alluvium	Big Sioux aquifer	0–30	Black to brownish-black organic-rich silt, clay, and fine sand. Fluvial
		Late Pleistocene	Wisconsinan	Glacial outwash		4–48	Fine to coarse, poorly sorted sand and fine to coarse pebble gravel with thin (3- to 5-feet thick) interbedded clay and till layers in some areas. Fluvio-glacial melt
		Early and Middle Pleistocene	Pre-Illinoian	Glacial till	Glacial till confining unit	0–120	Brownish-gray to gray with yellowish-brown to reddish-brown in upper oxidized zones of nonsorted, nonstratified sediments with a compact, silty, clay-rich matrix with sand to boulder-sized clasts. Glacial deposits
Mesozoic	Late Cretaceous	--	--	Split Rock Creek Formation	Bedrock aquifers	0–245	Sedimentary deposits of fine to coarse well-sorted quartzose sand interbedded with siltstone, shale, and claystone in a local topographic depression
Proterozoic	--	--	--	Sioux Quartzite		About 1,500	Thick gently dipping sequence of pink or reddish to tan-colored, siliceous, iron-stained orthoquartzite with minor interbedded mudstone and conglomerate layers

Figure 8. Generalized stratigraphic section of the model area.

2018) and well drillers' lithologic logs (South Dakota Department of Environment and Natural Resources, 2018b). Mean thickness of the Big Sioux aquifer is 34 ft and ranges from 0 to 96 ft in the model area (Valseth and others, 2018; South Dakota Department of Environment and Natural Resources, 2018b). The aquifer is thickest in the center of the Big Sioux River floodplain and thins out at the edges where the underlying glacial till confining unit is exposed at the land surface (fig. 6). In the southern part of the model area, the aquifer widens and becomes thinner with pockets of deeper deposits. Hydraulic conductivity estimates for the Big Sioux aquifer typically range from 50 to 1,500 feet per day (ft/d; table 3). The estimated maximum well yield of the Big Sioux aquifer is about 1,000 gallons per minute (gal/min) where the aquifer is greater than 25 ft thick (Lindgren and Niehus, 1992).

An NMR survey was completed in the model area to further characterize the hydraulic properties of the Big Sioux aquifer. An NMR survey is a borehole geophysical method used to estimate subsurface hydrogeologic properties. The NMR data were collected during June 13–15, 2017, at nine observation wells completed in the Big Sioux aquifer (appendix 1). Hydraulic conductivity determined from the NMR survey ranged from about 43 to 286 ft/d (appendix 1; table 1.1).

Glacial Till Confining Unit

The second hydrogeologic unit in the model area is an expanse of glacial till that is exposed at the land surface and also underlies the Big Sioux aquifer (figs. 6 and 8). In general, the glacial till acts as a lower hydraulic conductivity confining unit in the model area consisting of a glacially deposited, nonsorted, nonstratified sediments with a compact mixture of a silty, clay-rich matrix with sand to boulder-sized clasts (Lindgren and Niehus, 1992). Glacial deposits from glacial advances and retreats during the Pleistocene Epoch cover a large part of the United States (Bayless and others, 2017). Glacial deposit textures range from very fine (clay) deposits to coarse (sand or gravel, or both) deposits. Included in these deposits are glacial tills, which are heterogeneous mixes of fine- and course-textured materials. Glacial tills are present in eastern South Dakota, east of the Missouri River (Bayless and others, 2017; fig. 1), and in general, exist throughout the model area except where the glacial till is eroded away and the underlying bedrock is exposed at the land surface or directly underlies the Big Sioux aquifer (fig. 7). The estimated thickness of the glacial till confining unit ranged from 0 to about 120 ft (fig. 8). The thinnest parts of the glacial till confining unit are typically at the margins of the model area (fig. 6). The glacial till confining unit typically has a low hydraulic conductivity, with estimates ranging from $1.0x10^{-6}$ to 10.0 ft/d (table 3). Because of its low hydraulic conductivity, the glacial till confining unit is typically a poor source of water, except where it locally contains thin, discontinuous sand and gravel lenses. In these thin and discontinuous sand and gravel lenses, the glacial till confining unit can yield as much as 5 gal/min to wells (Lindgren and Niehus, 1992).

Bedrock Aquifers

The third hydrogeologic unit in the model area represents the combined Split Rock Creek and Sioux Quartzite bedrock aquifers. The Split Rock Creek and Sioux Quartzite bedrock aquifers exhibit distinct lithologic and hydrogeologic characteristics; however, for the purposes of this study, the aquifers were included in the groundwater-flow model and conceptualized as a single hydrogeologic unit.

Table 3. Previously published hydraulic properties in or near the model area.

[ft/d, foot per day; --, not available or not applicable]

Source	In study area	Location	Method	Hydraulic conductivity (ft/day)	Storage coefficient (dimensionless)	Specific yield (percent)	Riverbed hydraulic conductivity (ft/day)
Big Sioux aquifer							
Ellis and others (1969)	Yes	Big Sioux River Basin south of Dell Rapids and north of Sioux Falls, South Dakota	Aquifer tests	268–633; mean: 428	--	--	--
Ellis and others (1969)	No	Big Sioux River Basin north of Dell Rapids, South Dakota	Aquifer tests	96–1,069; mean: 451	--	--	--
Jorgensen and Ackroyd (1973)	Yes	Minnehaha County, South Dakota	Aquifer tests	--	--	--	0.5–1.0
Koch (1980)	No	Brookings, Deuel, and Hamlin Counties, South Dakota	Aquifer tests	500–1,500	--	10–17	--
Koch (1982)	Yes	Minnehaha County, South Dakota	--	200–400	--	10–20	--
Hansen (1988)	No	Moody County, north of Dell Rapids, South Dakota	--	200–450	--	20	--
Putnam and Thompson (1996)	No	About 90 miles north of Sioux Falls, South Dakota, in Codington and Grant Counties, South Dakota	Aquifer tests	50–500	0.1–0.2	[a]12–[b]38	--
Niehus and Thompson (1998)	No	Lincoln and Union Counties, South Dakota	--	200–400	--	20	--
Eldridge and Medler (2019)	Yes	Minnehaha County in northern part of Sioux Falls, South Dakota	Rising head slug tests	90–270; mean: 171	--	--	--
Glacial till confining unit							
Koch (1980)	No	Brookings, Deuel, and Hamlin Counties, South Dakota	Groundwater model calibration	10.0	--	--	--
Hendry (1982)	No	Alberta, Canada	--	5×10^{-4}	--	--	--
Heath (1983)	--	--	--	1×10^{-6}–1.0	--	--	--
Bedrock aquifers							
Split Rock Creek aquifer							
Pence (1996)	No	Northeast of Sioux Falls in Minnehaha County, South Dakota	Aquifer tests	23.0–61.0	--	--	--
Putnam (1998)	No	Southeast Minnehaha County, South Dakota	Groundwater model calibration	--	0.00026	20	--
Sioux Quartzite aquifer							
Putnam (1998)	No	Southeast Minnehaha County, South Dakota	--	--	0.0001	20	--

[a]In the unsaturated zone.

[b]In the saturated zone.

The Split Rock Creek aquifer is composed predominantly of one to five layers of sedimentary deposits ranging from fine to coarse well-sorted quartzose sand interbedded with 4- to 45-ft thick layers of siltstone, shale, and claystone of the Split Rock Creek Formation (Lindgren and Niehus, 1992). The extent and thickness of the Split Rock Creek aquifer was not identified specifically for this study because the aquifer was not clearly identified in lithologic logs or from the geophysical investigations completed in the model area (Valseth and others, 2018). However, Lindgren and Niehus (1992) indicated that the Split Rock Creek aquifer thickness as determined from well logs ranges from 0 to 86 ft thick in the model area and underlies about 139 mi^2 in Minnehaha County, S. Dak. In the model area, the Split Rock Creek aquifer is primarily overlain by glacial till and underlain by Sioux Quartzite. The Split Rock Creek aquifer is not aerially extensive in the model area; however, the aquifer underlies glacial till in the south-central part of the model area (Lindgren and Niehus, 1992). Hydraulic conductivity estimates for the Split Rock Creek aquifer typically range from 23 to 61 ft/d (Putnam, 1998). Properly constructed wells completed in the Split Rock Creek aquifer may yield as much as 500 gal/min where the cumulative thickness exceeds 75 ft, but yields usually are much less because of smaller thicknesses, interbedded layers of silt and clay, and cementation of the sand grains (Lindgren and Niehus, 1992).

The Sioux Quartzite aquifer exists in the fractured zones of the massive Sioux Quartzite in the model area. The Sioux Quartzite is a pink or reddish- to tan-colored, siliceous, iron-stained orthoquartzite with minor mudstone and conglomerate layers (Tomhave, 1994). The Sioux Quartzite underlies the model area in Minnehaha County and is exposed at the land surface in many places (fig. 6). The Sioux Quartzite is broken into blocks by well-developed vertical and horizontal jointing, and the spacing of the joints varies greatly in exposures from a few inches to several feet apart (Tomhave, 1994). The Sioux Quartzite is generally shallowest in the northern part of the model area and deeper toward the middle and southern parts of the model area. The thickness of the Sioux Quartzite is not known; however, a conservative estimate of the Sioux Quartzite thickness is about 1,500 ft (Rothrock and Otton, 1947). The interbedded layering of the mudstone and conglomerates in the Sioux Quartzite are so thoroughly lithified that the pore spaces are almost entirely filled with cement, causing the Sioux Quartzite to be nearly impermeable (Rothrock and Otton, 1947). Reported yields from properly constructed wells completed in the Sioux Quartzite aquifer are as much as 150 gal/min but generally are less than 50 gal/min. The yield to wells depends on the extent of the local fracturing and interconnection of fractures in the Sioux Quartzite (Lindgren and Niehus, 1992).

Potentiometric Surfaces

Several potentiometric surfaces for the Big Sioux aquifer were used to determine the general direction of groundwater flow and hydraulic gradients in the model area. Previously published potentiometric surfaces for the Big Sioux aquifer in the model area were mapped by Ellis and others (1969) and Lindgren and Niehus (1992). Ellis and others (1969) estimated the mean hydraulic head in the Big Sioux aquifer for August for 1963–66 (fig. 9*A*), and Lindgren and Niehus (1992) estimated the mean hydraulic head in the Big Sioux aquifer for September 1986 (fig. 9*B*). Lines of apparent groundwater flow were drawn perpendicular to the potentiometric contours on the potentiometric surfaces of Ellis and others (1969) and Lindgren and Niehus (1992). The apparent groundwater-flow direction arrows indicate a general groundwater gradient from north to south and toward perennial streams, which indicates that, in general, groundwater flows from the margins of the aquifer, and from areas of higher elevation, to the streams and rivers in the model area.

In comparison to Ellis and others (1969) and Lindgren and Niehus (1992), groundwater levels were compiled for the model area and used to create an estimated potentiometric surface for the Big Sioux aquifer representative of March 23, 2017 (fig. 10). Field-measured groundwater and surface-water levels were obtained during the following three measurement periods: March 23, 2017, May 4, 2017, and from June 11 through June 14, 2017 (U.S. Geological Survey, 2018; fig. 10). Established discharge and stream stage relations were used to estimate stream stage altitude at USGS streamflow measurement sites that were lacking published stream stage during the measurement periods. Additionally, water levels were estimated at control points placed on the Big Sioux River using the National Elevation Dataset digital elevation model (DEM; Gesch, 2007; Gesch and others, 2002; U.S. Geological Survey, 2017) and were adjusted by the offset between the DEM value and the stream stage altitude estimated on March 23, 2017.

All water levels were corrected to March 23, 2017, because that date had the greatest number of water-level measurements at wells. Before applying corrections, any multiple groundwater levels measured at a well during a measurement period were averaged to generate a single-observation dataset representative of that measurement period. Water-level changes were calculated from the March and June measurement periods and used to interpolate a continuous surface of water-level changes in the model area using the ArcGIS Topo to Raster geoprocessing tool (Esri, 2011). The surface of water-level changes was used to obtain estimated water-level changes at wells with measurements completed only during the June 11–14, 2017, measurement period. The extracted water-level changes were then applied to the water levels obtained during the June 11–14, 2017, measurement period to calculate estimated water levels for March 23, 2017. The applied water-level corrections were minimal (less than plus or minus 2.0 ft).

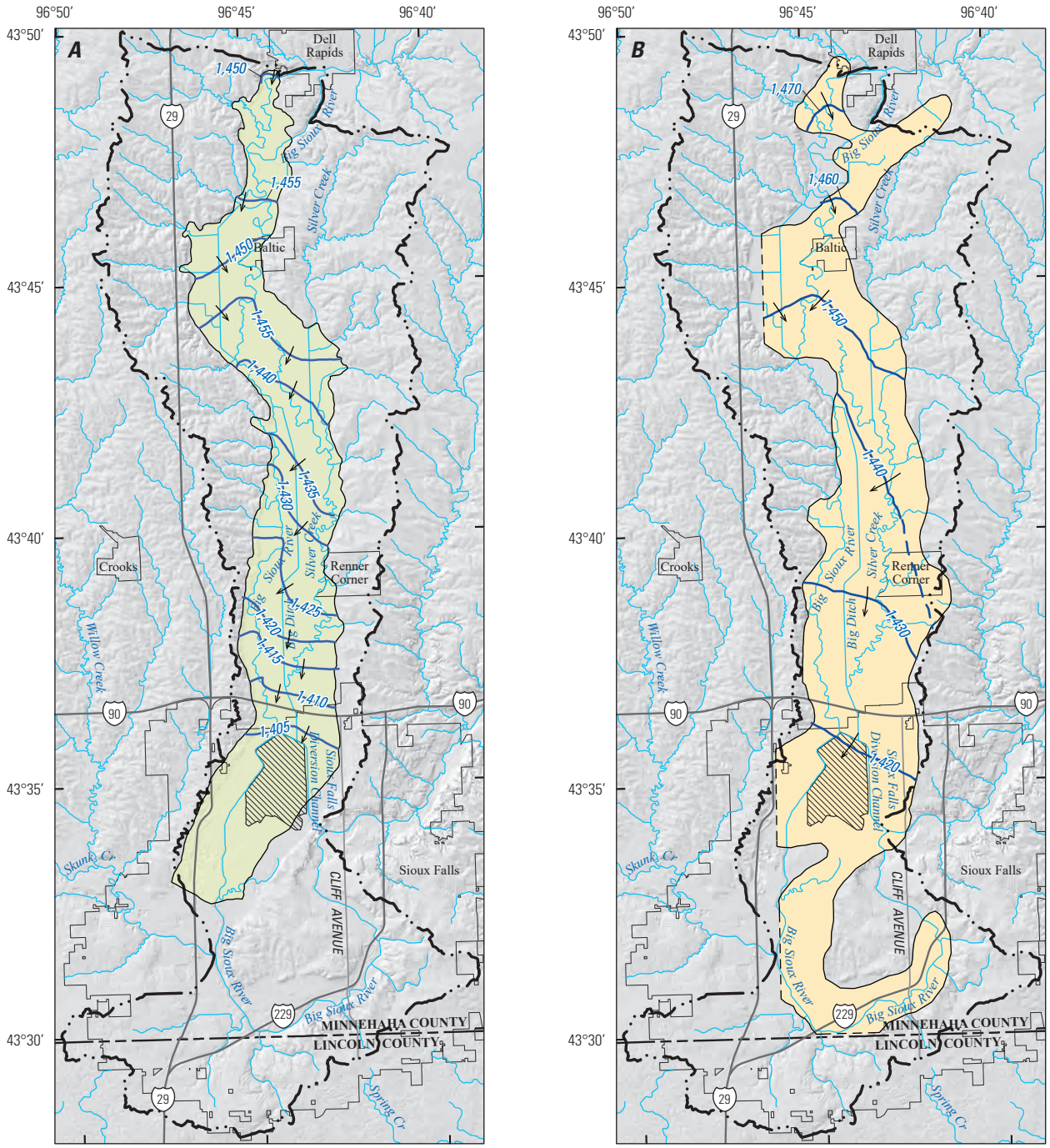

Base modified from U.S. Geological Survey digital data, various scales
Hillshade from digital elevation model (Gesch, 2007; Gesch and others, 2002)
Universal Transverse Mercator projection, zone 14 N.

EXPLANATION

- **Sioux Falls Regional Airport**
- **Big Sioux aquifer extent**—Modified from Ellis and others (1969)
- **Big Sioux aquifer extent**—Dashed indicates edge of the unmapped area; modified from Lindgren and Niehus (1992)
- **Model area boundary**
- **Apparent direction of groundwater flow**—Modified from *A*, Ellis and others (1969) and *B*, Lindgren and Niehus (1992)
- 1,420 **Potentiometric contour**—Shows average observed elevation at which water level would have stood in tightly cased well, in feet. Dashed where approximately located. Contour interval 10 feet. Datum is North American Vertical Datum of 1988

Figure 9. Previously published potentiometric surfaces of the Big Sioux aquifer from *A*, Ellis and others (1969); and *B*, Lindgren and Niehus (1992).

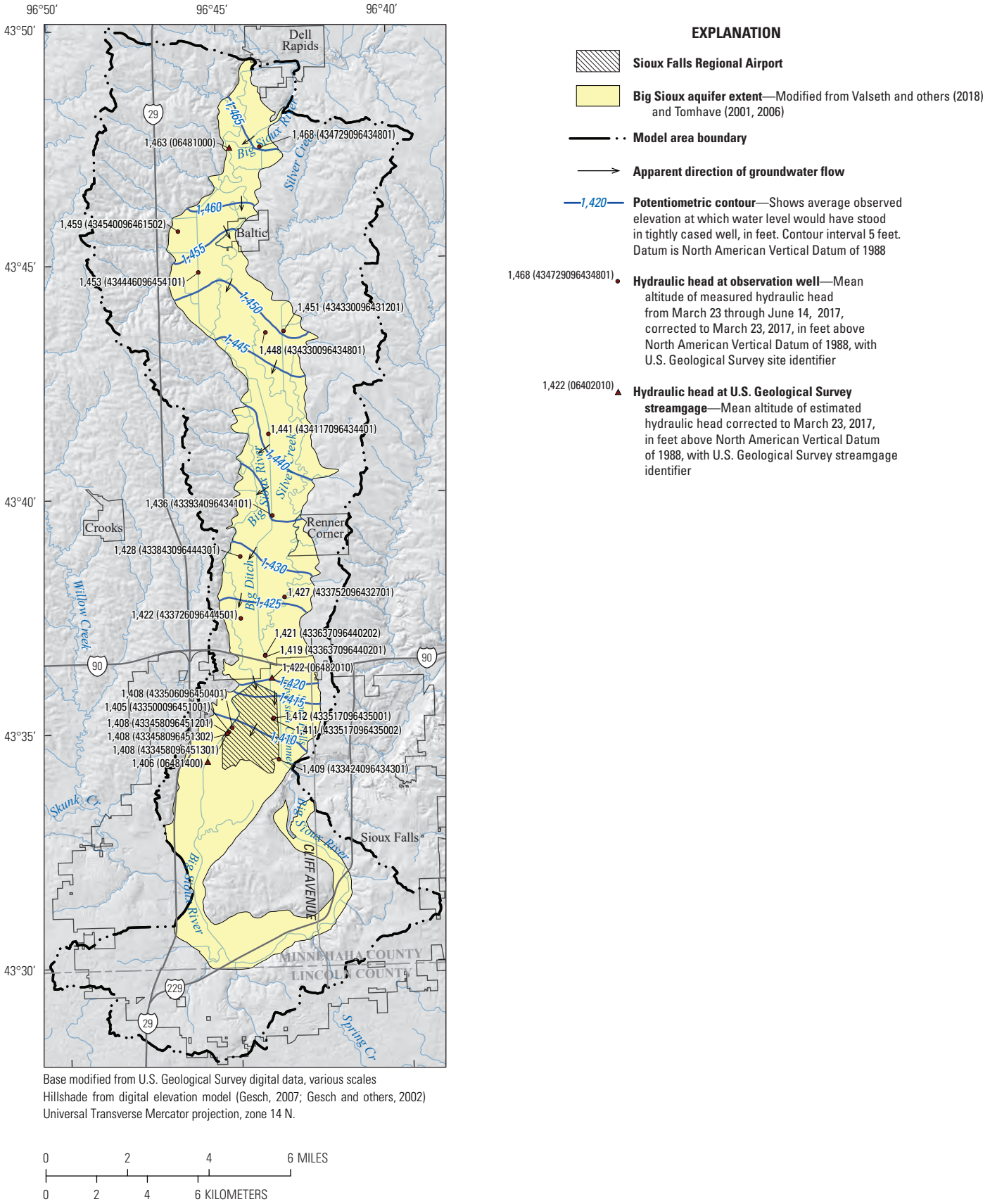

Figure 10. Estimated potentiometric surface of the Big Sioux aquifer, hydraulic head altitudes corrected to March 23, 2017.

An iterative process was used to remove mounds, depressions, or other visual anomalies in the potentiometric map of the Big Sioux aquifer for March 23, 2017 (fig. 10). The iterative process used the following steps: (1) an intermediate potentiometric surface was created using the March 23, 2017, corrected water levels and control points on the Big Sioux River at 5-ft intervals using the ArcGIS Topo To Raster geoprocessing tool (Esri, 2011); (2) potentiometric surface anomalies were visually identified by comparing the estimated contours to computer-simulated water-level maps from Koch (1980); (3) where potentiometric surface anomalies were observed, control points along the Big Sioux River were either resampled or removed or contours were manually corrected; and (4) steps 1–3 were repeated until potentiometric surface anomalies were minimized. Anomalies were typically from estimated water-level altitudes at the control points placed along the Big Sioux River because the estimated altitudes were determined based on the DEM altitude. Contour lines near the Sioux Falls Regional Airport were adjusted manually to remove potentiometric surface anomalies and to ensure groundwater-flow directions were hydrologically reasonable.

Groundwater-flow directions were interpreted from the potentiometric surface of the Big Sioux aquifer for March 23, 2017, and the directions are represented as arrows in figure 10 drawn perpendicular to potentiometric contours. Groundwater-flow direction arrows shown in figure 10 generally indicate groundwater flows from the margins of the Big Sioux aquifer toward the Big Sioux River. Interpreted groundwater-flow directions generated from the estimated potentiometric surface were similar to those interpreted from Ellis and others (1969) and Lindgren and Niehus (1992).

Water Budget

Primary recharge and discharge components for the Big Sioux aquifer in the model area include inflows from stream seepage, deep percolation of precipitation on the land surface (precipitation recharge), and seepage from hydrologically connected aquifers, and outflows from discharge to streams, direct evapotranspiration of groundwater, groundwater withdrawals, and seepage to the hydraulically connected aquifers (Koch, 1982; Ellis and others, 1969). Lindgren and Niehus (1992) estimated that 75–85 percent of precipitation in the model area is eventually removed by evapotranspiration, 5–10 percent of precipitation discharges as streamflow, and 5–20 percent of precipitation recharges the aquifers.

Groundwater inflows and outflows for 1970–79 for the Big Sioux aquifer for an area between the Sioux Quartzite flow barriers (fig. 6) were estimated by Koch (1982). Groundwater inflows are approximately split between stream seepage and precipitation recharge, and groundwater outflows are dominated by withdrawals. Koch (1982) estimated groundwater inflows from stream seepage (about 47 percent of total groundwater inflow) and recharge from precipitation (about 53 percent; table 4). Koch (1982) estimated groundwater discharge to streams was about 36 percent of total groundwater outflow and evapotranspiration was about 3 percent. Groundwater withdrawal estimated by Koch (1982) accounted for about 62 percent of total groundwater outflow. Koch (1982) did not estimate groundwater flux (inflow or outflow) to hydraulically connected aquifers because of the lower hydraulic conductivity of the underlying hydrogeologic units and assumed that net groundwater storage gain or loss (difference in groundwater storage inflow and outflow) was minimal. Lindgren and Niehus (1992) estimated that the total volume of water in storage for the Big Sioux aquifer in Minnehaha County, S. Dak., was about 190,000 acre-feet (about 61.9 billion gallons) by multiplying the mean thickness by the areal extent of the aquifer using an estimated porosity of 20 percent.

Precipitation Recharge

In the model area, the Big Sioux aquifer, glacial till confining unit, and bedrock aquifers outcrop at the land surface and receive recharge resulting from infiltration of precipitation that falls on the land surface. An SWB model (Westenbroek and others, 2010) was used to calculate spatially and temporarily varying estimates of precipitation recharge (SWB-estimated recharge) in the model area for 1949–2017. Annual

Table 4. Published groundwater budget components for the Big Sioux aquifer in the model area.

[ft^3/s, cubic foot per second; Mgal/d, million of gallons per day; --, not estimated or negligible]

Recharge or discharge component	Modified from Koch (1982)[a]		
	Rate (ft^3/s)	Rate (Mgal/d)	Percent of total
Groundwater recharge (inflow)			
Stream seepage	14.4	9.3	47.4
Recharge from precipitation	16.0	10.3	52.6
Groundwater inflow from other aquifers	--	--	--
Storage	--	--	--
Total recharge	**30.4**	**19.6**	**100.0**
Groundwater discharge (outflow)			
Groundwater discharge to streams	10.8	7.0	35.8
Evapotranspiration	0.8	0.5	2.6
Groundwater withdrawal	18.6	12.0	61.6
Groundwater discharge to other aquifers	--	--	--
Storage	--	--	--
Total discharge	**30.2**	**19.5**	**100.0**

[a]Estimated water budget for the Big Sioux aquifer between Dell Rapids and Sioux Falls, South Dakota, for 1970–79.

recharge for 1949 and monthly recharge for 1950–2017 was estimated using the SWB model. The SWB model is a two-dimensional distributed-parameter model based on the approach of Thornthwaite and Mather (1957) and was used to estimate groundwater recharge as infiltration below the root zone to each model cell on a daily time step. The SWB model inputs include daily precipitation and air temperature and cell-by-cell land cover classification, soil type parameters, and general surface-water-flow direction. A complete overview of the SWB model is available in appendix 2, and the SWB model input and output files are available in the accompanying USGS data release (Eldridge and Davis, 2019).

SWB-estimated recharge for 1949 was used to approximate steady-state recharge and was typically highest in the northern part of the model area and near streams (fig. 11). The SWB-estimated steady-state recharge ranged from 0.0 to 46.7 in. with a mean of 2.0 in. The SWB-estimated steady-state recharge distribution was similar to the mean annual SWB-estimated recharge for 1950–2017 (fig. 2.1). Input annual precipitation for 1945–2017 for the SWB model ranged from 11.4 to 38.3 in., with a mean of 25.3 in. Annual SWB-estimated recharge ranged from 0.06 to 5.90 in., with a mean of 2.1 in. (fig. 12) and was generally lower than previous estimates near the model area (table 5). The SWB-estimated annual recharge as a percentage of annual precipitation for 1950–2017 ranged from 0.3 to 20.0 percent, with a mean of 8.0 percent, and corresponded favorably to estimates that ranged from 5 to 20 percent (Lindgren and Niehus, 1992). Monthly SWB-estimated recharge for 1950–2017 ranged from 0.027 in. for August to 0.71 in for March (Eldridge and Davis, 2019). Annual and monthly trends in SWB-estimated recharge corresponded to trends in precipitation and temperature in the model area with higher recharge rates in March during spring thawing and snowmelt and lower recharge rates in the fall during periods of higher temperatures and lower monthly precipitation (table 1).

Evapotranspiration

In the model area, evapotranspiration from groundwater (ETg) is from direct evaporation from the saturated groundwater regime as well as from plant transpiration (Wilson and Moore, 1998). Potential evapotranspiration (PET) is the amount of water that could be removed from the saturated groundwater regime by evapotranspiration if there never was a deficiency of water in the soil for use by vegetation (Wilson and Moore, 1998). In general, ETg is greatest (equal to PET) when the water table is at the land surface and decreases linearly to an extinction depth (typically below the root zone of plants). Previous estimates of PET in the model area range from 21.0 to 41.0 inches per year (table 5). Estimates of ETg for the model area were not available. Actual ETg in the model area was calculated by the numerical model, as described in the "Numerical Model" section of this report.

The SWB model (Westenbroek and others, 2010) was constructed primarily to calculate estimates of recharge for the model area, but also was used to provide spatially and temporarily varying estimates of PET in the model area for 1949–2017 (appendix 2; Eldridge and Davis, 2019). In the model area, PET was calculated by the method of Hargreaves and Samani (1985) using the daily mean air temperature between 43.46 and 43.83 degrees north latitude. The SWB-estimated PET for 1949 was used to approximate steady-state PET and was about 36 in. (fig. 11). Annual SWB-estimated PET for 1950–2017 ranged from 29.1 to 40.3 in., with a mean of 33.9 in. (fig. 12) and compared favorably with published estimates near the model area (table 5).

Withdrawal

Withdrawal in the model area is primarily from groundwater; however, surface-water withdrawal in the model area also existed near the Sioux Falls Regional Airport (Sioux Falls Diversion Dam and Weir) and at a transfer pump (wetlands pump) north of Sioux Falls (fig. 1). The Sioux Falls Diversion Dam and Weir and the Sioux Falls Diversion Channel routes a percentage of the streamflow in the Big Sioux River down a flood mitigation canal near the Sioux Falls Regional Airport (fig. 1), and the wetlands pump transfers water from the Big Sioux River to Big Ditch (fig. 1) during the spring and summer. Groundwater and surface-water withdrawals applied in the model are described in the following sections.

Groundwater Withdrawal

Groundwater withdrawals for production wells in the model area were included in the groundwater-flow model. Groundwater withdrawals for irrigation, domestic, or livestock uses were not considered in the model area because previous investigators indicated that these withdrawals were less than 0.05 percent of total groundwater outflow in the model area (Koch, 1982).

Production wells in the model area are near Baltic and Dell Rapids and are generally within and about 6 miles north of the Sioux Falls Regional Airport area (fig. 13). Most of the groundwater from the Sioux Falls Regional Airport area is water captured from the Big Sioux River; however, Jorgensen and Ackroyd (1973) estimated about 10 percent of the groundwater withdrawn by wells was from underflow through the aquifer based on withdrawals in 1968.

Groundwater withdrawals rates for production wells in the model area were provided by the city of Sioux Falls (Jeff Dunn, Principal Engineer Water-Main, city of Sioux Falls, written commun., 2017) and the Minnehaha Community Water, Corporation (Scott Buss, Executive Director, Minnehaha Community Water, Corporation, written commun., 2018). The monthly mean groundwater withdrawal rates are available in the accompanying USGS data release (Eldridge and Davis, 2019).

Groundwater withdrawals for 45 production wells within and about 6 miles north of the Sioux Falls Regional Airport area were available for 1995–2017. Withdrawal records for the

Table 5. Published recharge or discharge component and extinction depth estimates for the Big Sioux aquifer from previous studies.

[in/yr, inch per year; ft, foot]

Source	Period	Location	Recharge or discharge component	Method of estimation	Rate (in/yr)	Evapotranspiration extinction depth (ft)
Koch (1980)	--	Brookings, Hamlin, and Duel Counties, South Dakota	Recharge	Water-table fluctuation; groundwater model calibration	3.29–6.57	--
			Potential evapotranspiration	Groundwater model calibration	33.0	5.0
Koch (1982)	1967–78	North of Sioux Falls, South Dakota	Recharge	Water-table fluctuation	[a]7.6; [b]6.9; 10.1	--
			Potential evapotranspiration	Percent of mean annual lake evaporation	33.0	5.0 and 10.0
Hansen (1988)	1970–79	North of Dell Rapids, South Dakota	Recharge	Water-table fluctuation	3.6–9.3; mean: 6.5	--
			Potential evapotranspiration	Mean annual pan evaporation	21.0–41.0; mean: 31.0	[c]5.0 and 10.0
Putnam and Thompson (1996)	1978–85	About 90 miles north of Sioux Falls, South Dakota, in Codington and Grant Counties, South Dakota	Recharge	Water-table fluctuation	[d]2.9–5.8	--
			Potential evapotranspiration	Percent of pan evaporation	mean: [e]34.7	--
Niehus and Thompson (1998)	1976–94	Lincoln and Union Counties, South Dakota, south of Sioux Falls, South Dakota	Recharge	Water-table fluctuation	2.14–12.96; mean: 7.54	--
			Potential evapotranspiration	74 percent of pan evaporation	[f]39.4	[g]5.0

[a]Initial estimate for numerical groundwater flow model.

[b]Calibrated value using inverse statistical calibration methods.

[c]5.0 feet extinction depth away from the Big Sioux River; 10.0 feet extinction depth near Big Sioux River.

[d]Primarily during March through June; little during winter.

[e]Zero during January, February, March, November, and December.

[f]Zero during November, December, January, February, March, and April.

[g]From Koch, 1982.

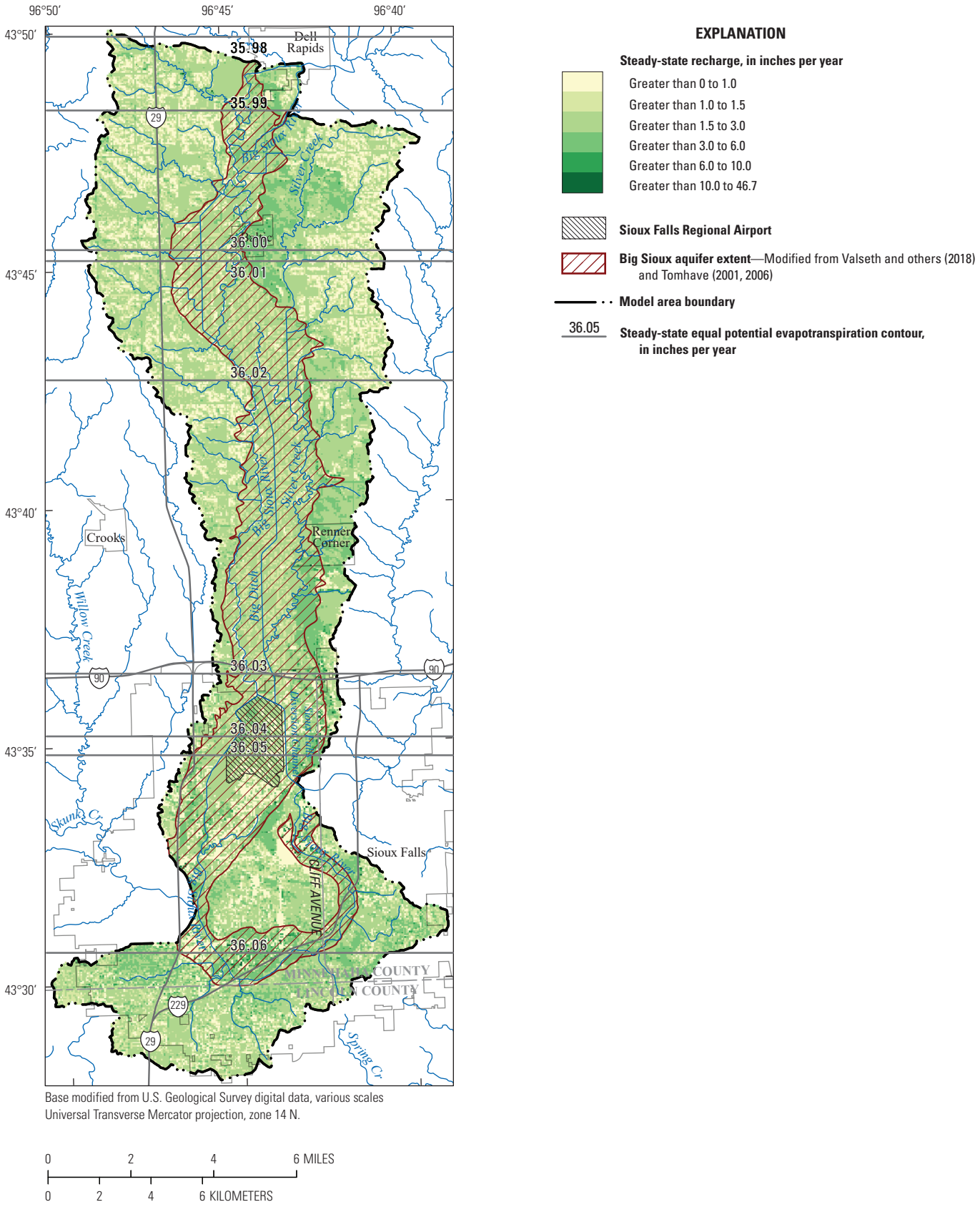

Figure 11. Spatial distribution of steady-state recharge and contours of potential evapotranspiration from the Soil-Water-Balance model.

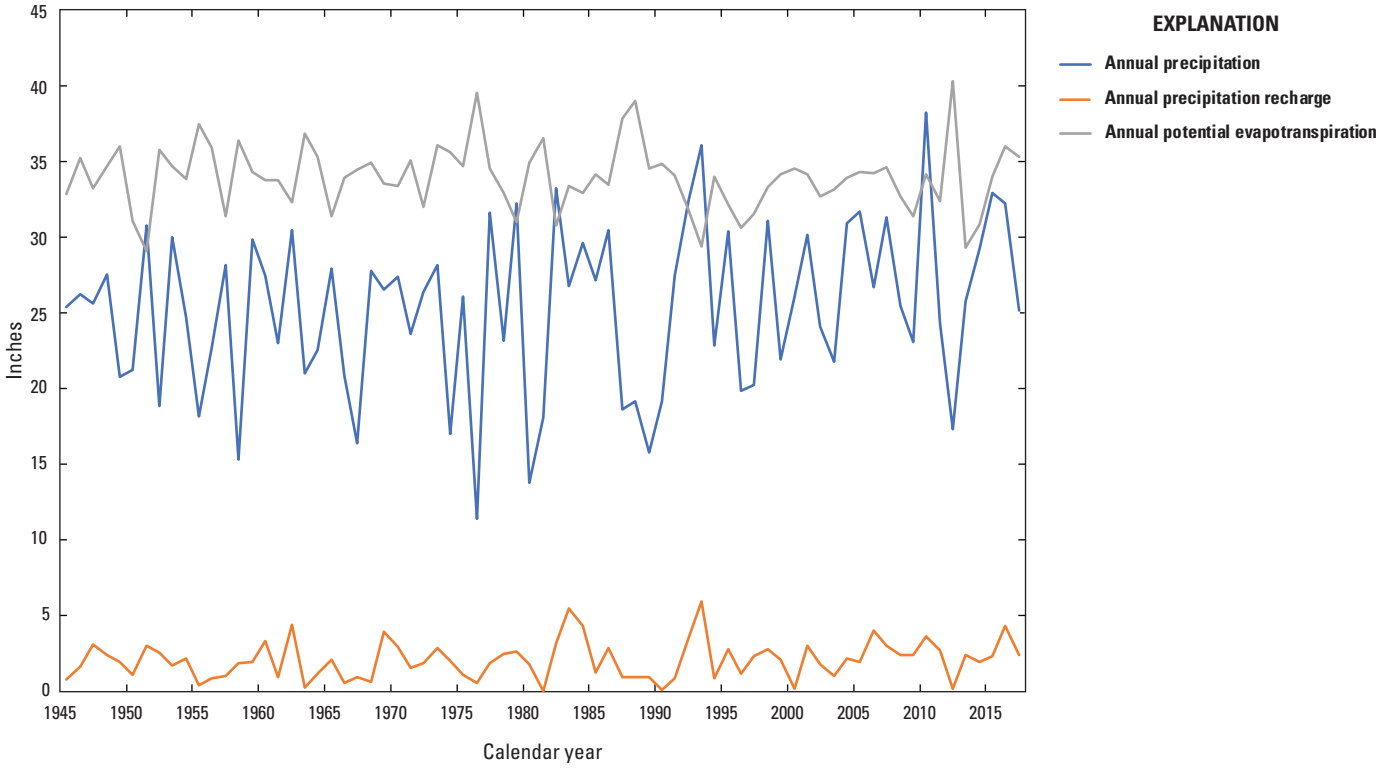

Figure 12. Annual precipitation, precipitation recharge, and potential evapotranspiration from the Soil-Water-Balance model for 1950–2017.

production wells were reported as a change in meter readings for a number of days. Discrepancies, such as dates that were out of order or changes in meter reading methods, were corrected. Withdrawals from individual production wells ranged from 0 to 90 million gallons per month. Total withdrawals from all wells ranged from 0 to 700 million gallons per month. Groundwater withdrawals for periods without records were estimated by correlating monthly population estimates with monthly groundwater withdrawal for 1995–2017. The mean monthly population-correlated withdrawal rates for 1950–1994 ranged from 4.7 Mgal/d for December to 7.3 Mgal/d for July. Reported and estimated monthly mean groundwater withdrawal for production wells within and about 6 miles north of the Sioux Falls Regional Airport area for 1950–2017 ranged from 0.2 to 22.8 Mgal/d (fig. 14).

Groundwater withdrawals near Baltic and Dell Rapids, S. Dak., were available for 15 production wells for 1979–2017. Monthly mean groundwater withdrawal for these production wells ranged from 0.3 to 4.4 Mgal/d (fig. 14).

Surface-Water Withdrawal

The city of Sioux Falls controls two nonconsumptive diversions on the Big Sioux River, primarily for flood mitigation purposes (Andy Berg, Environmental/Storm Water Manager, city of Sioux Falls, written commun., 2017). The first diversion is north of the Sioux Falls Regional Airport (fig. 1; Sioux Falls Diversion Dam and Weir) and is controlled by a dam and weir. The dam and weir divert a percentage of streamflow from the Big Sioux River into a diversion channel that flows to the east, bypassing the Sioux Falls Regional Airport and the southern part of the city. The diverted streamflow eventually discharges back into the Big Sioux River near USGS streamgage 06482020 (fig. 1). The U.S. Army Corps of Engineers began construction of the diversion, dam and weir, and other flood control measures for the city of Sioux Falls in 1956 and completed the projects in 1965 (U.S. Army Corps of Engineers, 1990). The Sioux Falls Diversion Dam and Weir and Sioux Falls Diversion Channel began operating in 1961 (Jorgensen and Ackroyd, 1973). The project included about 11 miles of stream channel improvements in the city, about 3 miles of the diversion channel, and 27 miles of levees. Minimum streamflow in the Big Sioux River through the city is maintained at about 400 ft^3/s (Lebeda Consulting, 2016). The city of Sioux Falls attempts to maintain the streamflow at USGS streamgage 06482000 (fig. 1) at less than 1,100 ft^3/s by balancing the observed streamflow at the USGS streamgages 06481000 and 06481500 (fig. 1) with the streamflow in the diversion channel (Andrew Berg, Environmental/Stormwater Manger, city of Sioux Falls, written commun., 2017). Additionally, a minimum inflow of 200 ft^3/s normally is maintained in the Sioux Falls Diversion Channel to ensure that some backwater remains in Silver Creek. The maximum streamflow allowed in the diversion channel is typically 500 ft^3/s.

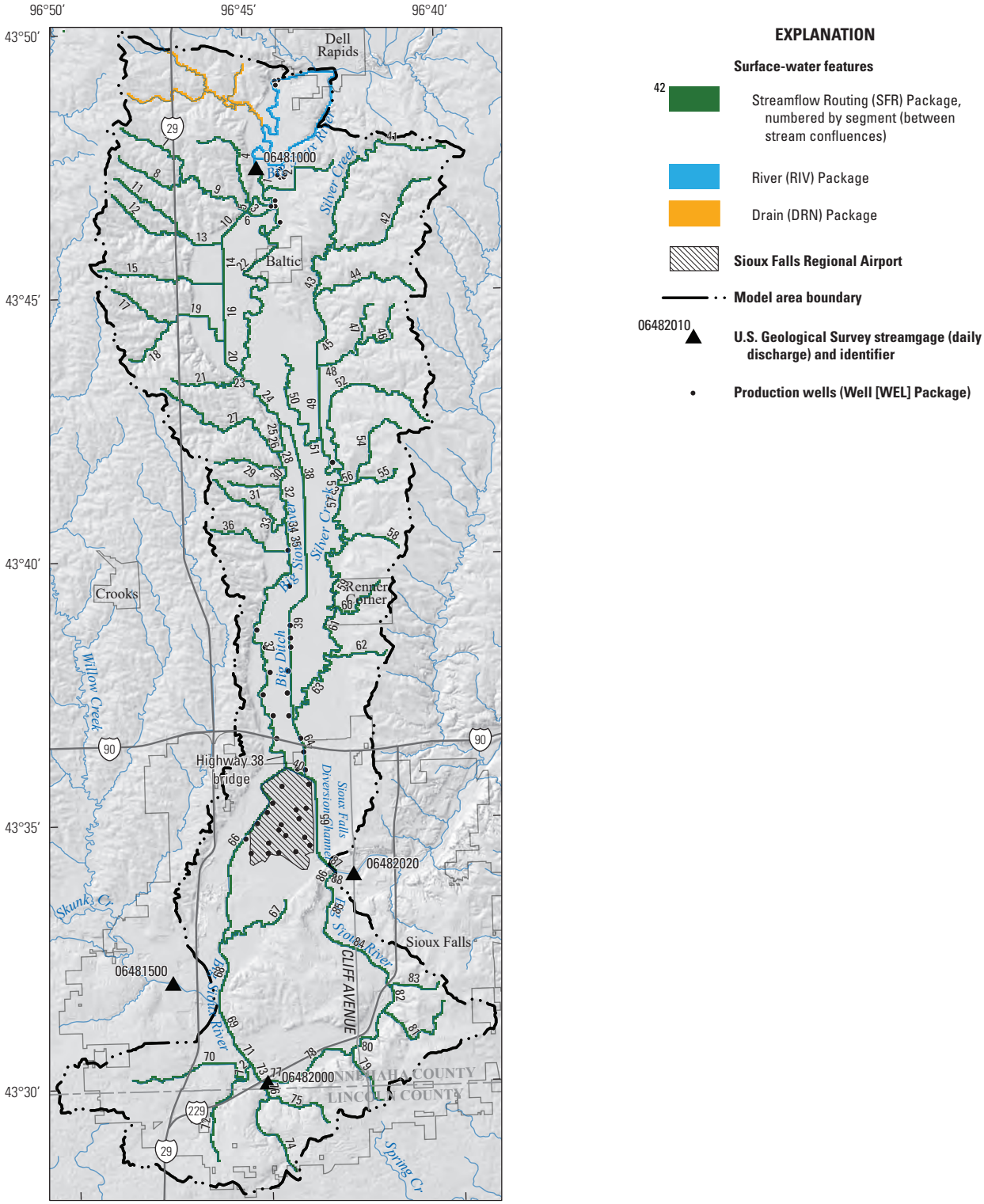

Figure 13. Hydrologic features and corresponding MODFLOW Packages represented in the numerical model.

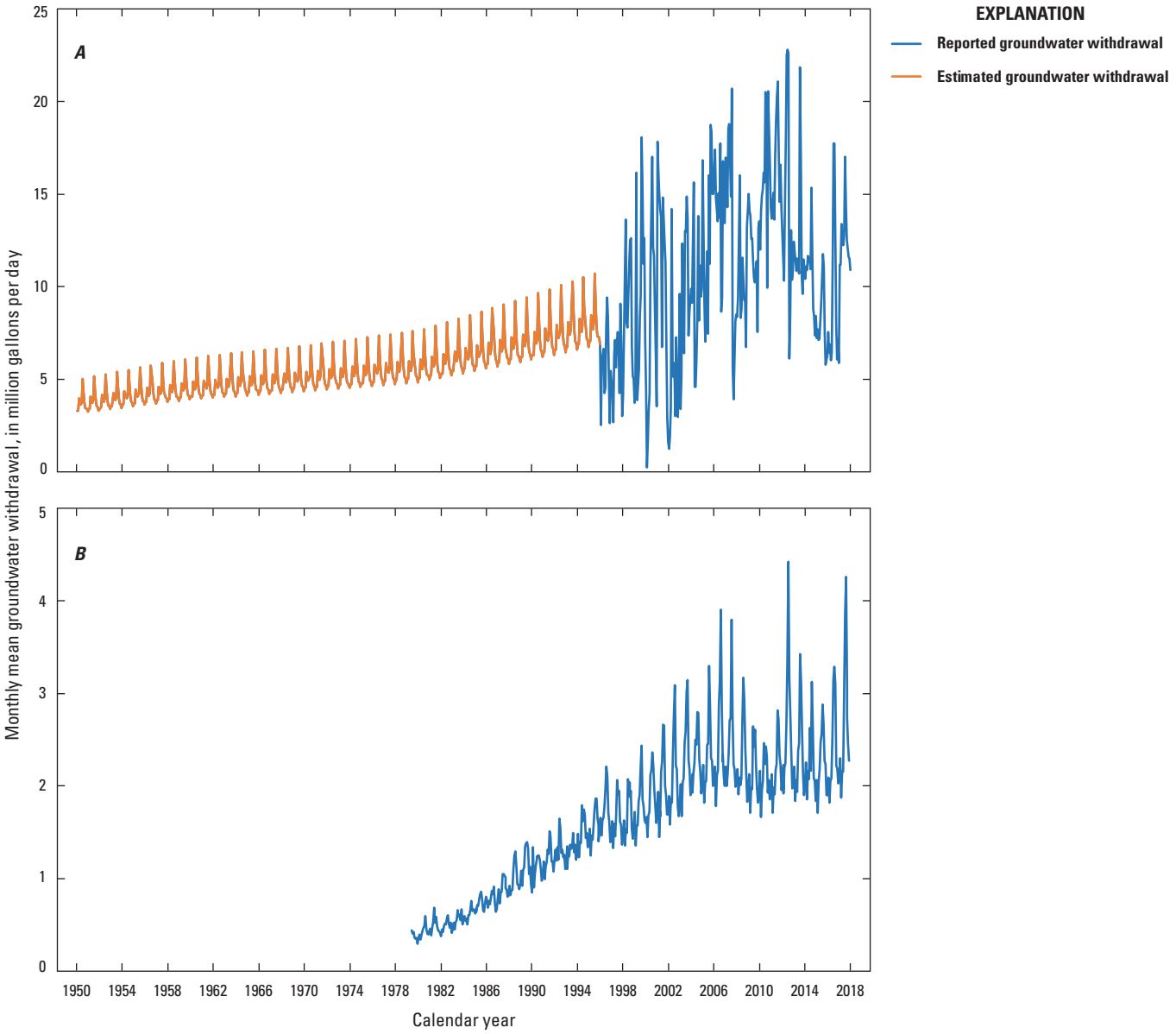

Figure 14. Reported and estimated monthly mean groundwater withdrawals for *A*, production wells located within and about 6 miles north of the Sioux Falls Regional Airport area; and *B*, production wells located between Dell Rapids and Baltic, South Dakota. (Data available in Eldridge and Davis, 2019.)

The second diversion controlled by the city of Sioux Falls transfers streamflow from the Big Sioux River to Big Ditch (fig. 1) by use of a transfer pump named the wetlands pump. The wetlands pump is about 5 miles north of the city of Sioux Falls near the Big Sioux River (fig. 1). During summer, when streamflow in the Big Sioux River is high, the city uses the wetlands pump to transfer water from the Big Sioux River by pipe into Big Ditch. The pump has only a single operating rate of 7,000 gal/min. The city maintained weekly records of pump operation from 2006 through 2017 (Tim Stefanich, Water Division Environmental Engineer, city of Sioux Falls, written commun., 2018), which were used to estimate wetlands pump transfer rates. These estimates are provided in the "Numerical Model" section of the report.

Groundwater and Surface-Water Interactions

Water in the Big Sioux aquifer is in hydraulic connection with the Big Sioux River and its tributaries in the model area (Koch, 1982); therefore, groundwater discharge to and groundwater recharge from surface water exists in the model area. During dry periods, the base flow of the Big Sioux River is primarily water released from groundwater storage, and during periods of high streamflow, water from the river recharges

the aquifer through the streambanks (Jorgensen and Ackroyd, 1973). Jorgensen and Ackroyd (1973) and Koch (1982) completed seven low-flow seepage studies during 1964–80 between Dell Rapids and Renner Corner, S. Dak., to quantify the groundwater discharge to streams (positive streamflow gain) and groundwater recharge from streams (negative streamflow gain or streamflow loss) in the model area—three low-flow seepage studies were completed during the fall, two were completed during late winter, and two were completed during spring and early summer. The seepage studies indicated that, at the time of the studies, streamflow gain between Dell Rapids and Renner Corner ranged from −5 to 10 ft^3/s, and between Renner Corner and State Highway 38, streamflow gain ranged from −20 to 3 ft^3/s (Koch, 1982). Additionally, the seepage studies indicated that streamflow gain typically was observed between Dell Rapids and Renner Corner and streamflow loss typically was observed between Renner Corner and the State Highway 38 bridge (Koch, 1982; fig. 1). Koch (1982) also estimated mean annual streamflow gain of 4.9 ft^3/s for 1970–79 between USGS streamgages 06481000 and 06482020 that resulted from discharge from groundwater and overland runoff. Jorgensen and Ackroyd (1973) concluded that the seepage runs indicated that groundwater moves from the stream to the aquifer near the Sioux Falls Regional Airport.

Neupane and others (2017) estimated groundwater discharge and groundwater recharge to streams in the Big Sioux River Basin based on geochemical tracers and concluded that the rate of groundwater discharge into the Big Sioux River increases from upstream to downstream. Neupane and others (2017) estimated groundwater discharge to the Big Sioux River in the Big Sioux River Basin based on radon activity in water samples collected along the Big Sioux River during May through July 2015. Based on radon activity measurements, the mean estimated groundwater discharge to the Big Sioux River in the Big Sioux River Basin ranged from 14.2 to 18.2 ft^3/s and in the model area, ranged from 20.22 to 60.28 ft^3/s (Neupane and others, 2017).

Streamflow gains and losses can be estimated by subtracting streamflow at an upstream streamgage, or the sum of streamflow from contributing upstream streamgages, from streamflow at a downstream streamgage (Koch, 1970). Determining whether the calculated gains and losses are real or apparent can be difficult when streamflow is greater than base flow. Apparent streamflow gains and losses exist when the monthly streamflow gain (or loss) is offset in the following month, or in some cases months, by the same magnitude of streamflow loss (or gain). Floods, riverbank groundwater storage, and reservoir operations create the conditions for apparent streamflow gains and losses. Cumulative streamflow gains and losses can be used to graphically determine whether the calculated streamflow gains and losses are real or apparent (Koch, 1970). Streamflow data were available for USGS streamgage 06482020 for October 1971 through December 2017 (U.S. Geological Survey, 2018); therefore, streamflow gains and losses were calculated in the model area by subtracting the streamflow at upstream USGS streamgages 06481000 and 06481500 from the streamflow at downstream USGS streamgage 06482020 for the same period (fig. 15). Cumulative streamflow gains and losses also were calculated for October 1971 through December 2017 to determine whether the calculated monthly streamflow gains and losses were real or apparent. Times at which streamflow gain and streamflow loss exist in the model area can be qualitatively determined using figure 15, but the mechanism of gain or loss, or both (surface-water runoff, groundwater recharge, groundwater discharge, or evapotranspiration) cannot be determined (Koch, 1970).

The calculated monthly streamflow gains and losses, indicated by positive and negative values on figure 15, respectively, include the total volume of water that passes USGS streamgage 06482020 downstream from USGS streamgages 06481000 and 06481500 in a given month and may include groundwater discharge to streams and groundwater recharge from streams, as well as overland runoff (Koch, 1970). Calculated monthly streamflow gains and losses ranged from −186,600 gal/min (−415.7 ft^3/s streamflow loss) to 264,800 gal/min (590.0 ft^3/s streamflow gain) for June 1984 and April 2011, respectively (fig. 15). Cumulative streamflow gains and losses are likely better estimates of multi-year real streamflow gain or loss and, as a result, include a component of groundwater discharge to streams and streamflow loss (Koch, 1970). The slope of the cumulative streamflow curve on figure 15 was used as an indicator of sustained periods of streamflow gain (positive slope) or loss (negative slope) in the model area. Therefore, figure 15 was used as an indicator of periods when groundwater discharged to streams and groundwater was recharged by streams in the model area for October 1971 through December 2017. Periods of sustained streamflow gain included October 1971 through February 1972, June 1972 through February 1988, August 1992 through March 1995, April 1997 through September 2001, October 2003 through May 2007, and July 2010 through December 2017.

In the early 1960s, the Sioux Falls Diversion Dam and Weir and Sioux Falls Diversion Channel was installed north of the city of Sioux Falls to divert a portion of the Big Sioux River streamflow, effectively bypassing much of the city, for flood control measures. The addition of the diversion channel near the Sioux Falls Regional Airport, possibly modified groundwater gradients in the area by providing a length of stream where groundwater discharge to or groundwater recharge from surface water can exist; however, the weir on the diversion channel and the dam on the Big Sioux River may have formed stream-sediment traps that can reduce the hydraulic conductivity of the streambed material (Jorgensen and Ackroyd, 1973). A large volume of sediment has been deposited in the backwater behind the weir, in the backwater behind the dam, and in Silver Creek (fig. 1). This sediment, in general, is only moderately permeable and restricts surface-water recharge to the aquifer (Jorgensen and Ackroyd, 1973).

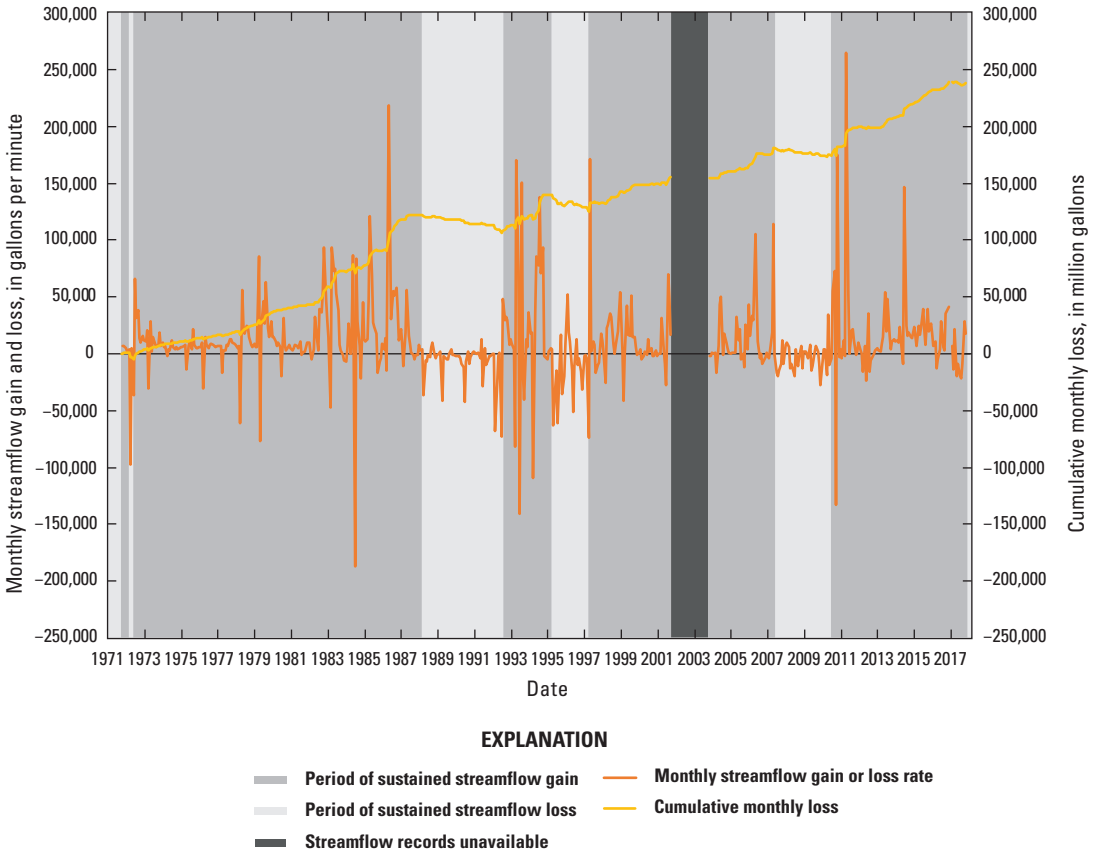

Figure 15. Estimated monthly streamflow gain and loss and cumulative monthly streamflow gain and loss between U.S. Geological Survey streamgages 06481000 (Big Sioux River near Dell Rapids, South Dakota) and 06482020 (Big Sioux River at North Cliff Avenue at Sioux Falls, S. Dak.) for October 1971 through December 2018.

Numerical Model

A numerical model was constructed and was used to simulate all aspects of the conceptual model for predevelopment (steady-state) and time-varying (transient) monthly conditions for 1950–2017. The numerical model was constructed using the USGS modular hydrologic simulation program, MODFLOW–6 (Langevin and others, 2017) and was calibrated using the PEST software, PEST++ (Welter and others, 2015). The numerical model represents a wide range in hydrologic conditions and can be used as a tool for (1) simulating hydrologic scenarios of interest to groundwater managers; (2) advancing understanding of groundwater budgets and their components such as recharge, discharge, and aquifer storage; (3) computing historical and projected system response to natural and anthropogenic stresses; and (4) determining likely sources of water supplied to wells in the model area. All numerical model input and output files are available in an accompanying USGS data release (Eldridge and Davis, 2019).

Numerical Model Design

MODFLOW–6 (Langevin and others, 2017) was used to simulate groundwater flow for the following three hydrogeologic units in the model area: (1) Big Sioux aquifer, (2) the glacial till confining unit, and (3) the combined Split Rock Creek and Sioux Quartzite bedrock aquifers. MODFLOW–6 solves the groundwater-flow equation for a set of discrete blocks, called "cells," and balances all inflows and outflows for each cell in the model area. Various components of the water budget were simulated using model packages, which are distributed with MODFLOW–6. A package is a part of the model that deals with a single aspect of the stimulation. The four types of packages available in MODFLOW–6 are Hydrologic/Internal, Hydrologic/Stress, Hydrologic/Advanced Stress, and Output Packages. Various packages of each type were used to simulate groundwater flow in the model area. The Hydrologic/Internal Packages calculate terms required to solve the groundwater-flow equation for each numerical model

cell or store the information needed to calculate these terms. Hydrologic/Stress and Hydrologic/Advanced Stress Packages in MODFLOW–6 formulate the coefficients in the groundwater-flow equation that describe an external or boundary flow and are used to calculate the flow between a numerical model cell and the package representing a particular stress; for example, the Well (WEL) Package calculates the coefficients describing flow between a numerical model cell and a well. Output Packages manage the printing and saving of numerical model results to output files.

MODFLOW–6 requires Hydrologic/Internal Packages. Required packages are determined based on the specification of grid information for the model area. Hydrologic/Internal Packages used in the numerical model were the Discretization (DIS), Initial Conditions (IC), Node Property Flow (NPF), and Storage (STO) Packages. The DIS Package was used to define the extent and geometry of layers included in the numerical model; the IC Package was used to provide initial starting hydraulic heads for each layer; the NPF Package was used to define the horizontal and vertical hydraulic conductivity for each layer; and the STO Package was used to define the aquifer storage properties for each layer. All available Hydrologic/Internal Packages, including those that are not used in the numerical model, are described in Langevin and others (2017).

Aquifer stress was simulated using Hydrologic/Stress and Hydrologic/Advanced Stress Packages. Hydrologic/Stress Packages used in the numerical model were the WEL, Recharge (RCH), and Evapotranspiration (EVT) Packages. The only Hydrologic/Advanced Stress Package used in the numerical model was the Streamflow Routing (SFR) Package. The WEL Package was used to simulate groundwater withdrawal from wells in the model area, the RCH Package was used to represent infiltration from precipitation in the model area, the EVT Package was used to represent ETg in the model area, and the River (RIV), Drain (DRN), and SFR Packages were used to represent the surface-water features in the model area. All available Hydrologic/Stress and Hydrologic/Advanced Stress Packages, including those that are not used in the numerical model, are described in Langevin and others (2017).

MODFLOW–6 Output Packages were used to generate output files associated with the numerical model simulation. The output files that were generated included hydraulic head and cell-by-cell flow terms for steady-state conditions and for each month of the simulation and are available in the accompanying data release (Eldridge and Davis, 2019). Additionally, Output Packages were used to generate time-series outputs for hydraulic head and streamflow.

Spatial and Vertical Discretization

The model area was spatially discretized with a grid consisting of square cells of uniform size that measured 200 ft on each side. The grid contained 260 columns (oriented north-south) and 675 rows (oriented east-west). About 196,400 cells were active in the model area (fig. 16). The projection used for geospatial data management was North American Datum, Universe Transverse Mercator, zone 14 north. The northwest corner of the model area was 2,211,800 ft north and 15,931,600 ft west. Numerical model spatial units were in feet.

The numerical model was vertically discretized into three layers based on the delineation of the aquifers and confining unit identified in the hydrogeologic framework. Model layer 1 represented the Big Sioux aquifer, layer 2 represented the glacial till deposits (glacial till confining unit), and layer 3 represented underlying bedrock aquifers. Model layer 1 represented the primary aquifer in the model area, layer 2 primarily represented a confining unit, and layer 3 was included as a secondary aquifer and was used to account for small amounts of interflow that may exist where the layer is directly connected to the overlying layers.

The spatial and vertical extent of layer 1 was primarily determined from geophysical investigations. Mapped surficial geology and aquifer presence identified in lithologic logs in the model area were secondary indicators of the spatial and vertical extent of layer 1. Model layer 2 existed throughout the model area except where quartzite was exposed at the land surface, or where the bedrock aquifers directly underlie the Big Sioux aquifer (figs. 6 and 16). The vertical extent of layer 2 was determined based on geophysical investigations and lithologic logs in the model area. Model layer 3 existed throughout the model area and was determined primarily based on mapped geology and lithologic logs. The extent of each model layer (fig. 16) was generalized to include potential areas of saturation in the model area. Parts of model layer 2 (the glacial till confining unit) were nonexistent between model layers 1 (Big Sioux aquifer) and layer 3 (bedrock aquifers) and were designated as “vertical pass-through” or “pinched” cells in the numerical model (fig. 16). In areas where layer 2 is “pinched,” MODFLOW–6 directly connects the overlying and underlying cells and effectively removes them from the numerical solutions of groundwater flow (Langevin and others, 2017). Active areas of each model layer were assigned a minimum thickness of 10 ft to help with model stability.

The top of the numerical model was representative of the mean land-surface altitude in each model cell. The mean land-surface altitude was determined based on a DEM for the model area (U.S. Geological Survey, 2017) and was assigned to the top of the uppermost active cell in the numerical model (fig. 16). The base of model layers 1 and 2, which represented the Big Sioux aquifer and glacial till confining unit, respectively, was determined primarily based on the interpretation of an AEM survey (Valseth and others, 2018). In areas where the AEM survey did not provide enough information for the delineation of the base of the Big Sioux aquifer and the base of the glacial till confining unit, aquifer and till presence identified in well logs (South Dakota Department of Environment and Natural Resources, 2018b) were used to determine the base of the Big Sioux aquifer and the glacial till confining unit. The base of model layer 3 was set to an arbitrary altitude

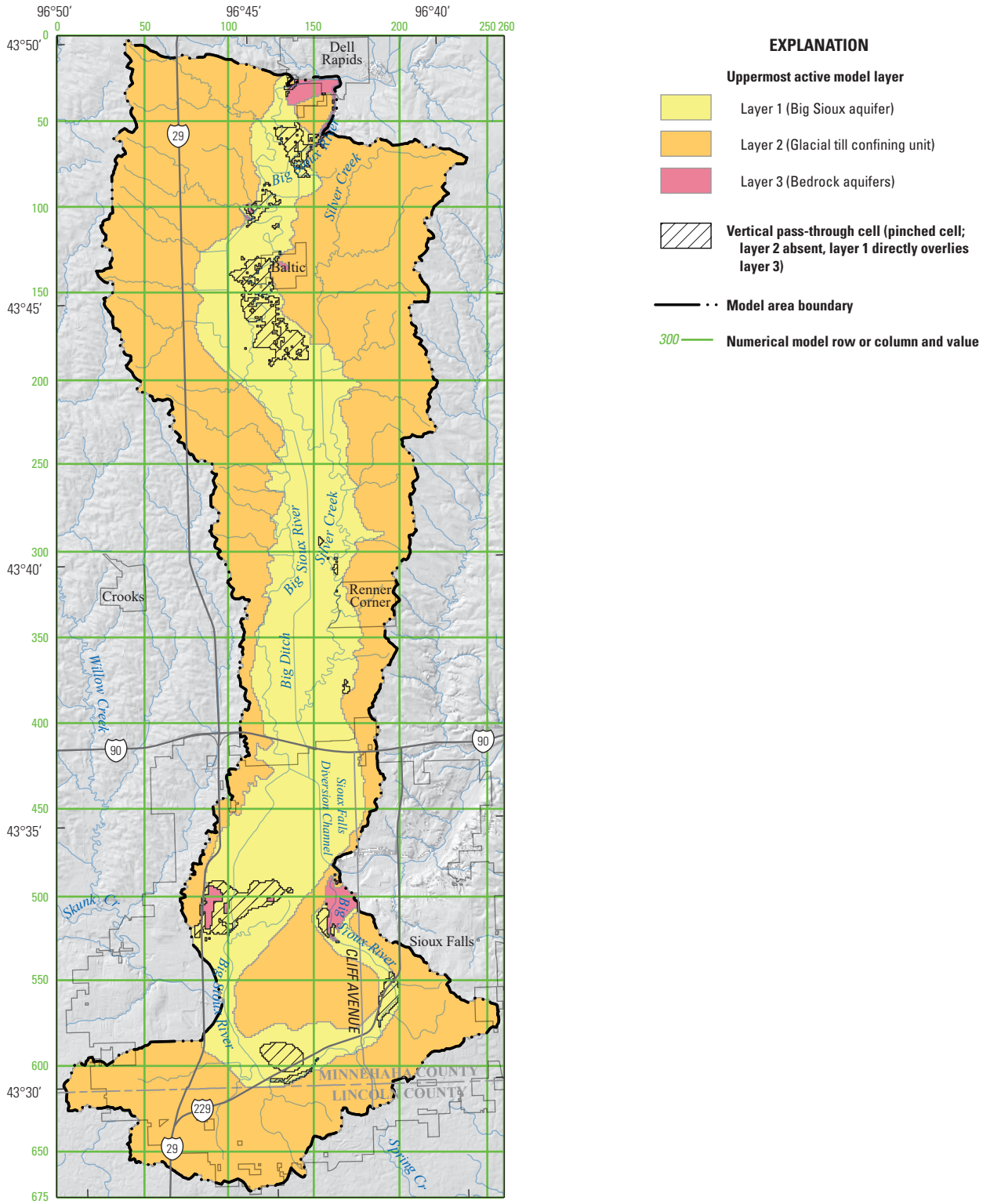

Figure 16. MODFLOW representation of hydrogeologic units and numerical model row and column locations.

of 850 ft. Altitudes of the top and bottom of each layer used in the numerical model are available in the accompanying USGS data release (Eldridge and Davis, 2019).

Temporal Discretization

The numerical model was temporally discretized into steady-state and transient stresses using blocks of time called "stress periods," within which all hydrologic stresses are constant and numerical model output applies to the end of each stress period. The numerical model was discretized into 817 stress periods. The first stress period was simulated in steady-state mode and was representative of predevelopment conditions before 1950 (steady-state) during which change in aquifer storage was not considered. Groundwater withdrawal before 1950 was not substantial; therefore, hydrologic stresses for 1949 were assumed to adequately represent steady-state conditions in the model area and were appropriate for providing initial conditions for the transient stress periods. The remaining 816 stress periods were simulated in transient mode and represented monthly conditions for 1950–2017. Aquifer stresses during the transient stress periods were representative of the mean of hydrologic stresses during each month. Aquifer storage was considered during the transient formulations of the groundwater-flow equation calculated by MODFLOW–6. The numerical model was constructed using temporal units of days.

Hydrogeologic Properties

Initial values and distributions of hydrogeologic properties for the numerical model were determined from geophysical investigations, slug tests, and previously published estimates. Geophysical investigations were used to approximate the horizontal variation in hydraulic properties and assign initial values in the numerical model. The spatial variation of resistivity of the Big Sioux aquifer at a depth of 21 ft (7 meters) from Valseth and others (2018) was assumed to adequately represent the horizontal variation of hydraulic conductivity in the Big Sioux aquifer.

A method was developed to interrogate the spatial distribution of resistivity in the Big Sioux aquifer from Valseth and others (2018) and apply that distribution to a subset of points (pilot points) from which values of hydraulic conductivity were interpolated to the numerical model grid. A set of pilot points were evenly distributed in the model area and were used to interrogate resistivity for the Big Sioux aquifer at each point. The method of kriging was used to generate a semivariogram for the resistivity values at pilot point locations that corresponded to the distribution of resistivity for the Big Sioux aquifer. Representative values of horizontal hydraulic conductivity from slug test (Eldridge and Medler, 2019) and NMR measurement locations (appendix 1) were used to create a relation between measured horizontal hydraulic conductivity and specific values of resistivity. The relation between measured horizontal hydraulic conductivity and resistivity was used to create an initial grid of horizontal hydraulic conductivity for the part of the model area that corresponded to the resistivity survey of Valseth and others (2018), and initial horizontal hydraulic conductivity at pilot points was extracted from this grid. Pilot points outside the resistivity survey from Valseth and others (2018) were assigned a horizontal hydraulic conductivity of 140 ft/d. Using the method of kriging and the semivariogram, the values of hydraulic conductivity were interpolated to the numerical model grid from the initial pilot point values. Hydraulic conductivity pilot points also were generated for model layers 2 and 3 and were distributed in each layer with densities proportional to the number of water-level observations in that layer. Additional pilot points were added at the sites where borehole geophysical methods were used to estimate hydraulic conductivity (fig. 17).

Initial values for horizontal and vertical hydraulic conductivity pilot points in each layer were set based on slug tests and geophysical investigations and were allowed to change during numerical model calibration. Initial values of horizontal hydraulic conductivity at pilot points for the Big Sioux aquifer (layer 1) ranged from 85.5 to 877.0 ft/d (table 6). Horizontal hydraulic conductivity pilot points for the glacial till confining unit (layer 2) and the bedrock aquifers (layer 3) were initially set to uniform values of 5.0 and 2.5, respectively (table 6). Vertical hydraulic conductivity values for all layers were initially assigned to about 10 percent of the horizontal hydraulic conductivity at the same location.

Aquifer storage properties consisted of specific yield and specific storage and were specified as constant for each model layer. Aquifer storage properties only were used during the formulations of the groundwater-flow equation during the transient part of the simulation. Initial values (table 6) were assigned based on literature values (table 3) and were adjusted further during numerical model calibration. Initial values of specific yield (dimensionless) used in the numerical model for the Big Sioux aquifer (layer 1), glacial till confining unit (layer 2), and bedrock aquifers (layer 3) were 0.12, 0.05, and 0.16, respectively (table 6). Initial values of specific storage (per foot) for layers 1, 2, and 3 were 7.25×10^{-5}, 3.0×10^{-7}, and 4.5×10^{-7}, respectively (table 6).

Boundary Conditions

Aquifer stresses in the numerical model were simulated using various MODFLOW–6 Hydrologic/Stress and Hydrologic/Advanced Stress Packages. Lateral and lower numerical model boundaries were simulated as no-flow boundaries and no specific package was used. Recharge from infiltration of precipitation in the model area was simulated using the RCH Package; direct ETg was simulated using the EVT Package; groundwater withdrawal was simulated using the WEL Package; and the interaction of groundwater and surface-water in the model area was simulated using RIV, DRN, and SFR Packages. Complete descriptions of MODFLOW–6 Hydrologic/Stress and Hydrologic/Advanced Stress Packages are available in Langevin and others (2017). The implementation of

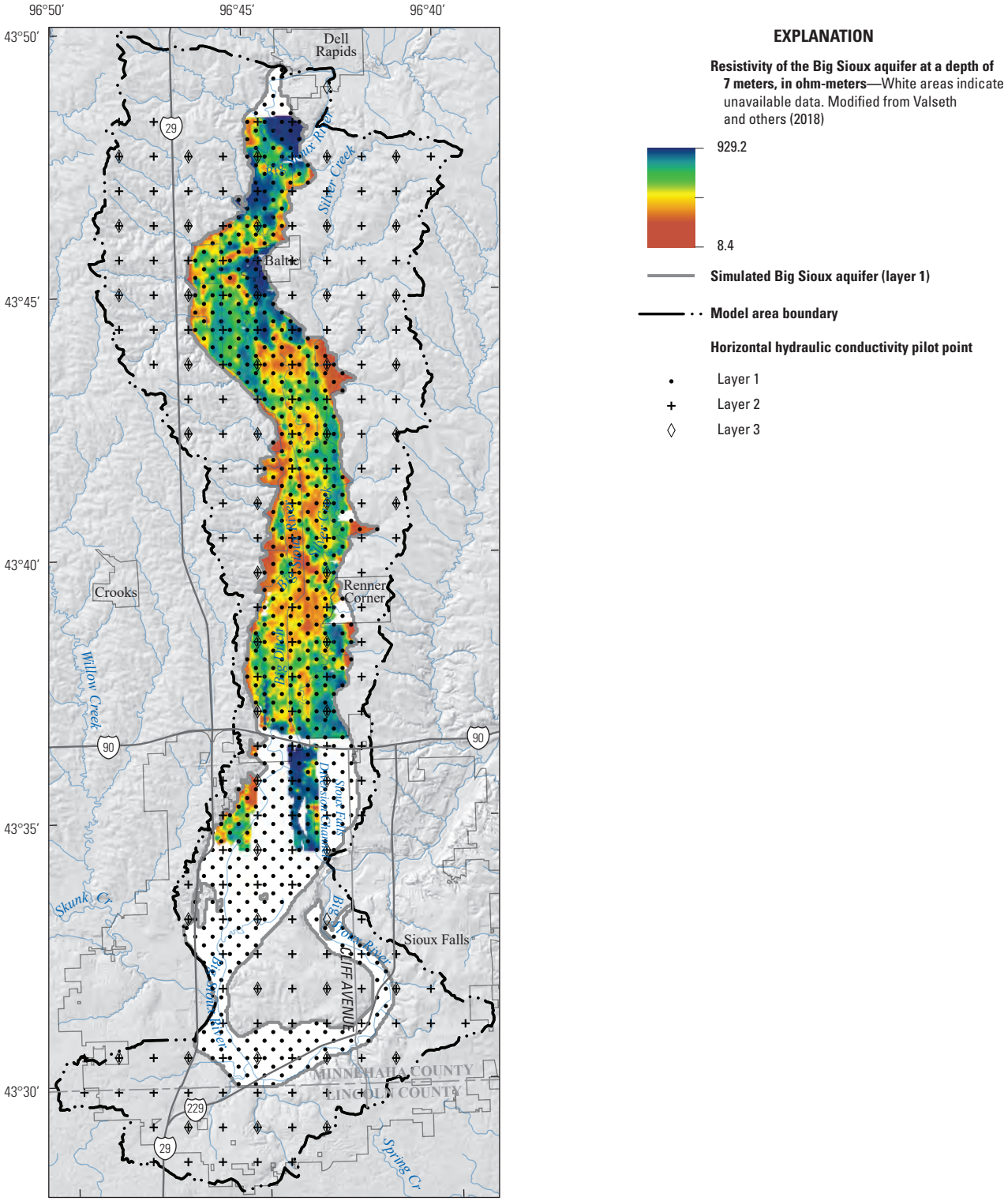

Figure 17. Spatial distribution of pilot points by model layer and distribution of resistivity of the Big Sioux aquifer.

Table 6. Summary of initial hydrologic property values assigned in the numerical model.

[*n*, number of unique adjustable values applied in model; ft/d, foot per day; ft, foot; --, not applicable]

Property	Model application	MODFLOW Package	Units	*n*	Minimum	Maximum	Mean
Big Sioux aquifer (layer 1)							
Horizontal hydraulic conductivity	Pilot points	Node Property Flow	ft/d	597	85.5	877.0	154.91
Vertical hydraulic conductivity	Pilot points	Node Property Flow	ft/d	284	10.5	65.2	15.16
Specific storage	Uniform in layer	Storage	per ft	--	--	--	7.25×10^{-5}
Specific yield	Uniform in layer	Storage	Dimensionless	--	--	--	0.12
Glacial till confining unit (layer 2)							
Horizontal hydraulic conductivity	Pilot points	Node Property Flow	ft/d	198	5.0	5.0	5.0
Vertical hydraulic conductivity	Pilot points	Node Property Flow	ft/d	198	0.5	0.5	0.5
Specific storage	Uniform in layer	Storage	per ft	--	--	--	3.0×10^{-7}
Specific yield	Uniform in layer	Storage	Dimensionless	--	--	--	0.05
Bedrock aquifers (layer 3)							
Horizontal hydraulic conductivity	Pilot points	Node Property Flow	ft/d	51	2.5	2.5	2.5
Vertical hydraulic conductivity	Pilot points	Node Property Flow	ft/d	51	0.25	0.25	0.25
Specific storage	Uniform in layer	Storage	per ft	--	--	--	4.5×10^{-7}
Specific yield	Uniform in layer	Storage	Dimensionless	--	--	--	0.16
Undifferentiated							
Streambed hydraulic conductivity	Uniform between stream confluences	Streamflow Routing, River, and Drain	ft/d	91	0.05	0.05	0.05

MODFLOW–6 Hydrologic/Stress and Hydrologic/Advanced Stress Packages in the numerical model is described in this section.

Lateral and Lower Boundaries

No-flow cells were assigned in the numerical model where the aquifers were nonexistent and at the edge of the Big Sioux River Basin (Eldridge and Davis, 2019). No-flow boundaries were assigned to layer 1 where the glacial till confining unit (layer 2) or bedrock aquifers (layer 3) were the uppermost active layers in the model area. The groundwater drainage basin was assumed to be coincident with the surface-water drainage basin in the model area; therefore, no-flow boundaries were assigned to layers 2 and 3 along the drainage basin boundary. The base of the numerical model also was represented with no-flow boundaries.

South of Dell Rapids and south of the Sioux Falls Regional Airport, subsurface ridges of Sioux Quartzite restrict groundwater flow in the Big Sioux aquifer (fig. 6). The Sioux Quartzite ridge near Dell Rapids was used to define the northern-most boundary of the numerical model. The Sioux Quartzite ridge south of the Sioux Falls Regional Airport was included in the numerical model; however, the model area extends south and east of the Sioux Quartzite ridge to include a full routing of the stream network in the numerical model bounded by USGS streamgages 06481000, 06481500, and 06482020.

Precipitation Recharge

Recharge from infiltration of precipitation on the land surface was simulated using the RCH Package. The RCH Package is designed to simulate aerially distributed recharge to the groundwater system (Langevin and others, 2017). The rate of recharge is specified for each stress period in units of feet per day, and the rate is multiplied by the cell horizontal area to obtain the recharge flow rate for each numerical model cell (Langevin and others, 2017). Spatially distributed recharge rates were estimated using the SWB model, described in the "Water Budget" section of this report and in appendix 2, and were used as initial estimates of recharge for the numerical model.

The SWB-calculated spatially distributed mean daily recharge rate for 1949 was used for the steady-state stress period in the numerical model and was assumed to adequately represent the spatial distribution of predevelopment recharge (fig. 11). Spatially distributed SWB-calculated monthly recharge rates were applied for the transient part of the simulation for 1950–2017. The SWB-calculated recharge rates, for steady-state and transient conditions, were adjusted during numerical model calibration using a single recharge multiplier and is described in the "Numerical Model Calibration Approach" section of this report. Spatially distributed estimates of monthly recharge used in the numerical model are available in the accompanying USGS data release (Eldridge and Davis, 2019).

Evapotranspiration from Groundwater

The ETg from direct evaporation of groundwater and from plant transpiration was simulated using the EVT Package. The EVT Package simulates the effects of plant transpiration and direct evaporation by removing water from the saturated groundwater regime (Langevin and others, 2017). ETg simulation was based on the following assumptions (Langevin and others, 2017): (1) when the water table is at or above a specified altitude (called the "ET surface" in this report), ETg loss is at a specified fixed rate; (2) when the depth of the water table below the ET surface exceeds a specified value (called the "extinction depth" in this report), ETg ceases; and (3) when between the "ET surface" and the "extinction depth," ETg varies in a piecewise-linear fashion with water-table altitude.

The rate of evapotranspiration was specified for each stress period in units of feet per day and represents PET in the model area, defined in the "Water Budget" section of this report. The PET rates are multiplied by the horizontal cell areas to obtain the PET flow rate for each numerical model cell (Langevin and others, 2017). The ET surface in the numerical model was set equal to the top of the model. Extinction depth was based on soil types and land covers. Extinction depths were initially calculated based the land cover and soil type for each model cell and assigned a value based on extinction depths reported by Shah and others (2007). Soil types were assigned to the soil categories used in the SWB model with sandy loam corresponding to soil type 1, loam corresponding to soil type 2, silt-loam corresponding to soil type 3, silt corresponding to soil type 4, and silty clay loam corresponding to soil type 5. Land cover types used for the SWB model were combined into the following three categories: bare soil, grass, and forest. A value that represented the intersection of soil type and land cover in each model cell was assigned an extinction depth from the same intersection listed by Shah and others (2007).

Spatially distributed PET rates were estimated using the SWB model, described in the "Water Budget" section of this report and in appendix 2 and were used as initial estimates of PET for the numerical model. The SWB-calculated spatially distributed annual PET rate for 1949 was used for the steady-state stress period in the numerical model and was assumed to adequately represent the spatial distribution predevelopment evapotranspiration (fig. 11). Spatially distributed SWB-calculated monthly PET rates were applied for the transient part of the simulation for 1950–2017. The spatially distributed SWB-calculated steady-state and transient PET rates were adjusted during numerical model calibration using a single evapotranspiration multiplier, described in the "Numerical Model Calibration Approach" section of this report. Spatially distributed estimates of PET used in the numerical model are available in the accompanying USGS data release (Eldridge and Davis, 2019).

Groundwater Withdrawal

Groundwater withdrawal from wells in the model area was simulated using the WEL Package (fig. 13). The WEL Package is designed to simulate features such as wells that withdraw water from or add water to the aquifer at a specified rate during a stress period, where the rate is independent of the cell area and the head in the cell (Langevin and others, 2017).

Groundwater withdrawal rates were specified for each stress period in units of cubic feet per day. Groundwater withdrawal before 1950 was assumed to be minimal; therefore, no withdrawals were specified during the steady-state stress period. Monthly mean groundwater withdrawal rates for municipal supply were assigned to the transient stress periods for 1950–2017. Groundwater withdrawal for irrigation, stock, and domestic uses existed in the model area but were small in comparison to all other water budget components; therefore, groundwater withdrawal for these uses was not included in the numerical model. Production well locations were converted to the equivalent model row, column, and layer coordinates. Simulated production well withdrawals are available in the accompanying USGS data release (Eldridge and Davis, 2019).

The WEL Package has an option to reduce the withdrawal rate of a well as the water-table altitude in the cell approaches the cell bottom. The flow reduction option is activated when the saturated cell thickness is less than a percentage of the cell thickness (Langevin and others, 2017). A uniform percentage of cell thickness was applied to the numerical model of 10 percent.

Surface-Water Features

Surface-water features in the model area contribute water to, or drain water from, the groundwater system, depending on the hydraulic head gradient between the feature and the groundwater regime. Streams and rivers were the only surface-water features represented in the numerical model and were categorized into the following two types: nonrouted streams and routed streams. Nonrouted streams were simulated using the RIV and DRN Packages, and routed streams were simulated using the SFR Package (Langevin and others, 2017; Langevin and others, 2018).

Routed streamflow for the Big Sioux River, its tributaries, and diversions between USGS streamgages 06481000 (Big Sioux River near Dell Rapids, S. Dak.) and 06482020 (Big Sioux River at North Cliff Avenue at Sioux Falls, S. Dak.) was simulated using the SFR Package (fig. 13). The SFR Package uses the continuity equation and assumption of piecewise steady (nonchanging in discrete periods), uniform (nonchanging in location), and constant-density streamflow. This assumption ensures that during all times, volumetric inflow and outflow rates are equal, and no water is added to or removed from storage in the surface channels, and the numerical model routes streamflow through a network of rectangular channels (which may include rivers, streams, canals, and ditches, and are referred to collectively as reaches in the remainder of the report; Langevin and others, 2017). In addition to calculating streamflow, the SFR Package also calculates the river/aquifer seepage.

The stream network represented by the SFR Package was divided into reaches with each reach representing a section of a stream that corresponds to a specific model cell (Langevin and others, 2017). Reaches were numbered sequentially beginning at USGS streamgage 06481000 and ending at USGS streamgage 60482020 (fig. 13). The sequential numbering provided a reference for routing surface-water flow among the SFR reaches. Attributes required for each SFR reach were length, width, gradient, top altitude of the streambed, streambed hydraulic conductivity, streambed thickness, and Manning's roughness coefficient of the stream channel. Stream length and width and streambed top altitude and thickness were assigned in units of feet, river gradients were assigned in units of feet per foot, streambed hydraulic conductivity values were assigned in units of feet squared per day, and Manning's roughness coefficients were unitless. Additional information used in the SFR Package included surface-water inflow to SFR reaches at USGS streamgages 06481000 and 06481500.

SFR reaches were assigned to the highest active numerical model layer. The length of each SFR reach was calculated using geographic information systems (GIS) geoprocessing tools by intersecting the stream features with the model grid, and the width of each SFR reach was estimated from aerial imagery (Esri, 2018). The stream network in the model area was segmented at river, tributary, or diversion confluences (hereafter referred to as "segments;" fig. 13). The length of each segment was calculated using GIS geoprocessing tools, and the upstream and downstream altitude of each segment were determined based on a DEM for the model area (U.S. Geological Survey, 2017). Downstream altitudes that were either equal to or higher than upstream altitudes, as determined from the DEM, were manually adjusted and set equal to 0.1 ft below the upstream altitude. The upstream and downstream altitudes and length of each segment were used to calculate river gradients for each SFR reach. River gradients less than 1.0×10^{-4} feet per foot were assigned a minimum gradient of 1.0×10^{-4} feet per foot. The upstream and downstream altitudes, length of each segment, and length of each SFR reach were used to calculate the riverbed top for midpoint of each SFR reach. Riverbed thicknesses for each SFR reach were assigned a uniform value of 1.0 ft. If the riverbed bottom altitude for individual SFR reaches (calculated by subtracting riverbed thickness from top altitude) was below the bottom of the uppermost active layer, the layer bottom altitude for that cell was assigned to 1.0 ft below riverbed bottom altitude. Subsequent layers were assigned a minimum thickness of 10.0 ft if needed. In some cases, this method produced reach altitudes that were above the top of the model layer to which the reach was assigned. The reach altitudes that were above the top of the numerical model were manually adjusted to ensure the altitude was below the top of the numerical model layer to which each reach was assigned. SFR reaches were initially assigned a uniform riverbed hydraulic conductivity of 0.05 ft/d, but this value was adjusted during numerical model calibration and is described in the "Numerical Model Calibration Approach" section of this report.

The mean streamflows for 1949 were used as stream inflows at USGS streamgages 06481000 (Big Sioux River near Dell Rapids, S. Dak.) and 06481500 (Skunk Creek at Sioux Falls, S. Dak.) for the steady-state stress period because 1949 was the earliest complete annual streamflow record available before the start of the transient numerical model. The mean daily streamflow for each month was used as stream inflow for the transient part of the simulation (1950–2017). Streamflow data were not available for USGS streamgage 06481500 from October 2001 through September 2003. The mean monthly fraction of streamflow between USGS streamgages 06481500 and 06481000 was used to estimate the inflow rates during the times of unavailable streamflow measurements (table 7). The fraction of streamflow was normalized to the streamflow at USGS streamgage 06481000 and then extrapolated to fill in the missing months of streamflow measurements at USGS streamgage 06481500.

The SFR Package also simulated streamflow diverted at two locations on the Big Sioux River called the wetlands pump and the Sioux Falls Diversion Dam and Weir (fig. 1). The monthly mean diversion rate from the Big Sioux River at wetlands pump was estimated based on records provided by the city of Sioux Falls (Tim Stefanich, Water Division Environmental Engineer, city of Sioux Falls, written commun., 2018) and was typically operated in the summer. Streamflow diverted at the Sioux Falls Diversion Dam and Weir was assumed to begin in June 1961. The diversion rate was set to a minimum of 200 ft^3/s. If streamflow immediately upstream from the diversion was less than 200 ft^3/s, then all streamflow was routed into the diversion and no streamflow remained in the Big Sioux River. Diverted streamflow values greater than 200 ft^3/s were calculated using the streamflow balancing method described in this section.

The Sioux Falls Diversion Channel streamflow was estimated using a method of balancing streamflow in the model area based on streamflow at USGS streamgages 06481000, 06481500, and 06482000. This method was necessary because streamflow was not recorded in the diversion, and nearby streamgage records did not have streamflow records available

Table 7. Mean monthly streamflow fractions applied to monthly streamflow at U.S. Geological Survey streamgage 06481000 (Big Sioux River near Dell Rapids, South Dakota) to estimate streamflow at U.S. Geological Survey streamgage 06481500 (Skunk Creek at Sioux Falls, S. Dak.) during periods without records.

Month	Streamflow fraction[a] (percent)
January	15
February	31
March	32
April	18
May	20
June	19
July	15
August	25
September	19
October	18
November	16
December	16

[a]Mean monthly streamflow at U.S. Geological Survey streamgage 06481000 divided by the mean monthly streamflow at U.S. Geological Survey streamgage 06481500 for January 1949 through September 2001 and October 2003 through December 2017.

for the model period. Equation 1 is the basic streamflow balance equation used to estimate streamflow in the Sioux Falls Diversion Channel.

$$Q_{div} = Q_{dr} + Q_{sk} + dQ - Q_{sf} \quad (1)$$

where

Q_{div} is the daily mean streamflow in the Sioux Falls Diversion Channel, in cubic feet per second;

Q_{dr} is the daily mean streamflow at USGS streamgage 06481000 (Big Sioux River near Dell Rapids, S. Dak.), in cubic feet per second;

Q_{sk} is the daily mean streamflow at USGS streamgage 06481500 (Skunk Creek at Sioux Falls, S. Dak.), in cubic feet per second;

dQ is the estimated daily mean combined streamflow gains and losses in the system, in cubic feet per second; and

Q_{sf} is the daily mean streamflow at USGS streamgage 06482000 (Big Sioux River at Sioux Falls, S. Dak.), in cubic feet per second.

The mean monthly value for dQ was estimated from daily streamflow records measured before installation and operation of the Sioux Falls Diversion Dam and Weir and the Sioux Falls Diversion Channel in 1961. During this time, *Qdiv* is zero because the diversion was not yet constructed, and equation 1 reduces to the following:

$$dQ = Q_{sf} - Q_{dr} - Q_{sk}. \quad (2)$$

Daily Q_{sf}, Q_{dr}, *and* Q_{sk} values were used to calculate a daily dQ value for the period when daily records were available at all three USGS streamgages. The daily dQ values were averaged by month (table 8). These mean monthly dQ values were then applied to all numerical model stress periods lacking a dQ value.

From 1960 through 2004, streamflow records were not available at USGS streamgage 06482000 (Big Sioux River at Sioux Falls, S. Dak.), and the Sioux Falls Diversion Channel discharge rate could not be calculated with equation 2 for this period. To estimate the streamflow in the diversion channel during 1960–2004, a ratio was calculated during the period when records were available for the three streamgages (2004–17). The ratio related the streamflow in the Sioux Falls Diversion Channel to the total streamflow in the system, using the following equation:

$$X = \frac{Q_{div}}{Q_{dr} + Q_{sk} + dQ} \quad (3)$$

where

X is the ratio of the streamflow in the Sioux Falls Diversion Channel to the combined streamflow at USGS streamgages 06481000 and 06481500 and the total streamflow gains and losses.

The mean monthly ratio of streamflows at each USGS streamgage were used for equation 3 (table 9). Negative or zero values of X were not used in the mean.

The mean monthly values for X and dQ were used to estimate the streamflow in the Sioux Falls Diversion Channel during the period of the numerical model using the following equation:

$$Q_{div} = X * (Q_{dr} + Q_{sk} + dQ). \quad (4)$$

The minimum Sioux Falls Diversion Channel streamflow was set to a value of 200 ft^3/s based on standard operating procedures used by the city of Sioux Falls. From equation 4, the maximum streamflow in the diversion was 6,743 ft^3/s in April 1997 and the mean was 505 ft^3/s.

The second diversion simulated was the wetlands pump (fig. 1). The monthly mean withdrawal diversion rate from the Big Sioux River at the wetlands pump was estimated based on 60 percent pump efficiency using the single operating rate of 7,000 gal/min and the time the pump was operated each month (Tim Stefanich, Environmental Engineer, city of Sioux Falls, written commun., 2018; fig. 18).

The Big Sioux River and the tributaries upstream from USGS streamgage 06481000 were simulated as nonrouted

Table 8. Mean monthly estimates of streamflow gain and loss before 1961 for the Big Sioux River near Sioux Falls, South Dakota downstream from U.S. Geological Survey streamgages 06481000 (Big Sioux River near Dell Rapids, South Dakota) and 06481500 (Skunk Creek at Sioux Falls, South Dakota) and upstream from U.S. Geological Survey streamgage 06482000 (Big Sioux River at Sioux Falls, South Dakota).

[Negative values indicate streamflow loss. Positive values indicate streamflow gain. ft^3/s, cubic foot per second]

Month	Streamflow gain or loss (ft^3/s)
January	2.1
February	2.2
March	−36.5
April	−102.6
May	14.5
June	27.6
July	14.6
August	3.0
September	6.6
October	3.2
November	0.5
December	2.6

Table 9. Mean monthly ratio of streamflow in the Sioux Falls Diversion Channel to the total streamflow in the model area.

Month	Ratio[a] (percent)
January	69.9
February	70.1
March	70.5
April	71.1
May	69.9
June	65.5
July	59.1
August	50.3
September	53.5
October	51.3
November	55.2
December	65.7

[a]Streamflow in the Sioux Falls Diversion Channel divided by combined streamflow at Dell Rapids, Skunk Creek, and combined stream gain and loss for the period between 2004 and 2017; *X* in equation 3.

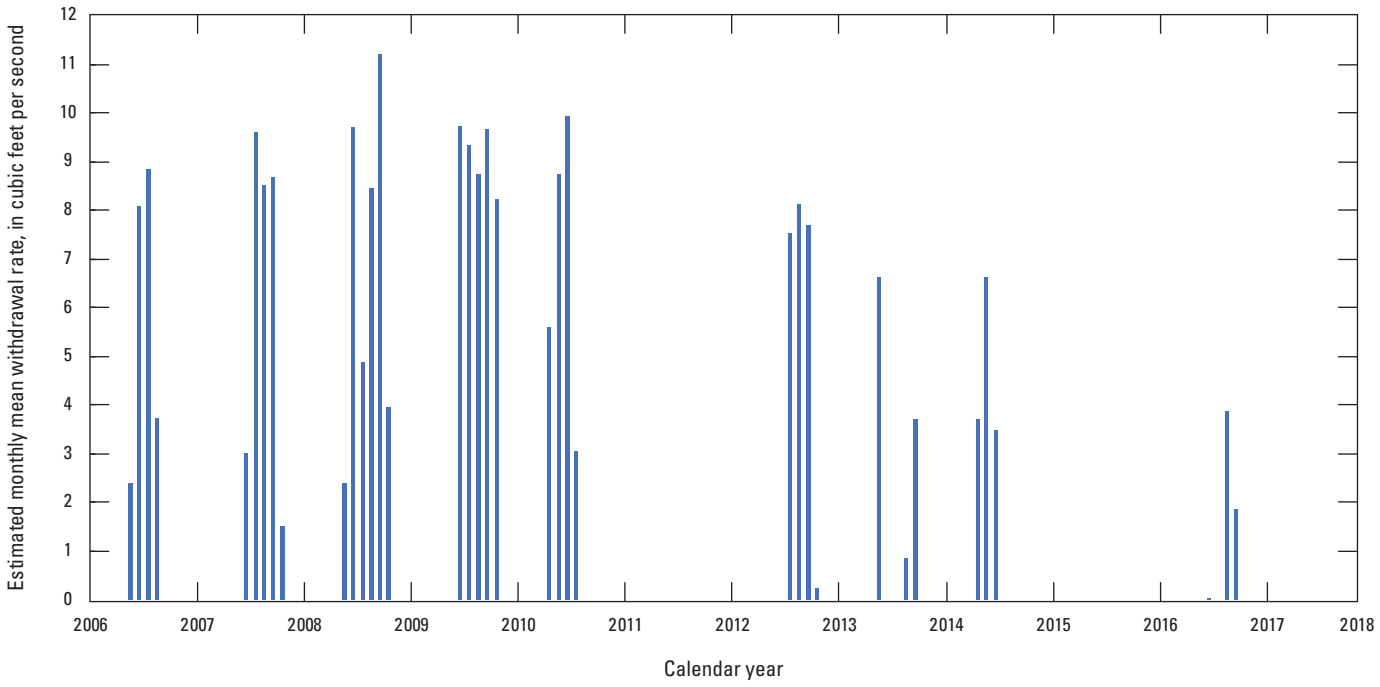

Figure 18. Estimated monthly mean withdrawal rates diverted into Big Ditch by the wetlands pump about 5 miles north of Sioux Falls, South Dakota, near the Big Sioux River.

streams using the RIV and DRN Packages, respectively (Langevin and others, 2017). The Big Sioux River and its tributaries upstream from USGS streamgage 06481000 were not simulated as routed streams using the SFR Package because surface-water inflow, a required input for the SFR Package, was not known for this part of the Big Sioux River. The purpose of the RIV Package is to simulate the effects of flow between surface-water features and groundwater systems; however, the RIV Package does not simulate surface-water flow in the river—only the river/aquifer seepage (Langevin and others, 2017). The Big Sioux River upstream from USGS streamgage 06481000 was simulated using the RIV Package and not the DRN Package (for the west and east branch; fig. 13) because the Big Sioux River is a perennial river and during the numerical model period, was assumed to contain water during every stress period. Ephemeral tributaries to the Big Sioux River upstream from USGS streamgage 06481000 were simulated using the DRN Package. The DRN Package is designed to simulate the effects of agricultural drains, springs, and other features that remove water from the aquifer at a rate proportional to the difference between the hydraulic head in the aquifer and some fixed head or altitude, called the drain altitude, only if the hydraulic head in the aquifer is above that altitude. If, however, the aquifer hydraulic head falls below the drain altitude, then the drain has no effect on the aquifer (Langevin and others, 2017). Tributaries to the Big Sioux River upstream from USGS streamgage 06481000 were simulated using the DRN Package and not the RIV Package because of the assumption that these streams do not contain surface water during all stress periods in the numerical model period.

The RIV Package was assigned to cells that intersected the west and east segments of the Big Sioux River upstream from USGS streamgage 06481000 (Big Sioux River near Dell Rapids, S. Dak.) and were assigned to the top numerical model layer in the cell (fig. 13). Attributes required to define each model cell simulated by the RIV Package (RIV cell) were the top altitude of the river bed, in feet above North American Vertical Datum of 1988 (NAVD 88); the stream stage altitude, in feet above NAVD 88; and conductance of the riverbed material, in feet squared per day. River bed top altitudes for each RIV cell were estimated by calculating a change in altitude for each RIV cell. The change in altitude per RIV cell was estimated by calculating the difference between the altitudes of the top of model cells at (1) the inlet of the Big Sioux River at the northern numerical model boundary and (2) the USGS streamgage 06481000 (determined from DEM; Gesch, 2007; Gesch and others, 2002; U.S. Geological Survey, 2017) and dividing by the number of RIV cells in each segment. The altitude change was applied to each RIV cell starting upstream from the RIV cell at USGS streamgage 06481000 and ending at the numerical model boundary. To assign the stream stage altitude to each RIV cell during the numerical model period, miscellaneous measurements of stream stage at streamgage 06481000 from USGS, recorded from January 13, 1950, to January 1, 2018 (U.S. Geological Survey, 2018), were used as a reference stream stage. The stream stage was calculated for each RIV cell upstream from USGS streamgage 06481000 using a stream stage multiplier to ensure that the stream stage was slightly shallower in upstream RIV cells than in downstream RIV cells. The stream stage multiplier was calculated by dividing the riverbed top altitude of the RIV cell at USGS streamgage 06481000 by the river bed top altitude for each RIV cell and applied to the altitude of the reference stream stage. Using this approach, the stream stage was calculated for each numerical model stress period and was applied to the riverbed top to calculate the stream stage altitude for each RIV cell. Conductance of the river bed material was calculated for each RIV cell using equation 5.

$$C_{nb} = \frac{K_{nb} L_{nb} W_{nb}}{b_{nb}} \tag{5}$$

where

C_{nb} is the hydraulic conductance of the streambed material, in feet squared per day;

K_{nb} is the hydraulic conductivity of the streambed material, in feet per day;

L_{nb} is the length of the stream as it crosses the cell, in feet;

W_{nb} is the width of the stream in the cell, in feet; and

b_{nb} is the thickness of the streambed material, in feet.

Hydraulic conductivity of the riverbed material was assigned an initial value of 0.05 ft/d. Separate riverbed hydraulic conductivity parameters were used for the west and east branches of the Big Sioux River upstream from USGS streamgage 06481000 and were allowed to adjust during numerical model calibration, discussed in the "Numerical Model Calibration Approach" section. The length of the river in each cell was calculated using GIS geoprocessing tools by intersecting the stream features with the numerical model grid. The width of river cells was estimated from aerial imagery. Upstream from USGS streamgage 06481000, all cells in the west branch of the Big Sioux were assigned a width of 155 ft and all cells in the east branch were assigned a width of 120 ft. Riverbed thickness was set to an arbitrary thickness of 1 ft for all cells.

The DRN Package was assigned to cells that intersected the Big Sioux River tributaries upstream from USGS streamgage 06481000 and was assigned to the top numerical model layer in the cell (fig. 13). Attributes required to define each numerical model cell simulated by the DRN Package (DRN cell) were drain altitude, in feet above NAVD 88, and conductance of the drain bed (streambed) material, in feet squared per day. The DRN Package in the numerical model was used to represent ephemeral streams; therefore, conductance was calculated for each DRN cell using equation 5. Drain altitudes were determined based on a DEM for the model area and were assigned based on the minimum DEM altitude in each DRN cell. Hydraulic conductivity of

the drain bed material was initially assigned a uniform value of 0.05 ft/d. All drains were assigned to a single drain bed hydraulic conductivity parameter and were allowed to adjust during numerical model calibration, described in the "Numerical Model Calibration Approach" section. The length of the drain in each cell was calculated using GIS geoprocessing tools by intersecting the stream features with the numerical model grid. Drain lengths in each cell ranged from about 10 to 340 ft. The width of river cells was estimated from aerial imagery and was 10 ft for all DRN cells. Drain bed thickness was set to an arbitrary thickness of 1.0 ft for all cells.

Numerical Model Calibration Approach

Model calibration is the process of estimating numerical model parameters to minimize the differences, or residuals, between hydraulic observations of interest and numerical model outputs. The hydraulic observations of interest that are used in model calibration hereafter are referred to as calibration targets. Together, all calibration targets are contained in the calibration dataset. Numerical model calibration was completed using the software package PEST++ version 4.1.12 (Welter and others, 2015). The model calibration process, using PEST++, completes a single numerical model simulation using a user-defined set of input parameters and compares numerical model outputs to the calibration dataset. Subsequent numerical model runs are applied with small changes in input parameters, and the numerical model outputs again are compared with the calibration dataset. The PEST++ software mathematically determines which input parameters to adjust to provide a better match between the calibration dataset and the numerical model outputs. The PEST++ software continues the process until the optimal set of input parameters is obtained, which provides the statistically best comparison of numerical model outputs and the calibration dataset. The transient numerical model was calibrated for steady-state and transient monthly conditions for 1950–2017. Calibration targets were observations of hydraulic head, changes in hydraulic head, monthly mean streamflow, and cumulative monthly stream discharge.

The PEST++ software implements the Gauss-Levenberg-Marquardt algorithm (Doherty, 2018; Doherty and Hunt, 2010) and the singular-value decomposition-based parameter estimation methodology (Tonkin and Doherty, 2005). The Gauss-Levenberg-Marquardt algorithm is a gradient-based search method that adjusts parameters by attempting to minimize the sum of the squared and weighted residuals.

The implementation of Tikhonov regularization and use of pilot points for estimation of spatial hydraulic properties using PEST++ allows for a large number of parameters to be optimized and estimated simultaneously. Regularization is the name given to a broad class of mathematical techniques that can be used to bring numerical stability to an otherwise overparameterized inverse problem through the introduction of an appropriate smoothness or other constraint on parameter values (Tikhonov 1963a, 1963b; Barbosa and Silva, 1994). Using regularization in conjunction with pilot points is a benefit because many more parameters can be estimated compared to the number of observations used for calibration (Doherty, 2003). The method of pilot points (Doherty, 2003), in which hydraulic conductivity is estimated for a set of point locations within the model area, was used to estimate vertical and horizontal hydraulic conductivity in the model area. The method of pilot points was used to interpolate a smooth hydraulic-conductivity field and apply the resulting spatially variable distribution of hydraulic conductivity to the numerical model grid.

Calibration Targets and Weighting

Model calibration is completed using a process called history matching. History matching refers to the process of attempting to closely match real-world hydraulic observations of interest (calibration targets) to model-simulated values for a defined period. In general, calibration targets are direct measurement values; for example, hydraulic head. However, in some cases, calibration targets may be calculated from measurement values; for example, changes in hydraulic head. History matching is accomplished by attempting to reduce the sum of squared weighted residuals, or the objective function, for all calibration targets. Each calibration target in the history matching process is assigned a weight, and a residual is the difference between a calibration target and model-simulated value. Each observation is assigned to a group of similar observation types. Calibration targets for hydraulic head and changes in hydraulic head were assigned to groups based on model layer, and calibration targets for monthly mean streamflow and cumulative monthly stream discharge each were assigned to their own group. Weighting adjusts the contribution of each residual to the overall objective function and combining calibration targets into groups ensures that no single observation type or group becomes a dominate contributor in the calibration process. Highly weighted calibration targets will have greater importance in the calibration process compared to calibration targets with lower weights because smaller changes in residual for highly weighted calibration targets will generate larger changes to the overall objective function. Calibration target weights were initially assigned so that each observation group had an approximately equal contribution to the overall objective function.

Hydraulic Head Measurements

Hydraulic head measurements were available for 763 wells in the model area and 9,582 available water-level observations were used to established calibration targets of hydraulic head and changes in hydraulic head for numerical model calibration (fig. 19). Water-level measurement dates ranged from July 3, 1956, through December 5, 2017; therefore, no hydraulic head targets were used before 1956. Water-level altitudes were obtained from South Dakota drillers' logs (South Dakota Department of Environment and Natural Resources, 2018a), observation well records (South

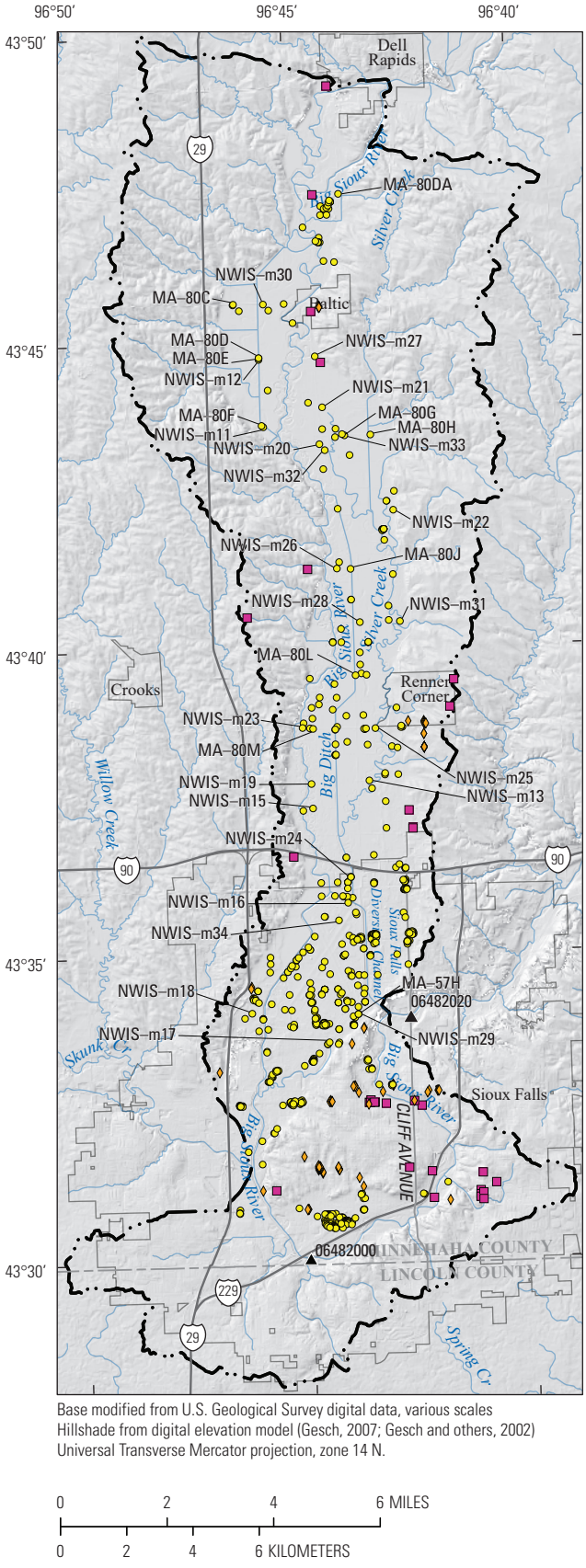

Figure 19. Location of hydraulic head and streamflow calibration targets in the model area.

Dakota Department of Environment and Natural Resources, 2018b), and National Water Information System water levels (U.S. Geological Survey, 2018). Water-level altitudes were calculated by subtracting the depth to water from (1) National Water Information System recorded well altitude, (2) state-recorded well altitude, or (3) land surface from a DEM.

Hydraulic head targets consisted of single water-level measurements and multiple water-level measurements recorded on different days but at a single well. Hydraulic head targets were separated into the following two groups for each model layer: (1) hydraulic head altitude targets, which were the absolute value of hydraulic head at the time of the measurement, and (2) hydraulic head change targets, which were calculated from water-level measurements in a series and were converted to a change in water level from the first recorded water-level measurement in the series. The hydraulic head target for single water-level measurements was assigned to the hydraulic head altitude target group. Hydraulic head targets for observation wells with multiple measurements were assigned to hydraulic head target groups in the following two ways: (1) the calibration target for the first recorded water-level measurement in the series was assigned to the hydraulic head altitude target group, and (2) the subsequent calibration targets were calculated and assigned to the hydraulic head change target group. Hydraulic head altitude targets and hydraulic head change targets accounted for 763 and 8,819 of the 9,582 hydraulic head targets, respectively. Most hydraulic head altitude targets were obtained from drillers' log records (South Dakota Department of Environment and Natural Resources, 2018b). Observation wells with multiple water-level measurements were primarily from State and Federal databases (South Dakota Department of Environment and Natural Resources, 2018a; U.S. Geological Survey, 2018).

Streamflow

Monthly mean streamflow and cumulative monthly stream discharge were used as calibration targets. Daily mean streamflow measurements at two USGS streamgages, 06482000 and 06482020 (U.S. Geological Survey, 2018), were used to calculate monthly mean streamflow and cumulative monthly stream discharge for calibration targets. Monthly mean streamflow for USGS streamgage 06482000 was calculated from daily mean streamflow measurements for September 1, 1943, through September 29, 1960, and for October 1, 2004, through December 31, 2017, and monthly mean streamflow for USGS streamgage 06482020 was calculated from daily mean streamflow measurements for October 1, 1971, to December 31, 2017. Streamflow targets were assigned a unique calibration group. Cumulative monthly stream discharge was calculated for USGS streamgages 06482000 and 06482020 by multiplying the monthly mean streamflow by the number of days in each month and adding each successive monthly discharge. Cumulative monthly stream discharge was assigned to a unique calibration group.

Groundwater and Surface-Water Interactions

Previously published estimates of groundwater discharge to and recharge from surface-water features (stream flux) in the model area were available (Jorgensen and Ackroyd, 1973; Koch, 1982; Neupane and others, 2017); however, these estimates were not used directly as calibration targets in the numerical model. The estimates of stream flux for the model area were used as general indicators of the groundwater and surface-water interactions that exist in the model area and were used to qualitatively assess the numerical model estimates of stream flux.

Calibration Parameters

Parameters adjusted during numerical model calibration were horizontal and vertical hydraulic conductivity, specific storage, specific yield, recharge and evapotranspiration multipliers, and streambed hydraulic conductivity. Horizontal and vertical hydraulic conductivity were estimated at pilot points distributed within the model area; specific storage and specific yield were assigned to uniform values in each layer in the model area; recharge and evapotranspiration multipliers were assigned uniformly for every stress period in the numerical model; and streambed hydraulic conductivity values were assigned uniformly between stream confluences in the SFR and RIV Packages and uniformly in the DRN Package.

Hydrogeologic Properties

Horizontal hydraulic conductivity values were calibrated at pilot point locations (fig. 17). Pilot points are discrete locations distributed throughout the model area that represent surrogate parameters from which horizontal and vertical hydraulic conductivity values are interpolated to the numerical model grid using a kriging algorithm (Doherty and Hunt, 2010). The pilot point locations were used to interrogate the spatial distribution of resistivity, described in the "Numerical Model Design" section of this report (fig. 17). Additional pilot points were included at locations where hydraulic conductivity values were estimated using slug tests (Eldridge and Medler, 2019) and NMR measurements (fig. 20; appendix 1). The use of pilot points and the method of kriging allows for a greater variation in hydraulic properties compared to using either a single value for each model layer or subdividing each layer into piecewise zones of uniform hydraulic conductivity. As a result, the process allows a smooth variation in hydraulic properties in the model area interpolated from estimated values at pilot points. Aquifer storage properties, including specific storage and specific yield, were uniform in each model layer, and initial values were set based on literature values (tables 3 and 6). Estimates of horizontal and vertical hydraulic conductivity and storage properties from literature were used to define the upper and lower allowable parameter bounds applied during numerical model calibration.

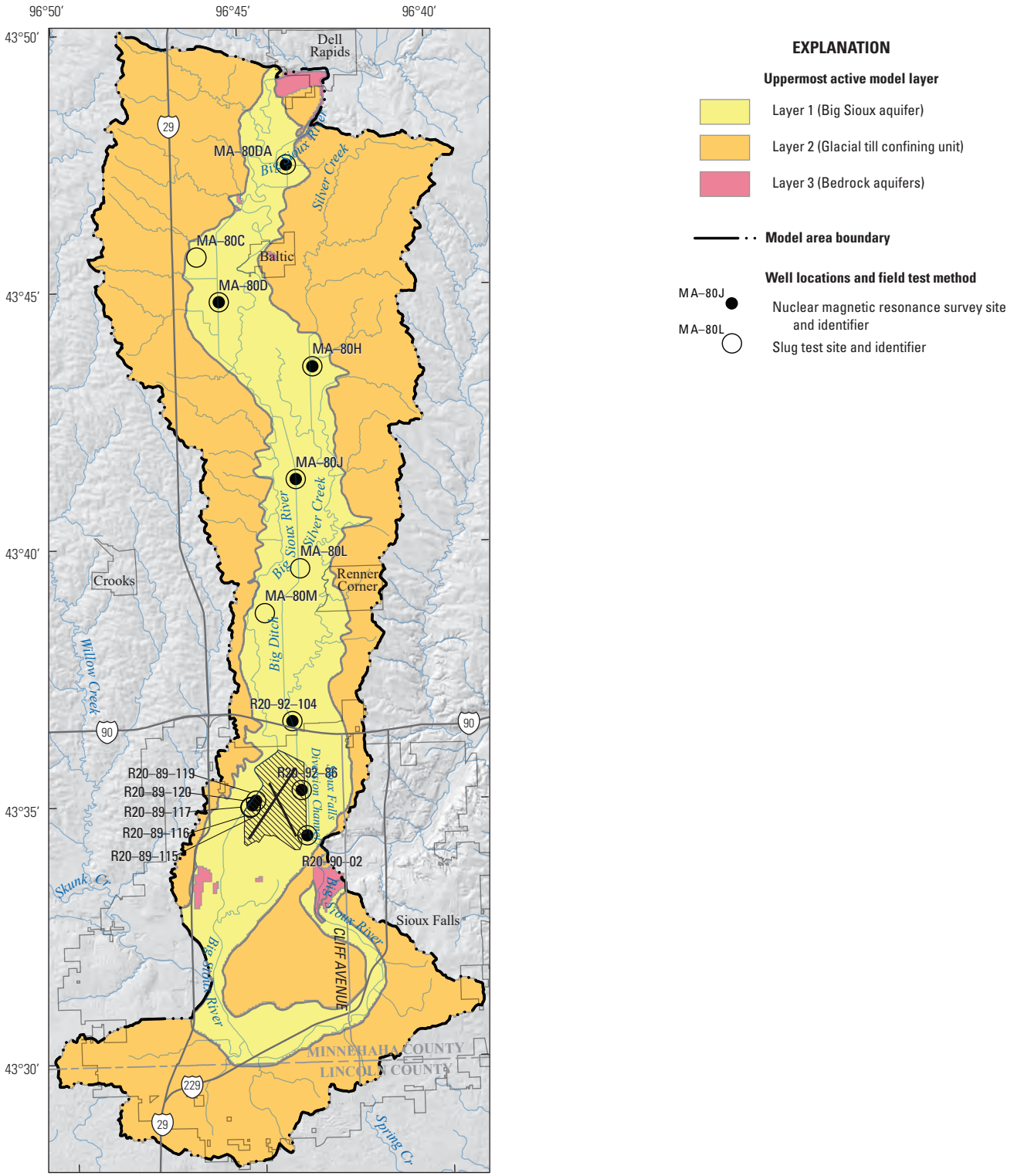

Base modified from U.S. Geological Survey digital data, various scales
Hillshade from digital elevation model (Gesch, 2007; Gesch and others, 2002)
Universal Transverse Mercator projection, zone 14 N.

Figure 20. Nuclear magnetic resonance (NMR) and slug test locations in the model area.

Streambed Hydraulic Conductivity

Streambed hydraulic conductivity parameters in the SFR, RIV, and DRN Packages were adjusted during the calibration process. Streambed hydraulic conductivity is a property that controls the stream flux simulated by the numerical model. Uniform values of streambed hydraulic conductivity were assigned to the SFR Package between stream confluences, indicated by numbered segments on figure 13. Uniform values of streambed hydraulic conductivity were used for the west and east branches of the Big Sioux River upstream from USGS streamgage 09481000 represented by the RIV Package in the numerical model (fig. 13). Uniform values of streambed hydraulic conductivity were used in the DRN Package. Previously published estimates of streambed hydraulic conductivity were used to define the upper and lower allowable parameter bounds applied during numerical model calibration.

Recharge and Evapotranspiration

The estimates of recharge and evapotranspiration were adjusted independently during the calibration process using recharge and evapotranspiration multipliers. The multipliers were applied uniformly to all numerical model stress periods (steady-state and transient stress periods) for the spatially varied SWB estimates used in the RCH and EVT Packages. Estimates of recharge from literature were used to define the upper and lower limits of recharge applied to the numerical model during calibration.

Calibration and Numerical Model Results

Calibration results included optimal parameter estimates, a comparison of calibration targets to model-simulated values, and a parameter sensitivity analysis. Optimal parameter estimates for horizontal and vertical hydraulic conductivity, specific yield, specific storage, streambed hydraulic conductivity, and recharge and evapotranspiration multipliers compared well with literature values. Optimal parameter estimates were obtained primarily on the basis of the automated comparison of model-simulated values to calibration targets of hydraulic head, changes in hydraulic head, monthly mean streamflow, and cumulative monthly stream discharge. Numerical model-simulated potentiometric surfaces, groundwater-flow directions, and groundwater budgets were qualitatively compared with those published in literature. Secondary assessments of numerical model performance also included a qualitative assessment of numerical model-simulated groundwater and surface-water interactions (stream flux) and the ability of the numerical model to adequately simulate the specified monthly mean groundwater withdrawal rates. A parameter sensitivity analysis was completed and used to indicate which parameters had the greatest effect on numerical model outputs. The parameter sensitivity analysis was completed using PEST++.

Optimal Parameter Estimates

The final calibrated parameter values of horizontal and vertical hydraulic conductivity, specific yield, specific storage, streambed hydraulic conductivity, recharge, and evapotranspiration were considered reasonable for the hydrogeologic materials and conditions in the model area for 1950–2017. In general, the mean calibrated parameter values were reasonably close to previously published values (tables 3 and 10). The mean horizontal hydraulic conductivity for the Big Sioux aquifer, estimated at pilot points during the calibration process, was about 158 ft/d and ranged from about 25 to 946 ft/d (table 10). Higher horizontal hydraulic conductivity values were typically in the northern part of the model area near Dell Rapids and Baltic and in the northern part of Sioux Falls near the Sioux Falls Regional Airport (figs. 21*A*). Calibrated mean vertical hydraulic conductivity for the Big Sioux aquifer was about 15 ft/d and ranged from about 10 to 66 ft/d at pilot point locations (table 10). Calibrated vertical hydraulic conductivities were generally close to the initial values (tables 6 and 10), and the areas with the highest vertical hydraulic conductivity corresponded to the areas of highest horizontal hydraulic conductivity (figs. 21*A* and 22*A*). The calibrated specific storage and specific yield for the Big Sioux aquifer were lower than the initial values and lower than most literature values at 3.54×10^{-5} and 0.05, respectively (tables 3, 6, and 10).

The mean calibrated horizontal hydraulic conductivity for the glacial till confining unit was similar to the initial mean value but higher than the values reported in most previous studies (tables 3, 6, and 10). Calibrated horizontal hydraulic conductivity, estimated during the calibration process at pilot points for the glacial till confining unit, was about 5 ft/d and ranged from about 0.8 to 46 ft/d (table 10). The highest horizontal hydraulic conductivities for the glacial till confining unit in the model area were in Sioux Falls at the junction of the Big Sioux River and the outlet of the Sioux Falls Diversion Channel (fig. 21*B*). Calibrated mean vertical hydraulic conductivity for the glacial till confining unit was about 0.5 ft/d and ranged from about 0.4 to 1.2 ft/d at pilot point locations. Areas of the highest vertical hydraulic conductivity typically corresponded to areas of high horizontal hydraulic conductivity, with the addition of higher areas northwest of Renner Corner and west of Baltic (figs. 21*B* and 22*B)*. Specific storage for the glacial till confining unit was lower than the initial value, but the specific yield was higher (tables 6 and 10). Calibrated specific storage for the glacial till confining unit was about 2.7×10^{-7}, and calibrated specific yield was 0.10.

The mean calibrated horizontal hydraulic conductivity values for the bedrock aquifers were higher than the mean initial values but typically lower than values reported in literature (tables 3, 6, and 10). Calibrated horizontal hydraulic conductivity, estimated during the calibration process at pilot points for the bedrock aquifers, was about 2.7 ft/d and ranged from about 0.3 to 11 ft/d (table 10). The highest calibrated horizontal hydraulic conductivity values in the bedrock layer were in the southern part of the model area and the lowest values were near the city of Sioux Falls and near the central part of

the model area (fig. 21*C*). Calibrated mean vertical hydraulic conductivity for the bedrock aquifers was about 0.2 ft/d and ranged from about 0.1 to 0.3 ft/d at pilot point locations. Areas of the highest vertical hydraulic conductivity were in the south and northwestern part of the model area (fig. 22*C*). Calibrated specific storage was similar to the initial value but lower than the values reported in previous studies (tables 3, 6, and 10). Calibrated specific yield was higher than the initial value and higher than the values listed in previous studies (tables 3, 6, and 10). Calibrated specific storage for the bedrock aquifers was 5.25×10^{-7}, and calibrated specific yield was about 0.3.

Calibrated streambed hydraulic conductivity from the SFR, RIV, and DRN Packages ranged from about 0.02 to 0.65 ft/d with a mean of about 0.07 ft/d (table 10). The calibrated streambed hydraulic conductivity values generally were smaller than those reported in literature (tables 3 and 10). The calibrated recharge multiplier was 1.7, and the calibrated evapotranspiration multiplier was 0.1.

Comparison of Calibration Targets to Simulated Equivalents

Numerical model performance was assessed primarily on its ability to match calibration targets for groundwater levels (hydraulic head), changes in hydraulic head, monthly mean streamflow, and cumulative monthly stream discharge. Hydraulic head altitude targets were assessed for 763 wells completed in the Big Sioux aquifer, glacial till confining unit, or bedrock aquifers. Hydraulic head change targets were assessed for wells completed only in the Big Sioux aquifer and bedrock aquifers for wells with more than one measurement. Monthly mean streamflow and cumulative monthly stream discharge targets were used for two the USGS streamgages with daily streamflow measurements in the model area.

Groundwater Levels

The 763 hydraulic head altitude targets for wells in the Big Sioux aquifer, glacial till confining unit, and bedrock layers used in numerical model calibration were compared with numerical model-simulated hydraulic head calculated at the same location and time as the observations. Positive and negative mean hydraulic head altitude residuals (observed minus simulated values) were evenly distributed spatially in the model area (fig. 23). The even distribution of positive and negative mean hydraulic head altitude residuals indicates that the numerical model results are not spatially biased.

Observed hydraulic head altitudes were plotted with simulated hydraulic head altitudes and compared to a 1:1 perfect-fit line (fig. 24), and hydraulic head altitude residuals were plotted using a histogram (fig. 25) to assess the overall model-to-measurement fit. Overall, simulated hydraulic head altitudes had a linear regression coefficient of determination (R^2) of 0.48. Hydraulic head altitude residuals for the glacial till confining unit and bedrock aquifers typically were greater in magnitude when compared to residuals in the Big Sioux

Table 10. Summary of numerical model-estimated (calibrated) aquifer properties by model layer.

[ft/d, foot per day; --, not applicable]

Property	Units	Minimum	Maximum	Mean
Big Sioux aquifer (layer 1)				
Horizontal hydraulic conductivity[a]	ft/d	25.39	946.44	157.61
Vertical hydraulic conductivity[a]	ft/d	10.42	65.76	15.14
Specific storage	per foot	--	--	3.54×10^{-5}
Specific yield	Dimensionless	--	--	0.05
Glacial till confining unit (layer 2)				
Horizontal hydraulic conductivity[a]	ft/d	0.81	45.55	4.99
Vertical hydraulic conductivity[a]	ft/d	0.37	1.19	0.50
Specific storage	per foot	--	--	2.74×10^{-7}
Specific yield	Dimensionless	--	--	0.10
Bedrock aquifers (layer 3)				
Horizontal hydraulic conductivity[a]	ft/d	0.25	10.99	2.71
Vertical hydraulic conductivity[a]	ft/d	0.14	0.34	0.24
Specific storage	per foot	--	--	5.25×10^{-7}
Specific yield	Dimensionless	--	--	0.26
Streambed hydraulic conductivity	ft/d	0.02	0.65	0.07

[a]Values from pilot point locations.

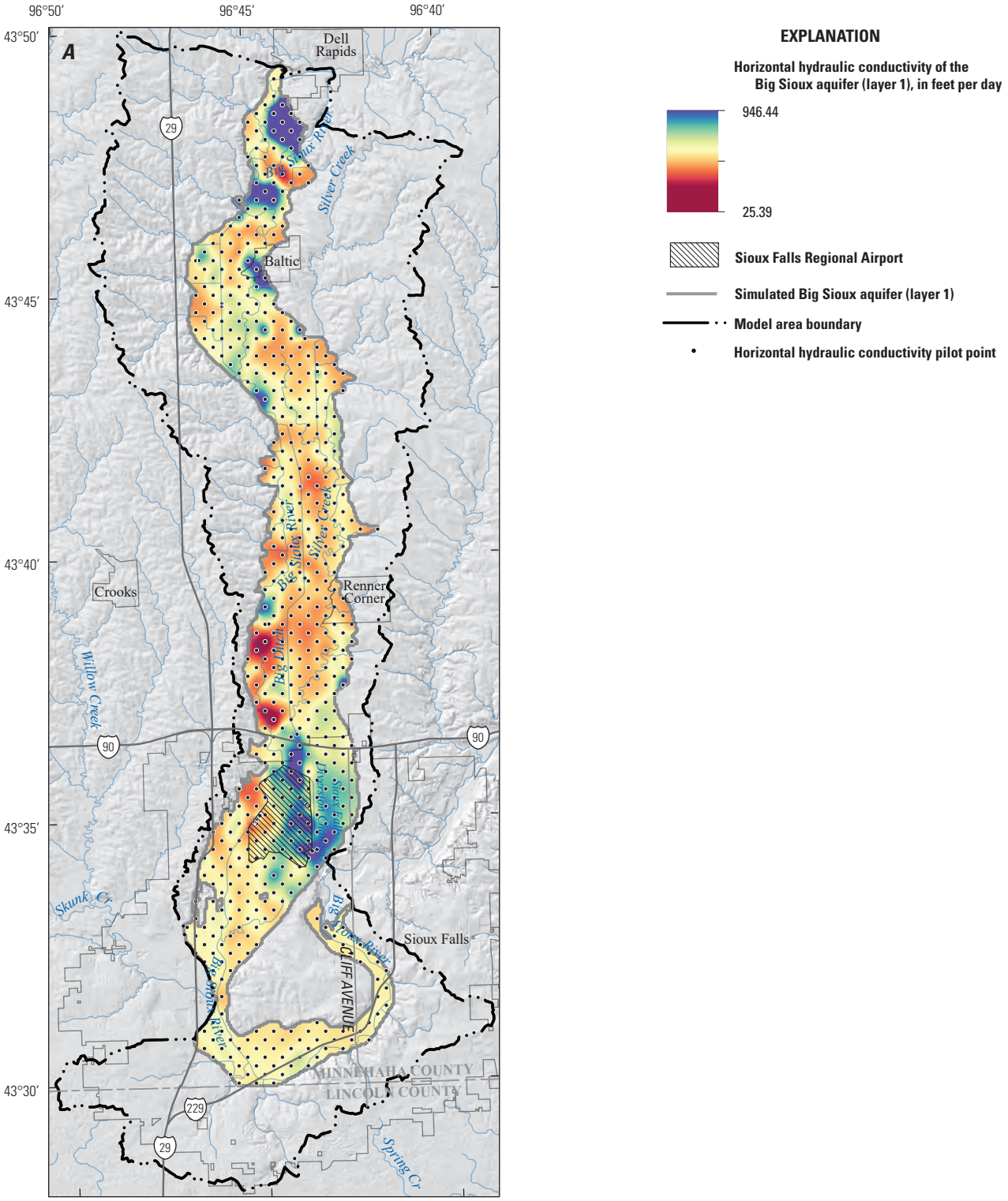

Figure 21. Calibrated horizontal hydraulic conductivity for *A*, Big Sioux aquifer (layer 1); *B*, glacial till confining unit (layer 2); and *C*, bedrock aquifers (layer 3).

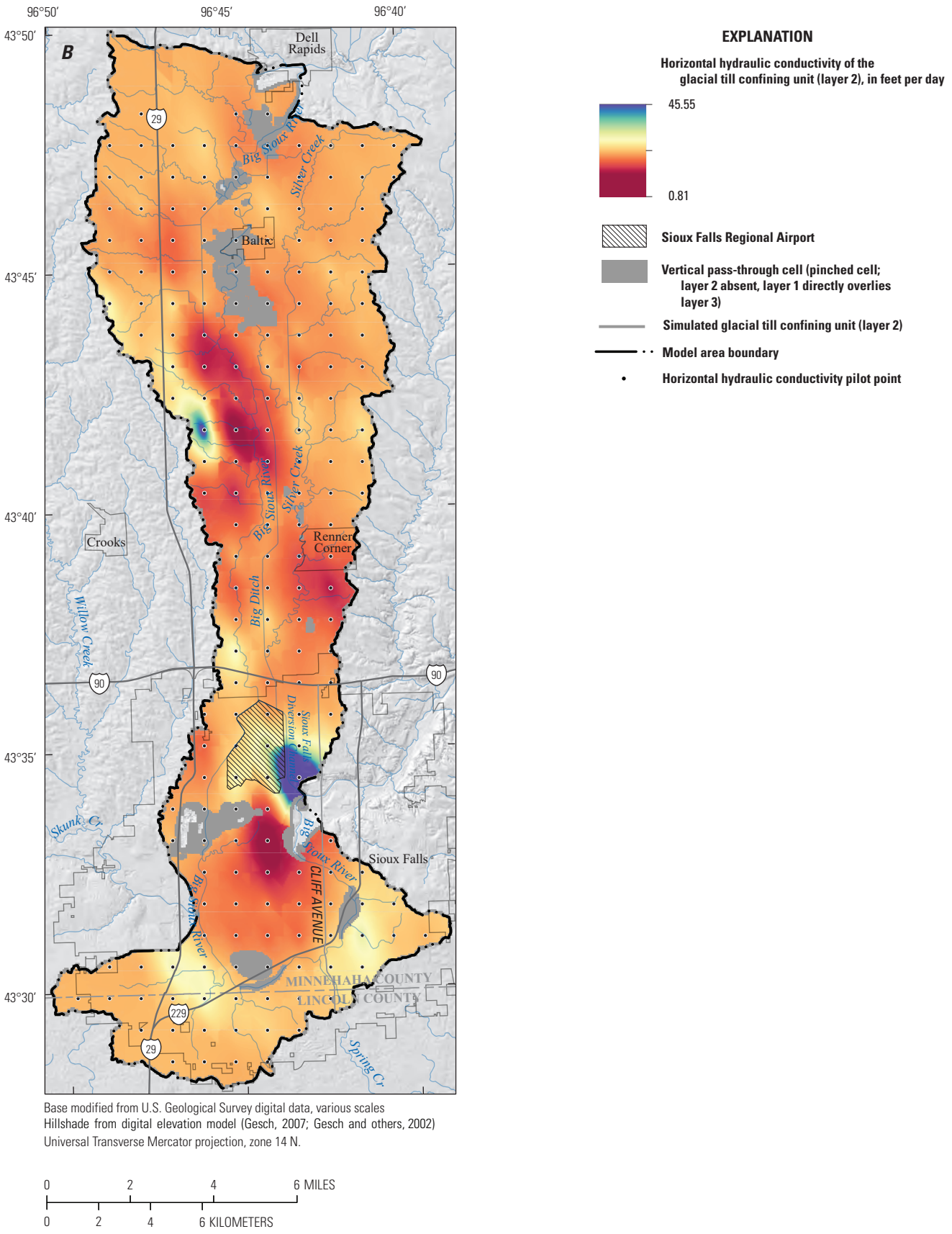

Figure 21. Calibrated horizontal hydraulic conductivity for *A*, Big Sioux aquifer (layer 1); *B*, glacial till confining unit (layer 2); and *C*, bedrock aquifers (layer 3).—Continued

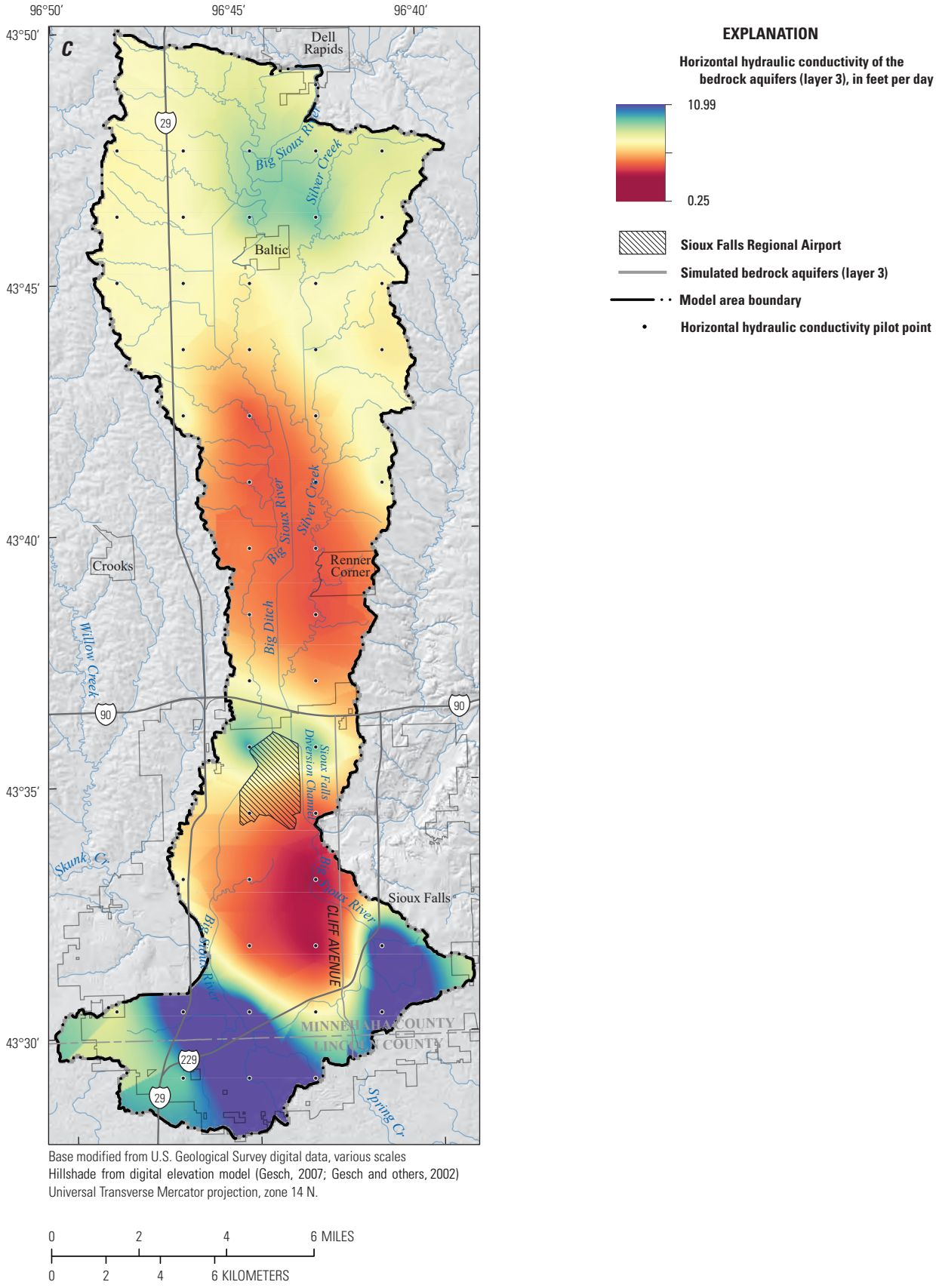

Base modified from U.S. Geological Survey digital data, various scales
Hillshade from digital elevation model (Gesch, 2007; Gesch and others, 2002)
Universal Transverse Mercator projection, zone 14 N.

Figure 21. Calibrated horizontal hydraulic conductivity for *A*, Big Sioux aquifer (layer 1); *B*, glacial till confining unit (layer 2); and *C*, bedrock aquifers (layer 3).—Continued

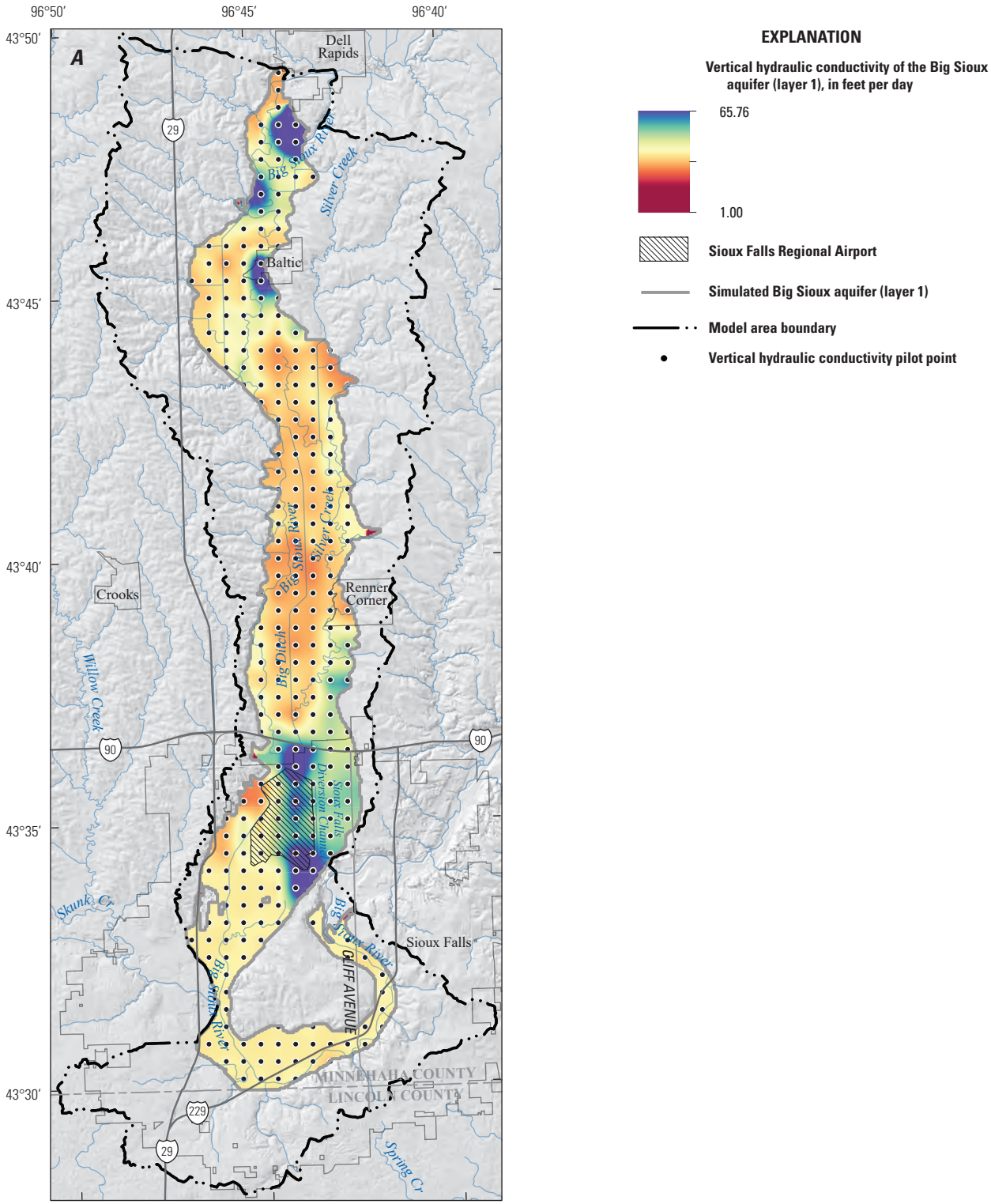

Figure 22. Calibrated vertical hydraulic conductivity for *A*, Big Sioux aquifer (layer 1); *B*, glacial till confining unit (layer 2); and *C*, bedrock aquifers (layer 3).

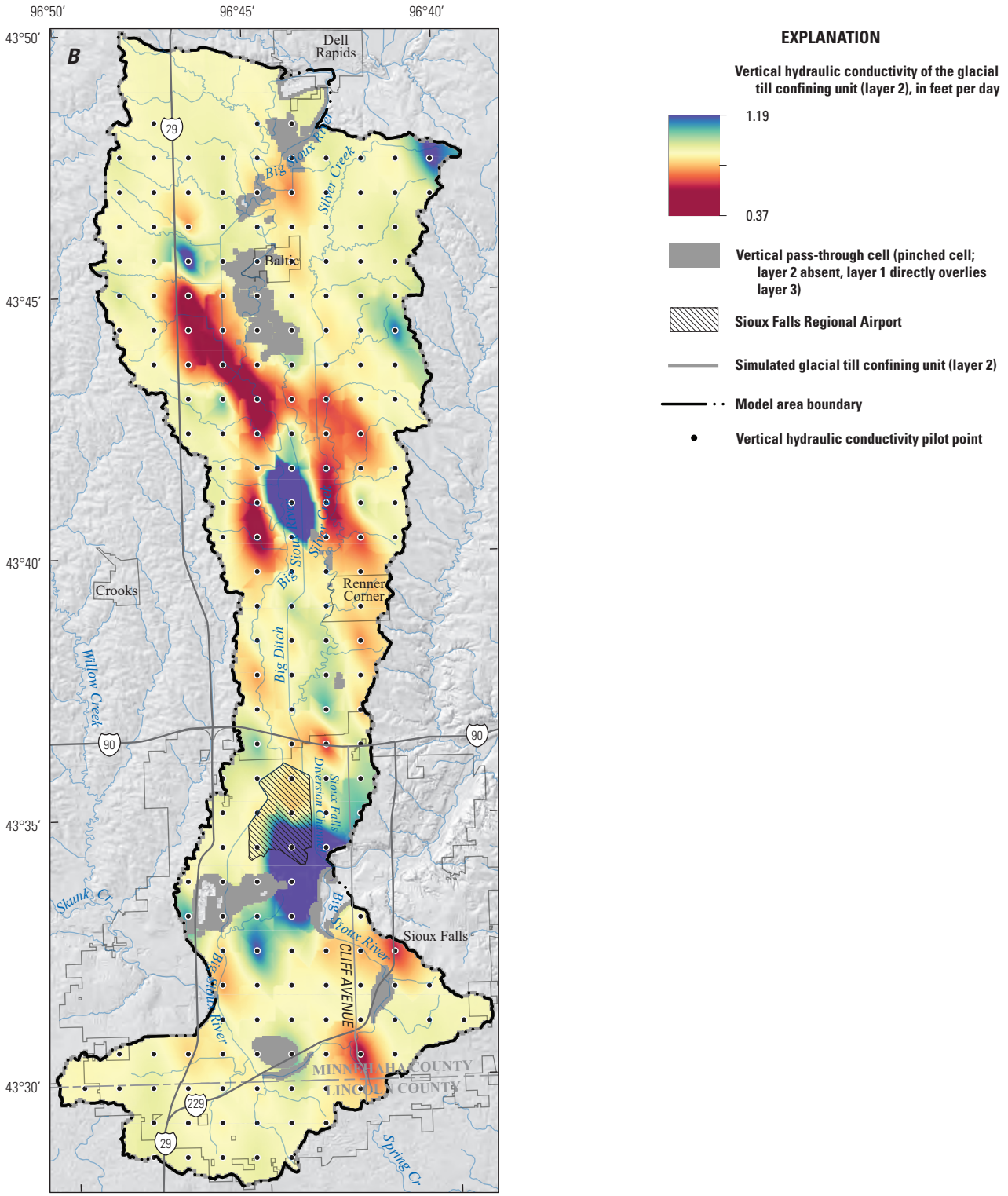

Figure 22. Calibrated vertical hydraulic conductivity for *A*, Big Sioux aquifer (layer 1); *B*, glacial till confining unit (layer 2); and *C*, bedrock aquifers (layer 3).—Continued

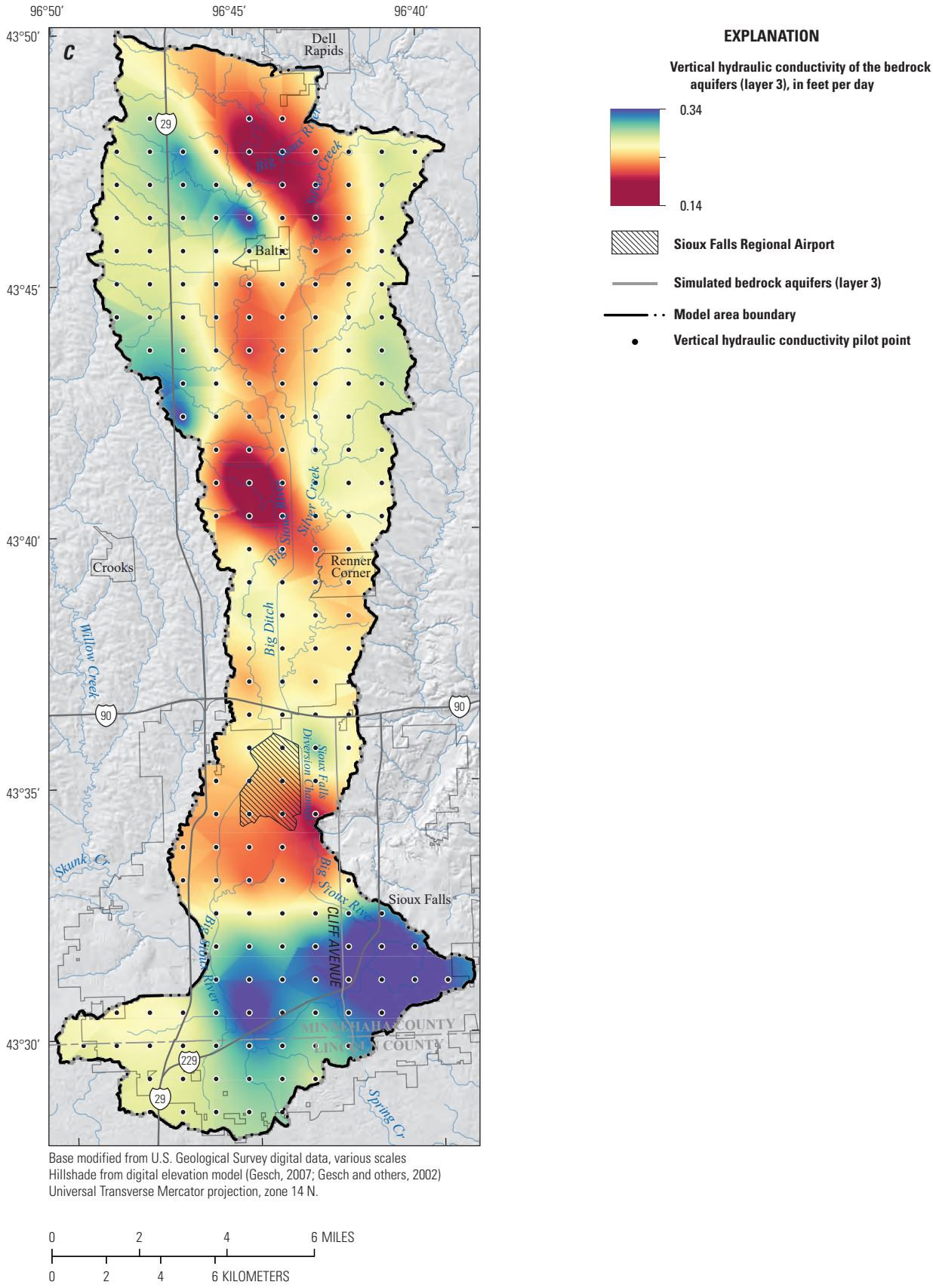

Figure 22. Calibrated vertical hydraulic conductivity for *A*, Big Sioux aquifer (layer 1); *B*, glacial till confining unit (layer 2); and *C*, bedrock aquifers (layer 3).—Continued

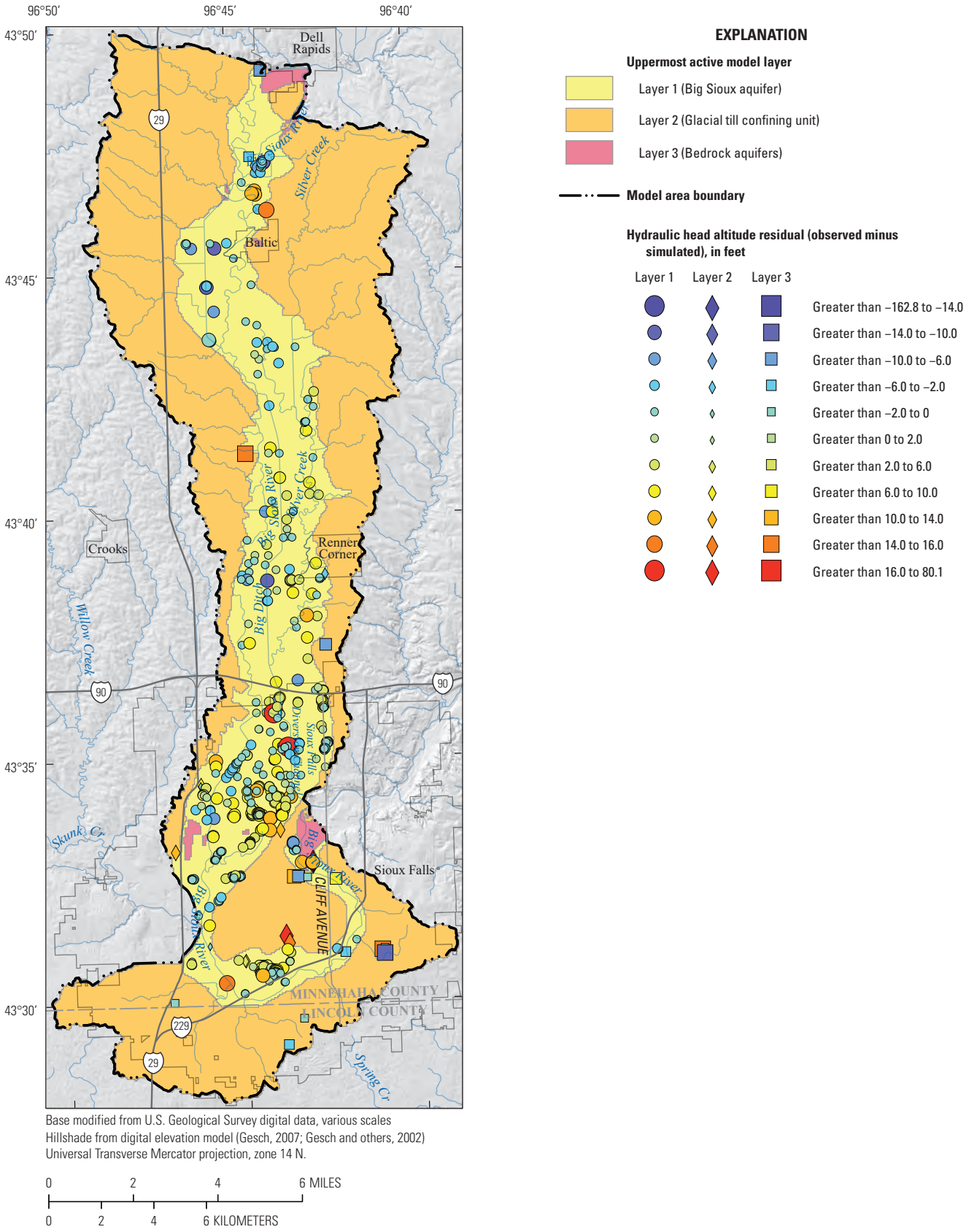

Figure 23. Residuals (observed minus simulated values), in feet, of hydraulic head altitude targets for 1950–2017 for the Big Sioux aquifer, glacial till confining unit, and bedrock aquifers in the model area.

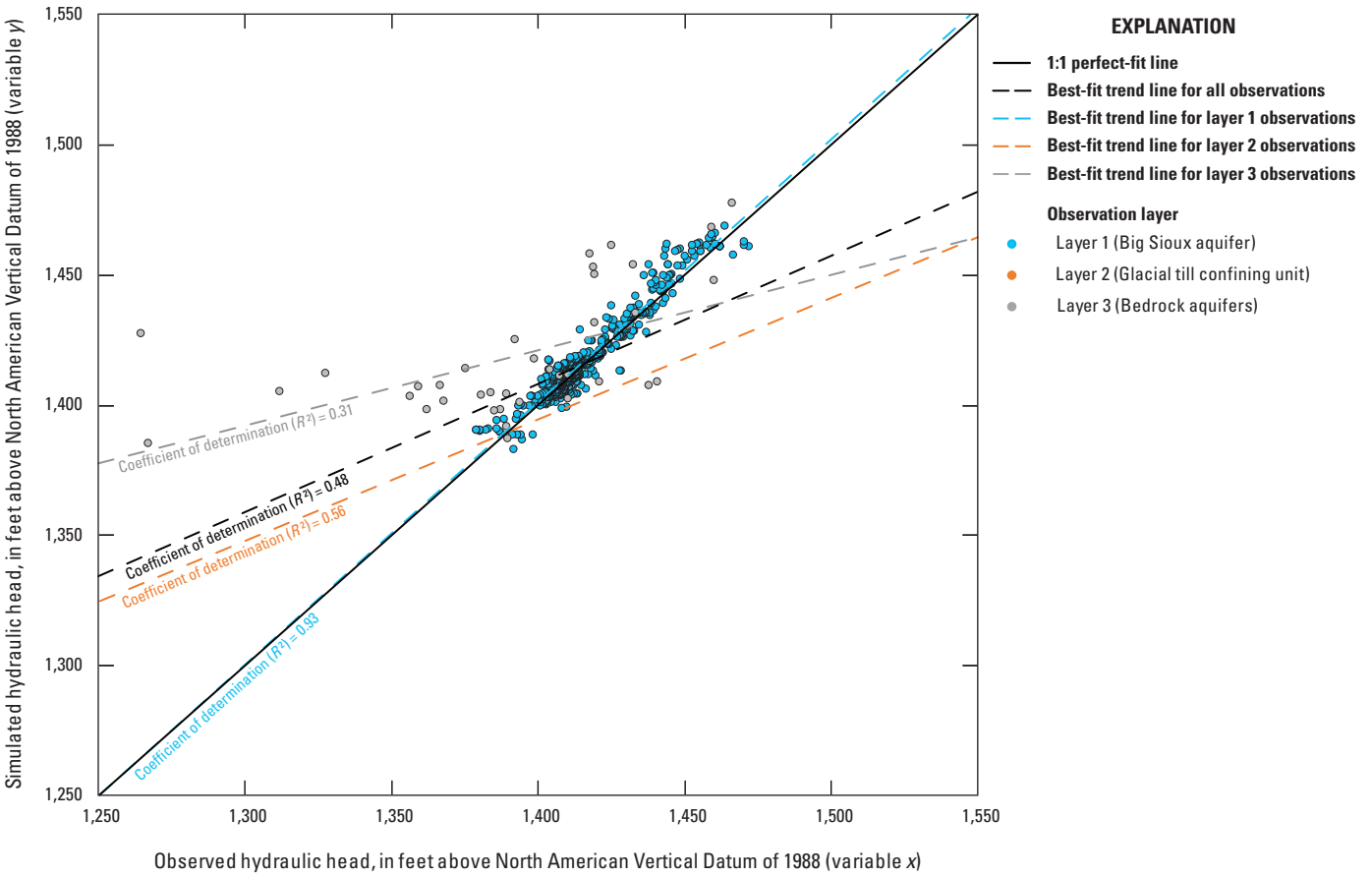

Figure 24. Observed and simulated hydraulic head for hydraulic head altitude targets for 1950–2017, by aquifer, including a best-fit line from linear regression. The 1:1 perfect-fit line also is shown for reference to visualize bias.

aquifer (figs. 23, 24, and 25). Simulated hydraulic head altitudes in the Big Sioux aquifer compared favorably with mean observed hydraulic head altitudes and had a linear regression R^2 of 0.93 (fig. 24). The numerical model does not simulate hydraulic head for the glacial till confining unit or the bedrock aquifers as accurately when compared to the simulated hydraulic head in the Big Sioux aquifer (indicated by the wider spread around the 1:1 line for hydraulic head altitudes in the confining unit and bedrock aquifers; fig. 24). In general, the numerical model slightly overestimated water levels for the Big Sioux aquifer (indicated by points above the 1:1 line for hydraulic head altitudes in the Big Sioux aquifer; fig. 24). The numerical model typically overestimated hydraulic head in the glacial till confining unit, indicated by points above the 1:1 line, and underestimated hydraulic head in the bedrock aquifers, indicated by points below 1:1 line. The linear regression coefficients of determination for the glacial till confining unit and bedrock aquifers were 0.56 and 0.31, respectively (fig. 24).

Hydraulic head altitude residuals for all numerical model layers ranged from −162.8 to 80.1 ft with a mean of −3.0 ft and standard deviation of 7.1 ft (table 11). Simulated hydraulic head altitudes more closely matched observed values for the Big Sioux aquifer than the glacial till confining unit and bedrock aquifers (table 11). Hydraulic head altitude residuals for the Big Sioux aquifer ranged from −17.9 to 15.3 ft, and residuals for the glacial till confining unit and bedrock aquifers ranged from −162.8 to 80.1 ft. The smallest absolute hydraulic head altitude residuals also were in the Big Sioux aquifer, and the largest absolute hydraulic head altitude were in the bedrock aquifers (table 11). About 61 percent of simulated hydraulic head altitudes for all layers were within plus or minus 2 ft of the observed values and 85 percent were within plus or minus 10 ft. The numerical model generally overestimated hydraulic head altitudes in the Big Sioux aquifer and bedrock aquifers and underestimated hydraulic head altitudes in the glacial till confining unit (fig. 25).

Hydraulic head change observations were not available for the glacial till confining unit; therefore, simulated hydraulic head changes were compared with observed values for only the Big Sioux aquifer and bedrock aquifers. Observed hydraulic head changes and simulated hydraulic head changes for observation wells with multiple water-level measurements were converted to a change in water level from the first recorded water level in the series. The observed change in water level and the simulated change in water level were

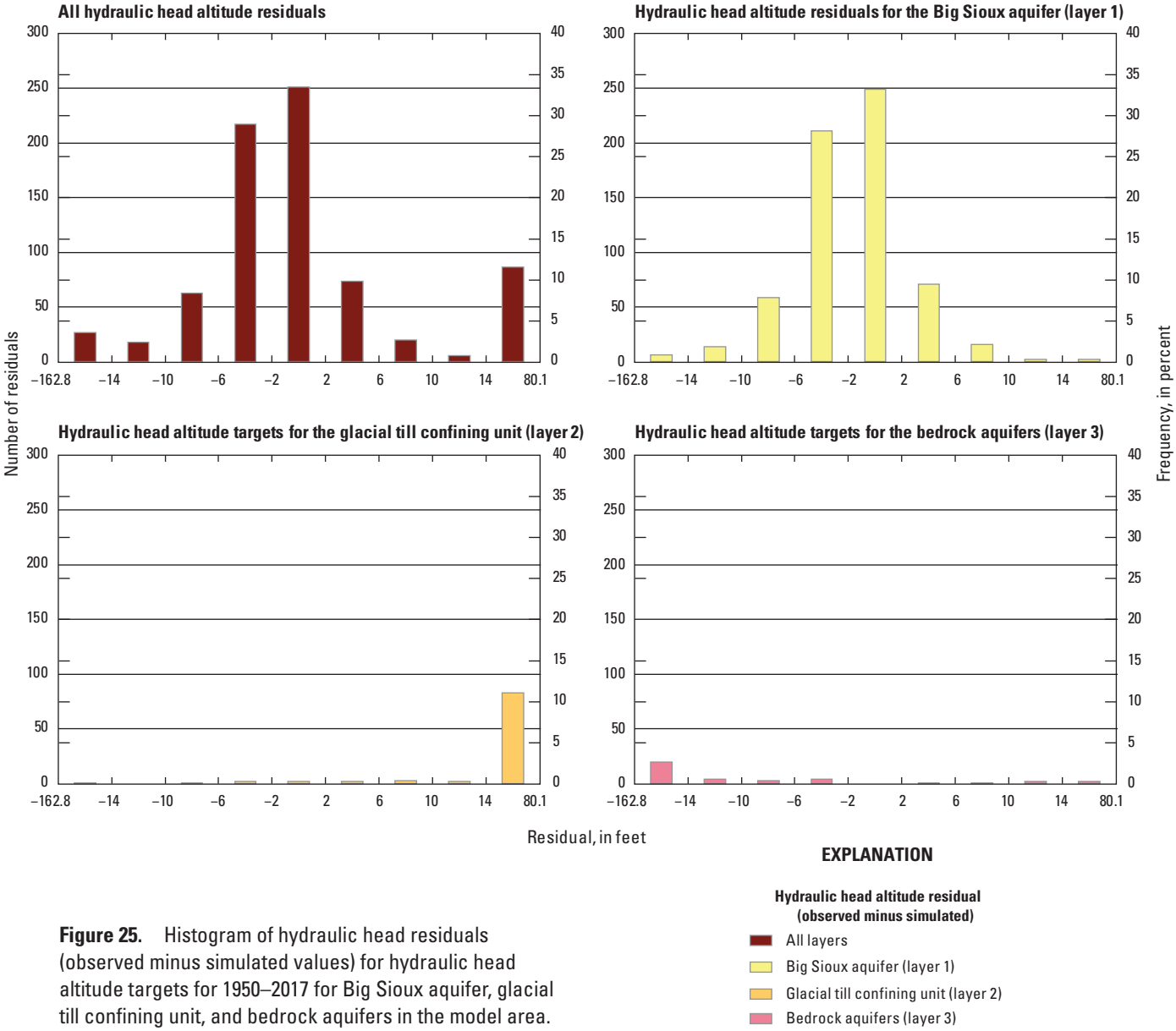

Figure 25. Histogram of hydraulic head residuals (observed minus simulated values) for hydraulic head altitude targets for 1950–2017 for Big Sioux aquifer, glacial till confining unit, and bedrock aquifers in the model area.

Table 11. Summary of hydraulic head altitude residuals (observed minus simulated values) for the Big Sioux aquifer, glacial till confining unit, and bedrock aquifers.

[*n*, number of observations; ft, foot]

Model layer	Aquifer	*n*	Residual[a]				Absolute residual[a]			
			Minimum (ft)	Maximum (ft)	Mean (ft)	Standard deviation (ft)	Minimum (ft)	Maximum (ft)	Mean (ft)	Standard deviation (ft)
1	Big Sioux aquifer	630	−17.9	15.3	−1.7	4.2	0.0	17.9	3.4	3.0
2	Glacial till confining unit	96	−83.5	80.1	31.8	21.0	0.3	83.5	33.9	17.4
3	Bedrock aquifer	37	−162.8	31.9	−26.3	37.7	2.0	162.8	31.4	33.5
All		**763**	**−162.8**	**80.1**	**−3.0**	**7.1**	**0.0**	**162.8**	**5.3**	**5.6**

[a]Residuals calculated as observed minus simulated values.

compared in the following three categories based on the direction of observed water-level change: (1) decreased water levels, (2) increased water levels, and (3) no change (table 12). An assessment of observed and simulated hydraulic head changes indicated that the numerical model typically underestimated hydraulic head changes in the model area (table 12). Underestimated hydraulic head changes accounted for 77.8 percent of all observations and overestimated hydraulic head changes accounted for 20.7 percent of all observations. Hydraulic head changes in the numerical model were underestimated by 84.3 and 75.1 percent of the observations in the decreasing and increasing categories, respectively. Most simulated hydraulic head change observations with no change in water levels were overestimated (table 12).

Observed and simulated hydraulic head hydrographs were created for the Big Sioux aquifer and bedrock aquifer for observation wells with more than three water-level observations during the numerical model period (fig. 26). The hydrographs are a visual representation of hydraulic head altitude and hydraulic head change observation targets. The earliest value in the hydrographs represents the hydraulic head altitude at the time of the first measurement at an observation well. Subsequent values in the hydrographs represent hydraulic head change targets assigned to each observation well and were added to the earliest value for plotting. A visual assessment of the hydrographs indicated that, in general, the numerical model overestimated initial water levels in the Big Sioux aquifer, but subsequent water-level changes were underestimated (fig. 26).

Streamflow

Monthly mean streamflow and cumulative monthly stream discharge at USGS streamgages 06482000 and 06482020 were used for numerical model calibration and were compared with the simulated values for the transient period (figs. 27*A–D*). Simulated hydrographs matched the general trends of observed increases and decreases in streamflow (figs. 27*A*, *C*). Larger magnitude streamflow was typically overestimated at USGS streamgage 06482000 (Big Sioux River at Sioux Falls, S. Dak.) and underestimated at USGS streamgage 06482020 (Big Sioux River at North Cliff Avenue at Sioux Falls, S. Dak.). Cumulative monthly stream discharge also was calculated to assess the ability of the numerical model to simulate the volume of streamflow in the model area. The numerical model reasonably estimated cumulative monthly stream discharge for the first 10–15 years of available streamflow records at both USGS streamgages (figs. 27*B*, *D*). After the first 10–15 years of available streamflow record, cumulative monthly stream discharge was closely estimated

Table 12. Summary of observed and simulated hydraulic head changes for the Big Sioux aquifer, glacial till confining unit, and bedrock aquifers.

[*n*, number of observations that decreased, increased, or had no change in water level; *s*, number of simulated values; <, less than; --, not applicable]

Observed water level change[a] direction	*n*	Simulated water level change[b] compared to observed water level change[a]	*s*	Percent of *s* in *n*	Percent of *s* in total
Decrease	3,533	Underestimated	2,980	84.3	33.8
		Overestimated	546	15.5	6.2
		Exactly estimated	7	0.2	0.1
		Subtotal	3,533	100.0	40.1
Increase	5,171	Underestimated	3,882	75.1	44.0
		Overestimated	1,278	24.7	14.5
		Exactly estimated	11	0.2	0.1
		Subtotal	5,171	100.0	58.6
No change	115	Overestimated	114	99.1	1.3
		Exactly estimated	1	0.9	<0.01
		Subtotal	115	100.0	1.3
		Total	**8,819**	**--**	**100.0**

[a]Observed water level changes were calculated for observation wells with multiple measurements; calculated by subtracting the earliest measured water level from subsequent water level measurements.

[b]Simulated water level changes were calculated at locations and times in the model corresponding to observation wells with multiple measurements; calculated by subtracting the earliest simulated water level from subsequent simulated water levels corresponding to observed water level change targets.

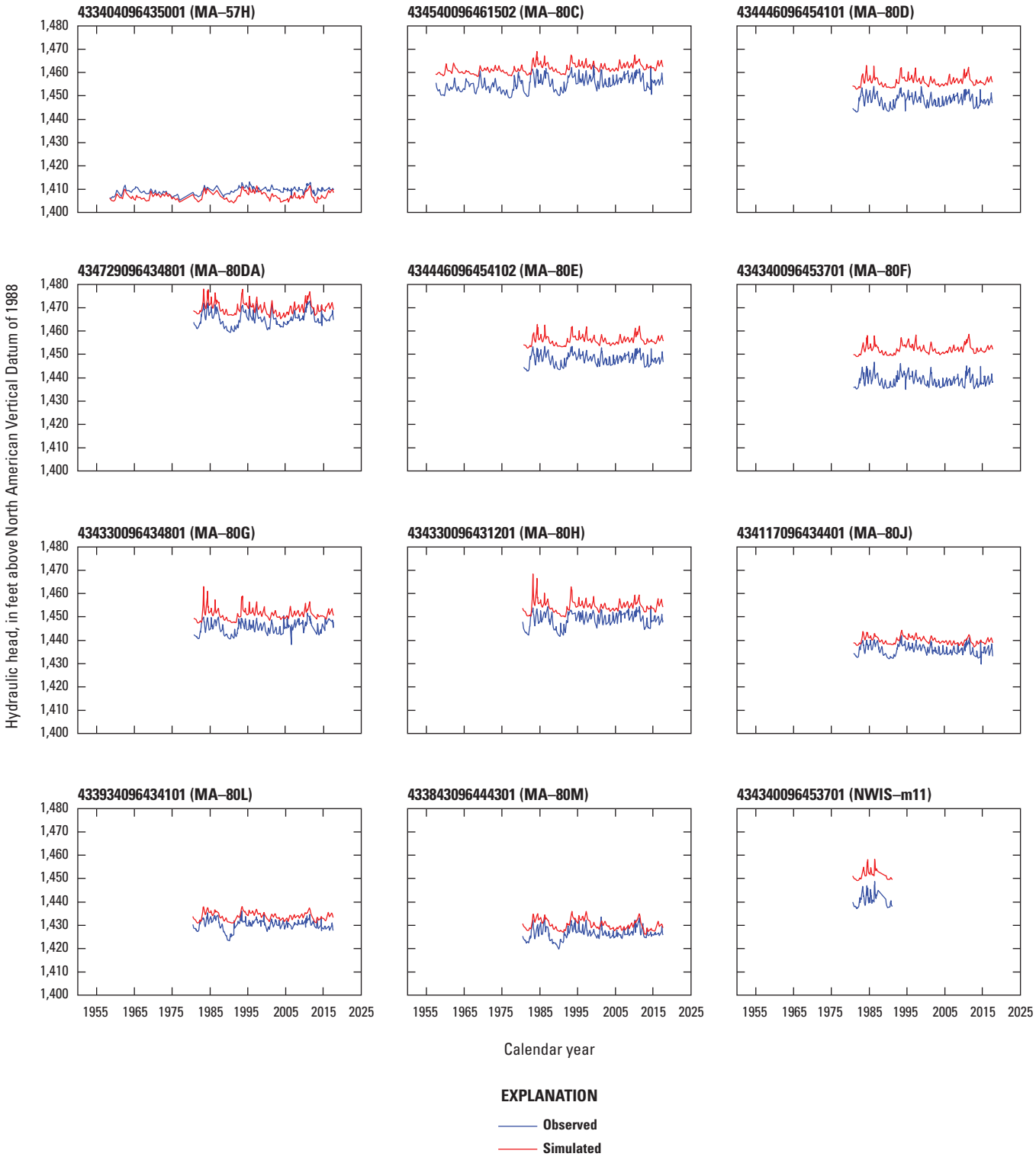

Figure 26. Hydrographs of observed and simulated hydraulic head for selected observation wells completed in the Big Sioux aquifer. Observation well locations are shown in figure 19.

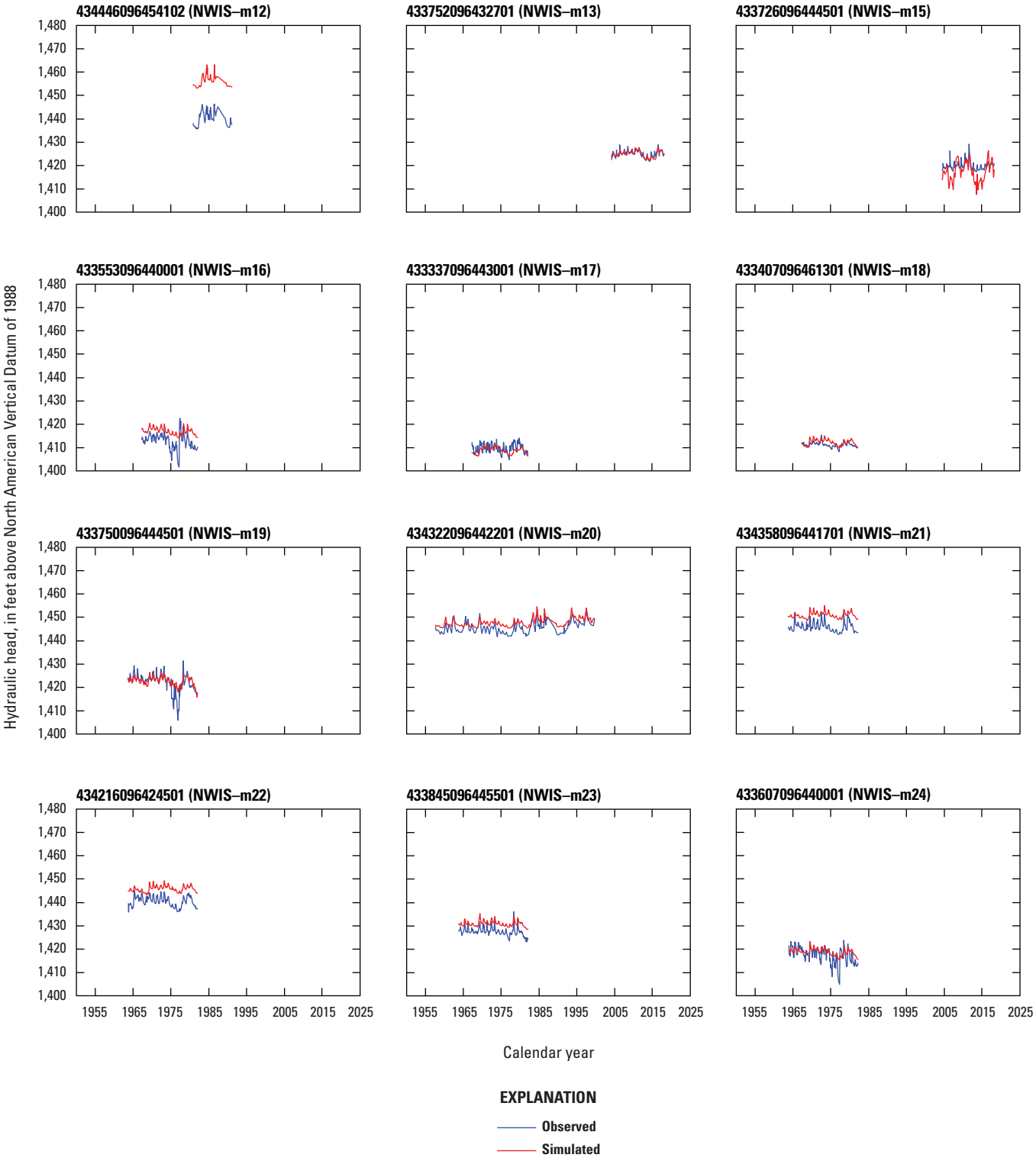

Figure 26. Hydrographs of observed and simulated hydraulic head for selected observation wells completed in the Big Sioux aquifer. Observation well locations are shown in figure 19.—Continued

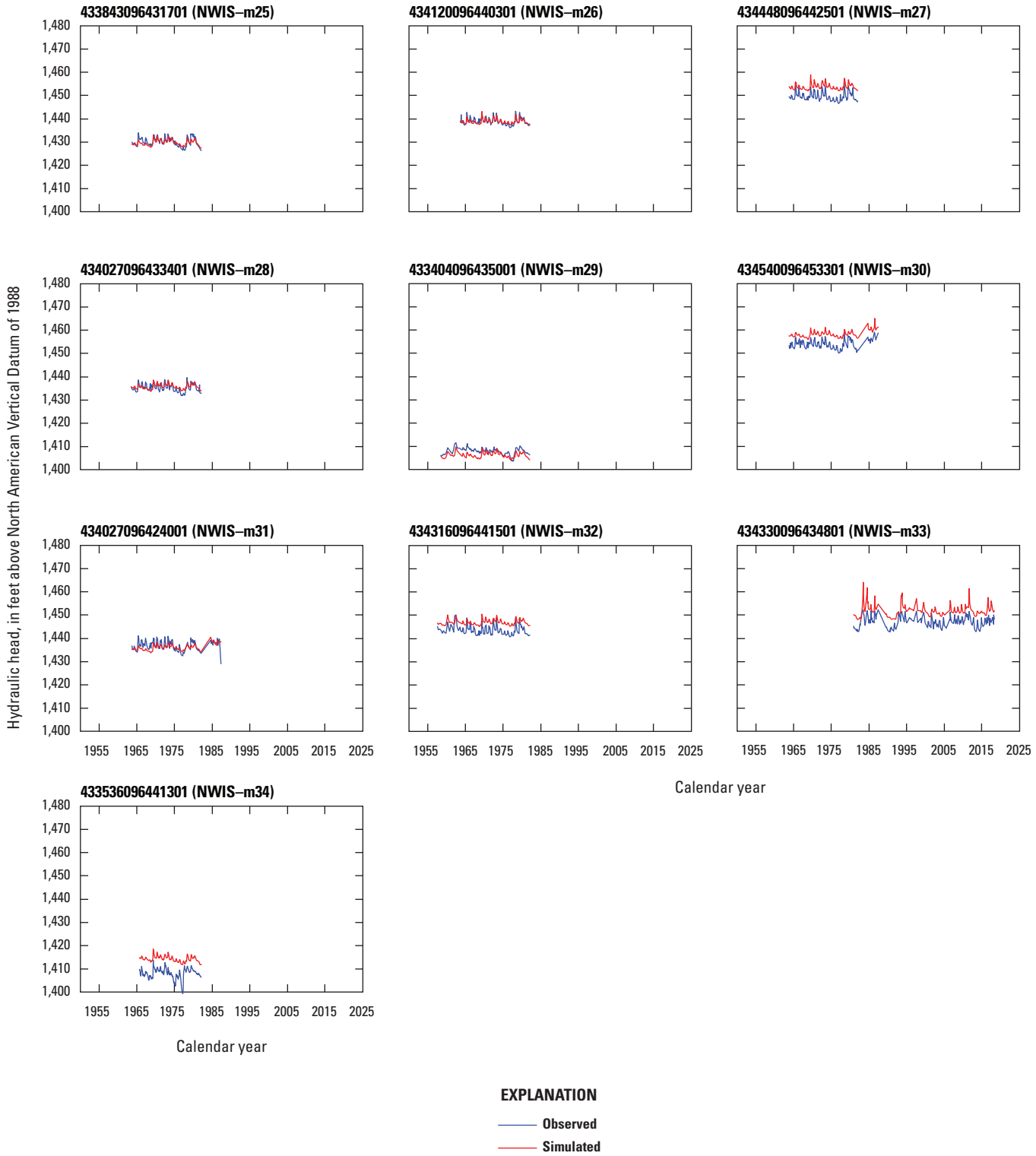

Figure 26. Hydrographs of observed and simulated hydraulic head for selected observation wells completed in the Big Sioux aquifer. Observation well locations are shown in figure 19.—Continued

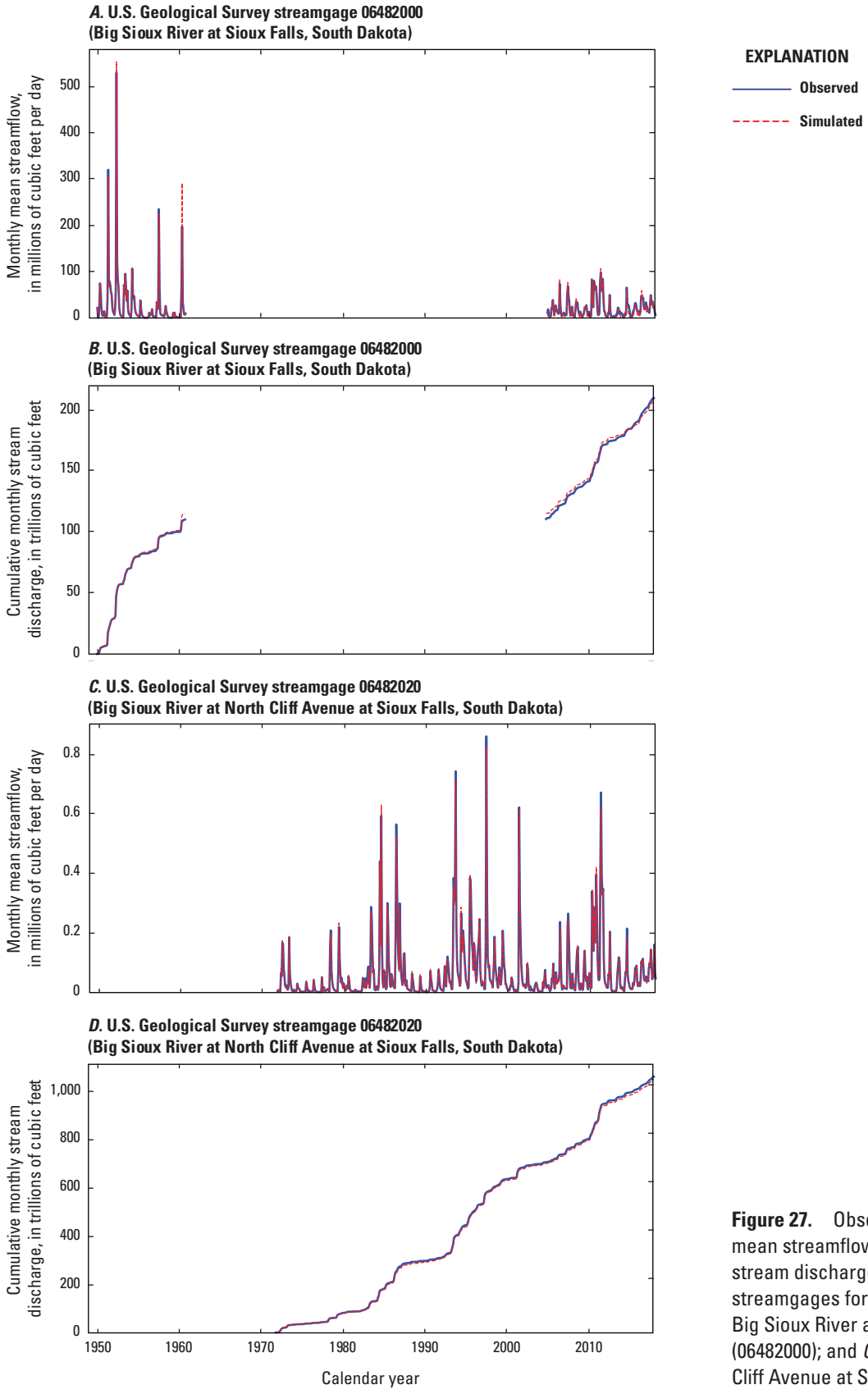

Figure 27. Observed and simulated monthly mean streamflow and cumulative monthly stream discharge at U.S. Geological Survey streamgages for the transient period. *A*–*B*, Big Sioux River at Sioux Falls, South Dakota (06482000); and *C*–*D*, Big Sioux River at North Cliff Avenue at Sioux Falls, S. Dak. (06482020).

for USGS streamgage 06482000 (Big Sioux River at Sioux Falls, S. Dak.) and underestimated at USGS streamgage 06482020 (Big Sioux River at North Cliff Avenue at Sioux Falls, S. Dak.).

Groundwater Flow

The numerical model was assessed by its ability to replicate groundwater-flow directions and hydraulic gradients, interpreted from potentiometric surfaces, for the Big Sioux aquifer as reported by Ellis and others (1969) and Lindgren and Niehus (1992). The simulated groundwater budget also was compared with a groundwater budget presented by Koch (1986). Additional indicators of numerical model performance were groundwater and surface-water interactions and discharge from wells.

Comparison of Simulated Potentiometric Surfaces

Simulated potentiometric surfaces and groundwater-flow directions for the Big Sioux aquifer were compared with those from literature and those described in the "Potentiometric Surfaces" section of this report (figs. 28*A–D*). The simulated potentiometric surface for August 1966 was compared with the potentiometric surface published by Ellis and others (1969; fig. 28*B*); the simulated potentiometric surface for September 1986 was compared with the potentiometric surface published by Lindgren and Niehus (1992; fig. 28*C*); and the simulated potentiometric surface for March 2017 was compared with the potentiometric surface estimated in the "Potentiometric Surfaces" section this report (fig. 28*D*). The simulated potentiometric surfaces generally compared well with previous potentiometric surfaces; however, local differences exist. In general, the simulated potentiometric surfaces were higher in the northern part of the model area and lower in the southern part of the model area compared with those presented in literature (figs. 28*B–D*). The simulated potentiometric surface for August 1966 ranged from about 12 ft higher to about 17 ft lower than what Ellis and others (1969) presented for the Big Sioux aquifer. The simulated potentiometric surface for September 1986 ranged from about 14 ft higher to about 18 ft lower than literature values (Lindgren and Niehus, 1992). The simulated potentiometric surface for March 2017 ranged from about 12 ft higher to 28 ft lower than what was estimated in the "Potentiometric Surfaces" section of this report. The greatest differences between the estimated and simulated potentiometric surfaces were in areas with groundwater withdrawals. Simulated groundwater-flow directions were generally from (1) north to south and (2) from the margins of the Big Sioux aquifer and areas of higher elevation toward rivers and streams (figs. 28*A–D*). Therefore, the character of the simulated groundwater-flow directions agrees favorably with those from literature and this report.

Simulated Groundwater Budget

The simulated groundwater budget characterizes inflows and outflows for the three model layers and includes groundwater fluxes among model layers in addition to inflow from and outflow to storage. Steady-state and mean annual groundwater budgets were calculated (figs. 29*A–B*), and the transient groundwater budgets were summarized for each calendar year (fig. 30). Groundwater withdrawal was not simulated during the steady-state stress period; therefore, the steady-state groundwater budget does not include a groundwater withdrawal component.

The simulated steady-state groundwater budget (fig. 29*A*) for the Big Sioux aquifer consisted of inflows from precipitation recharge (RCH Package) and stream infiltration (SFR and RIV Packages) and outflows from evapotranspiration (EVT Package) and groundwater discharge to streams (SFR, RIV, and DRN Packages). For the Big Sioux aquifer during the steady-state stress period, simulated inflow was 10.8 ft^3/s from precipitation recharge and 2.6 ft^3/s from stream infiltration (fig. 29*A*). Simulated steady-state inflow from groundwater flux to the Big Sioux aquifer from the underlying hydrogeologic units was 17.1 ft^3/s (fig. 29*A*). For the Big Sioux aquifer during the steady-state stress period, simulated outflow was 6.5 ft^3/s from evapotranspiration and 21.7 ft^3/s from groundwater discharge to surface-water features (fig. 29*A*). Simulated steady-state outflow through groundwater flux to the underlying hydrogeologic units was calculated as 2.1 ft^3/s.

Steady-state simulated inflow to the glacial till confining unit was from precipitation recharge and stream infiltration and was 19.2 and 0.5 ft^3/s, respectively (fig. 29*A*). During the steady-state stress period, the glacial till confining unit received inflow from groundwater flux from the Big Sioux aquifer and bedrock aquifers and was 2.0 and 7.5 ft^3/s, respectively. Outflows from the glacial till confining unit were from evapotranspiration and groundwater discharge to streams. Simulated steady-state outflows from the glacial till confining unit were 0.3 ft^3/s for evapotranspiration and 1.4 ft^3/s for groundwater discharge to surface-water features. Outflow through groundwater flux for the glacial till confining unit was 15.6 ft^3/s to the Big Sioux aquifer and 12.0 ft^3/s to the bedrock aquifers (fig. 29*A*).

Simulated steady-state inflow to the bedrock aquifers was from precipitation recharge, stream infiltration, and groundwater flux, and outflow was to evapotranspiration, groundwater discharge to streams, and groundwater flux (fig. 29*A*). Precipitation recharge and stream infiltration were 0.3 and 0.1 ft^3/s, respectively, for the bedrock aquifers in the steady-state stress period (fig. 29*A)*. Total simulated inflow through groundwater flux from the overlying hydrogeologic units was calculated as 12.1 ft^3/s. Simulated outflow from the bedrock aquifers was 0.1 ft^3/s for evapotranspiration and 3.5 ft^3/s for groundwater discharge to surface-water features (fig. 29*A*). Simulated steady-state outflow through groundwater flux to the overlying hydrogeologic units was calculated as 9.0 ft^3/s.

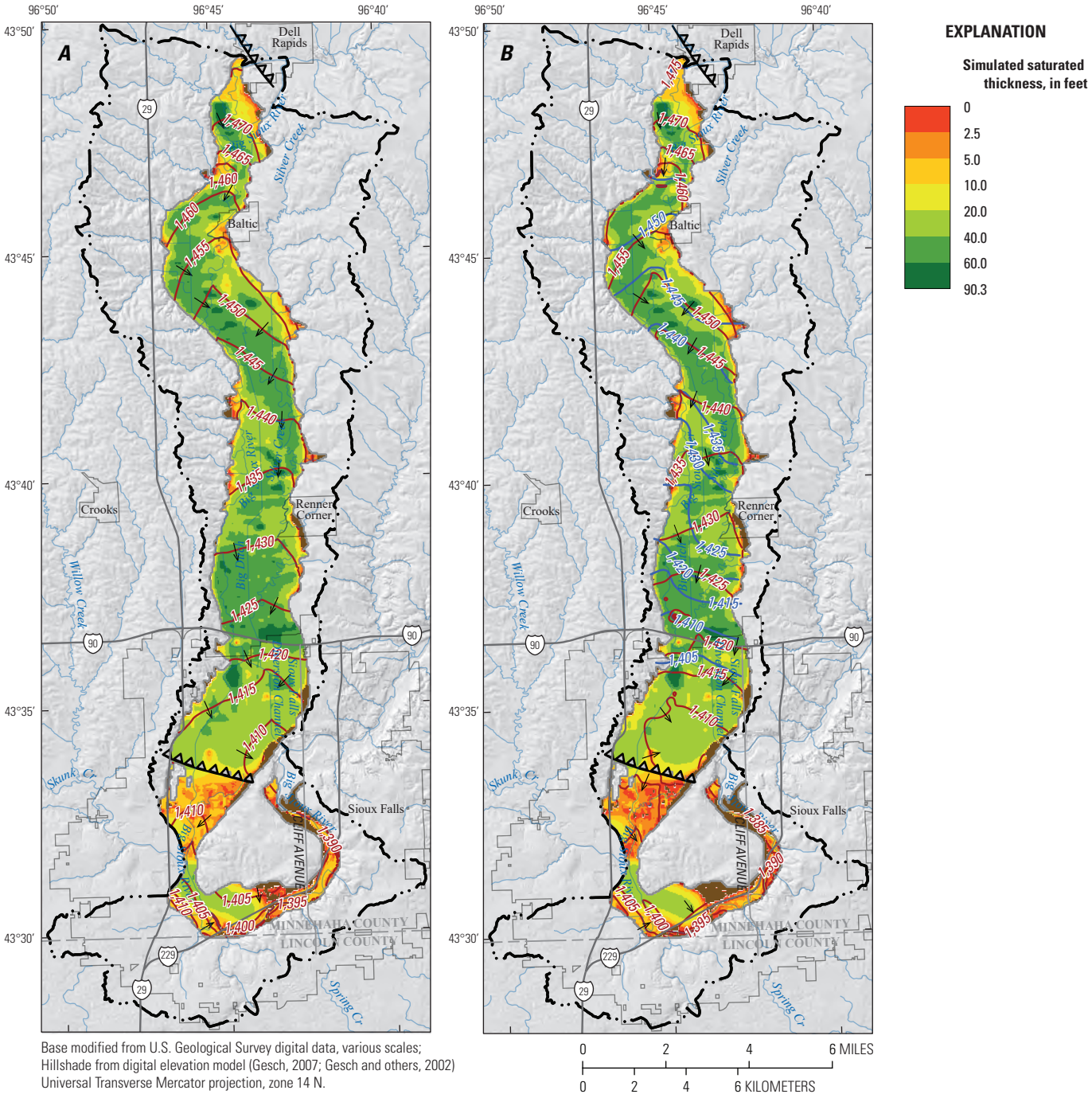

Figure 28. Simulated potentiometric surface, groundwater-flow directions, and saturated thickness of the Big Sioux aquifer for *A*, steady-state conditions; *B*, August 1966; *C*, September 1986; and *D*, March 2017. Estimated potentiometric contours are shown for reference from *B*, Ellis and others (1969; fig. 9); *C*, Lindgren and Niehus (1992; fig. 9); and *D*, March 2017 (fig. 10).

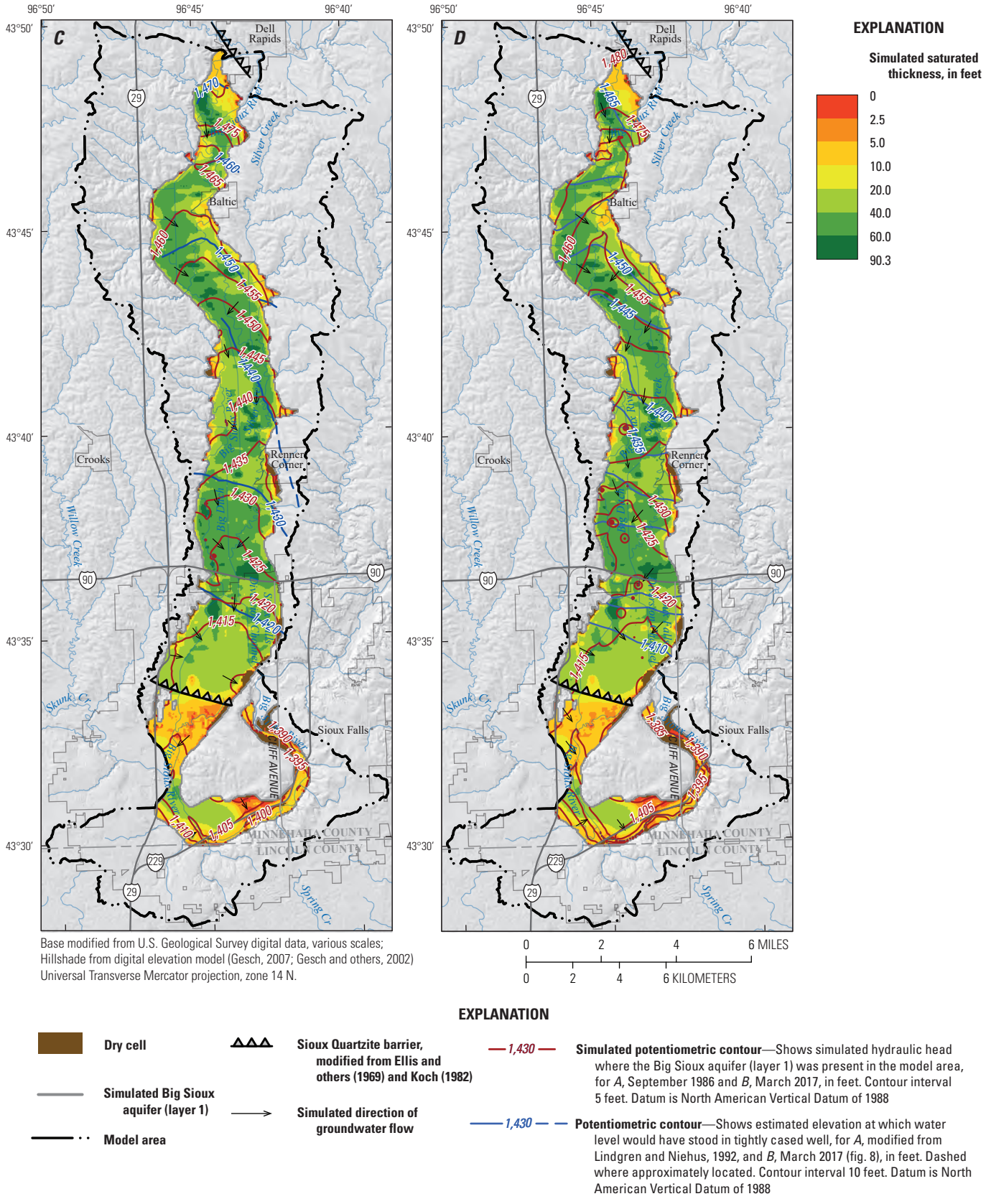

Figure 28. Simulated potentiometric surface, groundwater-flow directions, and saturated thickness of the Big Sioux aquifer for *A*, steady-state conditions; *B*, August 1966; *C*, September 1986;, and *D*, March 2017. Estimated potentiometric contours are shown for reference from *B*, Ellis and others (1969; fig. 9); *C*, Lindgren and Niehus (1992; fig. 9); and *D*, March 2017 (fig. 10).—Continued

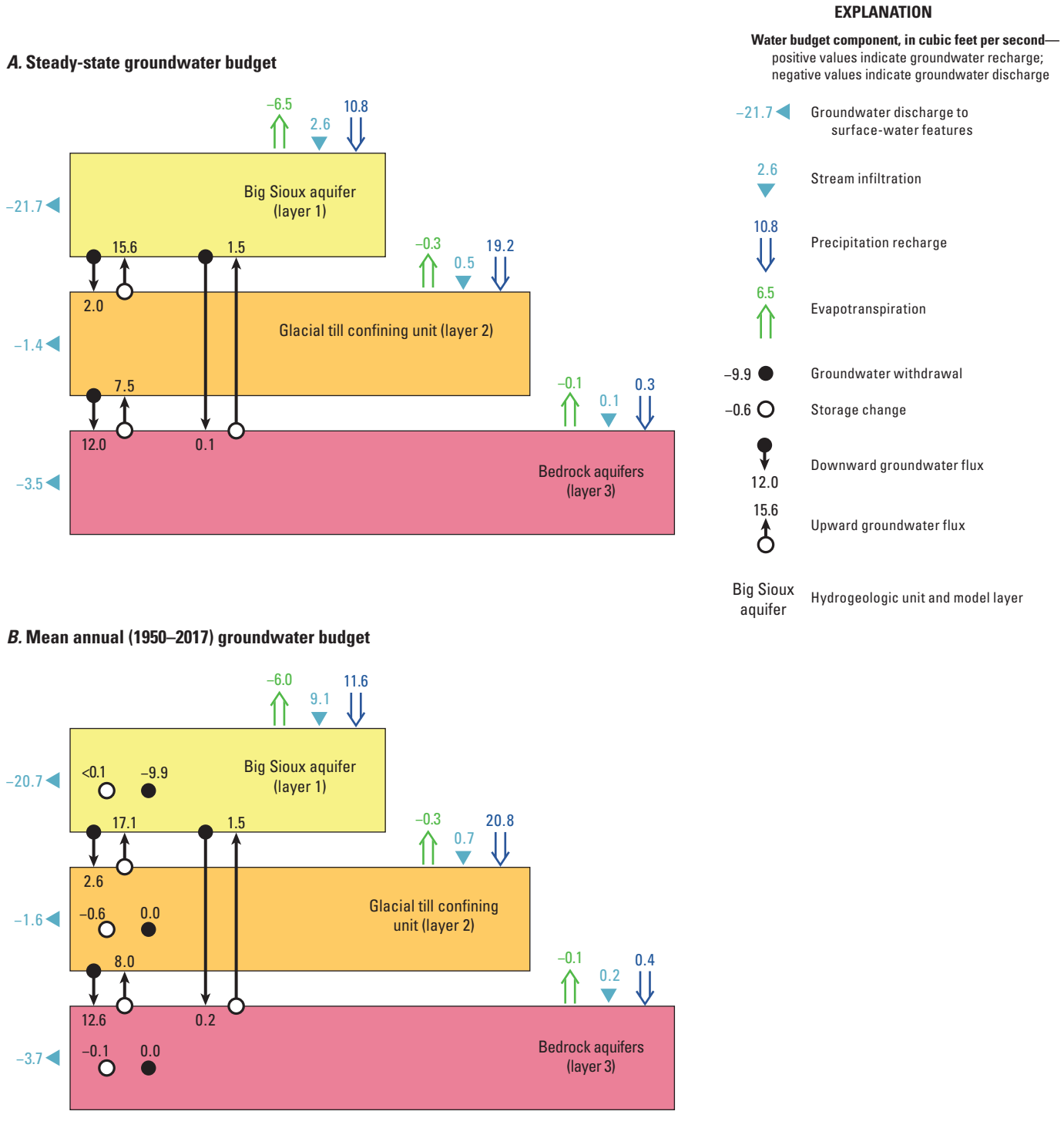

Figure 29. Simulated groundwater budgets for *A*, steady-state budget; and *B*, mean annual (1950–2017) budgets.

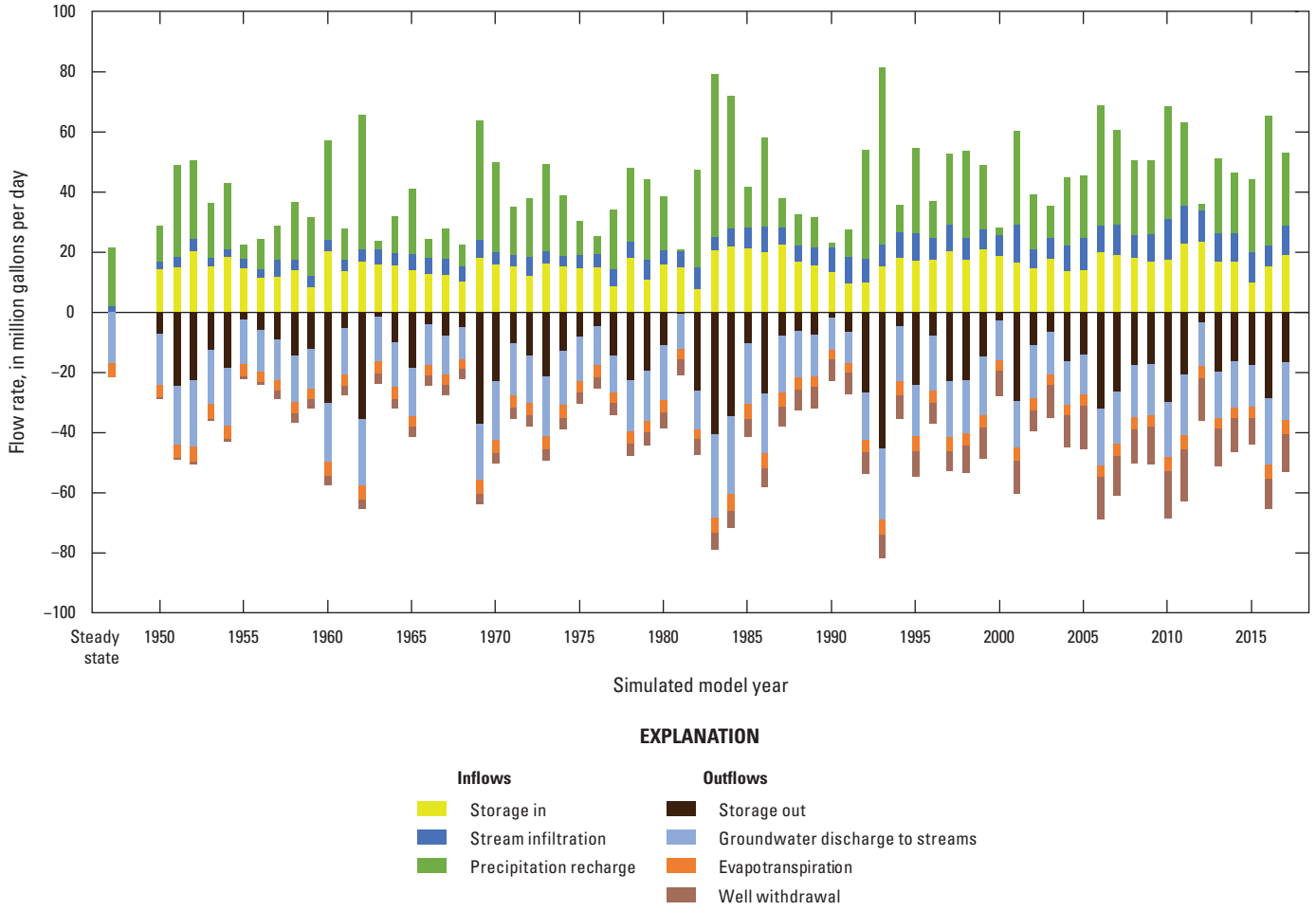

Figure 30. Simulated steady-state and transient annual groundwater-flow budgets. (Data from Eldridge and Davis, 2019.)

Simulated transient groundwater budgets for the numerical model consisted of inflow from storage, streams, and precipitation recharge and groundwater outflow to storage, streams, evapotranspiration, and wells (fig. 30). The length of each bar in figure 30 represents the total magnitude of the groundwater budget for each calendar year and can be used to visually characterize wet and dry periods in the model area; for example, 1993 was climatically wet and has the largest flows for all groundwater budget terms. Simulated groundwater inflow and outflow terms typically fluctuated annually and corresponded with climate variations during 1950–2017; however, groundwater withdrawal increased steadily from about 0.6 Mgal/d in 1950 to about 12.4 Mgal/d in 2017, with a maximum groundwater withdrawal of 17.3 Mgal/d in 2011. Flows to groundwater storage were typically offset by precipitation recharge; for example, during periods of higher precipitation, the simulated groundwater budget indicates an increase in water stored in the aquifers (storage out is greater than storage in), and during periods of lower precipitation, the simulated groundwater budget indicates a decrease in water stored in the aquifers (storage out is less than storage in). The minimum total simulated annual inflow and outflow was about 21.1 Mgal/d in 1981, and the maximum total simulated annual inflow and outflow was about 81.6 Mgal/d in 1993.

Numerical model-simulated mean annual groundwater budgets for 1950–2017 for the Big Sioux aquifer were calculated and compared with those from Koch (1986; table 4). Simulated mean annual inflows for the Big Sioux aquifer calculated from figure 29*B* consisted of 0.3 percent from storage, 23.1 percent from stream infiltration, 29.4 percent from precipitation recharge, and 47.2 percent through groundwater flux from other hydrogeologic units. Simulated mean annual outflows for the Big Sioux aquifer calculated from figure 29*B* consisted of about 52.5 percent groundwater discharge to streams, 15.2 percent to evapotranspiration, 25.1 percent to wells, and 7.1 percent through groundwater flux to other hydrogeologic units.

Previous investigators did not estimate changes in groundwater storage or inflow and outflow through groundwater flux for the Big Sioux aquifer. As a result, simulated inflow and outflow from groundwater storage and groundwater flux were ignored for comparative purposes. Simulated mean annual groundwater storage change was close to zero; therefore, the comparison between the numerical model-simulated

budget and the budget provided by Koch (1986) is acceptable. The rate of groundwater inflow for stream infiltration and precipitation recharge and discharge from groundwater withdrawal was lower than the estimates provided by Koch (1986) (table 4) but simulated mean annual groundwater discharge to streams and evapotranspiration were greater than estimates from Koch (1986) (table 4; fig. 29). Koch (1986) did not estimate the rate of groundwater exchange between the Big Sioux aquifer and underlying hydrogeologic units; however, the numerical model indicated that the exchange of groundwater through groundwater flux among aquifers in the model area is an important component of the groundwater budget for steady-state and transient conditions.

Groundwater and Surface-Water Interactions

Groundwater discharge to and recharge from surface-water features (stream flux) in the model area were used as an indicator of numerical model performance and to indicate the timing and location of surface-water seepage in the model area. The Big Sioux River is commonly understood to be in strong hydraulic connection with the underlying Big Sioux aquifer, with some segments receiving groundwater from the aquifer (gaining reaches) and other segments losing surface water to the aquifer (losing reaches) (Jorgensen and Ackroyd, 1973; Koch, 1982; Neupane and others, 2017). Losing and gaining reaches are not static and can change with time as the hydraulic gradient changes between the stream and underlying aquifer. The rate that water exchanges between the stream and adjoining aquifer depends on the hydraulic gradient and the hydraulic conductivity of the geologic materials between the stream and aquifer, which are normally characterized by the streambed materials (Barlow and Leake, 2012).

Groundwater fluxes were calculated for the steady-state stress period for each cell of the RIV, DRN, and SFR Packages in the model area and were used to illustrate segments of streams and tributaries that were gaining and losing (fig. 31). Groundwater discharge to streams (gaining streams) was observed where the simulated stream flux was negative, and stream infiltration (losing streams) was observed where the simulated stream flux was positive. During the steady-state stress period, groundwater and surface-water exchanges typically were observed in stream segments that intersected the Big Sioux aquifer (fig. 31). Nearly all streams overlaying the glacial till confining unit had zero flux during the steady-state stress period, indicating that in steady-state conditions, these segments were neither gaining nor losing. Much of the Big Sioux River was slightly gaining (0 to 0.05 ft^3/s) but segments north of Baltic and north of Sioux Falls were slightly losing (0 to 0.05 ft^3/s). Big Ditch, a tributary of Silver Creek, was gaining, losing, and neutral in the central, northern, and southern parts, respectively. The southern-most part of the Big Sioux River that flows through the city was primarily gaining.

Streamflow records indicated periods of sustained stream loss (fig. 15); however, these periods of sustained stream loss were not adequately represented by the numerical model. Net groundwater discharge to streams was simulated in every stress period and is indicated by the annual budgets in figure 30 (groundwater discharge to streams [outflow] minus stream infiltration [inflow]). Simulated monthly net groundwater discharge to streams ranged from 2.0 to 23.5 Mgal/d.

Discharge from Wells

In addition to evaluating groundwater discharge to and recharge from surface-water features in the model area, the ability of the calibrated numerical model to adequately simulate groundwater withdrawal was used as an indicator of properly applied model parameters. Reported monthly mean groundwater withdrawal was used as an input for the numerical model; however, MODFLOW–6 can reduce the specified groundwater withdrawal rate for cells that dewater the aquifer to a user-defined percentage of aquifer thickness. Groundwater withdrawals were only in the Big Sioux aquifer; therefore, the numerical model reduced groundwater withdrawal for wells that dewatered the Big Sioux aquifer to 10 percent of the aquifer thickness. The ability of the numerical model to adequately simulate groundwater withdrawal was used to indicate appropriately calibrated model parameters, including horizontal and vertical hydraulic conductivity, aquifer storage properties, precipitation recharge, and evapotranspiration applied in the numerical model. Specified monthly mean groundwater withdrawal applied to the transient part of the numerical model ranged from 0.38 to 24.98 Mgal/d, and simulated monthly mean groundwater withdrawal for the transient part of the numerical model ranged from 0.38 to 22.01 Mgal/d. The reduction of simulated groundwater withdrawal ranged from 0 to about 32 percent with a mean reduction of about 2 percent. Production wells with the largest reduction in simulated groundwater withdrawal were generally the northern-most wells near Renner Corner and Dell Rapids, S. Dak. (fig. 13). Specified monthly mean groundwater withdrawal and simulated monthly mean withdrawal rates are available in the accompanying USGS data release (Eldridge and Davis, 2019).

Numerical Model Parameter Sensitivity

Numerical model parameter sensitivity is a measure of the effect that a change in model input, such as various parameters, has on outputs, such as observation targets. During calibration, PEST++ modifies MODFLOW–6 input files by slightly adjusting a single numerical model parameter, by running the numerical model to generate output files, and by comparing the result to the outputs based on the initial parameter dataset. The change in values calculated at a target observation (Δ *observation*) divided by the change of a parameter value (Δ *parameter*) is the *sensitivity coefficient* or also called *parameter sensitivity*:

$$sensitivity\ coefficient = \frac{\Delta\ observation_i}{\Delta\ parameter_j} \quad (6)$$

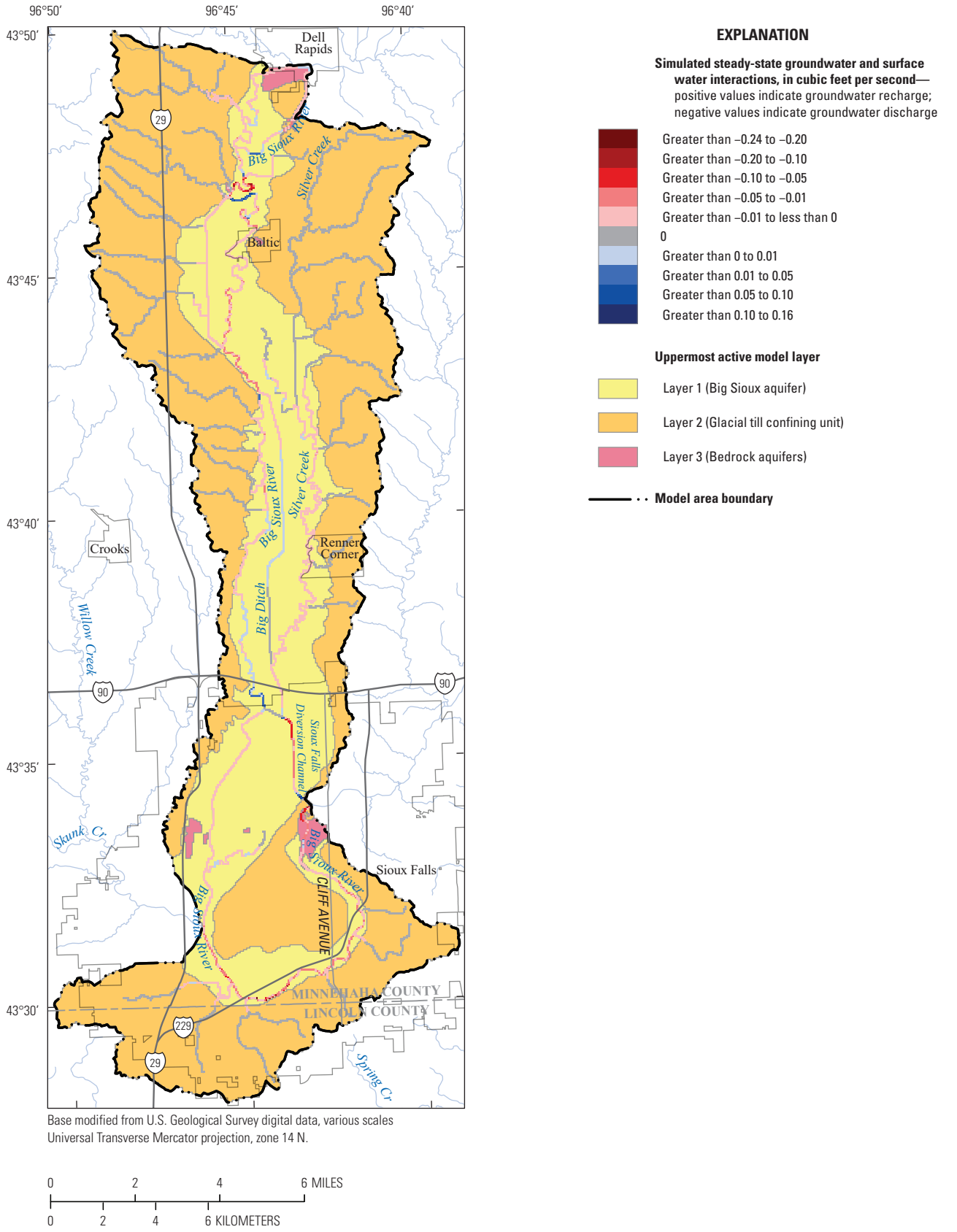

Figure 31. Simulated groundwater discharge to and recharge from streams (stream flux) in the model area during steady-state conditions.

where

$\Delta observation_i$ is the change in simulated value of the ith target observation, and

$\Delta parameter_j$ is the change in value of the jth calibration parameter.

The PEST++ software arranges the sensitivity coefficients in a matrix with i rows and j columns commonly called the Jacobian matrix or sensitivity matrix. Each PEST++ iteration spends most of the time calculating the Jacobian matrix because the numerical model must be run once for each adjusted parameter. The PEST++ software determines a composite sensitivity by using the Jacobian matrix to calculate a value related to the sensitivity with respect to each parameter for all observations (where observations are user-defined weighted). The composite sensitivity of parameter i (csp_i) is defined as follows:

$$csp_i = \frac{[\mathbf{J}^t\mathbf{Q}\mathbf{J}]^{½}_{ii}}{n} \quad (7)$$

where

$\mathbf{J}$ is the Jacobian matrix,

$\mathbf{J}^t$ is the transpose of the Jacobian matrix,

$\mathbf{Q}$ is the weight matrix, and

n is the number of zero-weighted observations (Doherty, 2018).

The composite sensitivity of parameter i is the normalized magnitude of the column of calculated target observations in the Jacobian matrix for that parameter (Doherty, 2018). After calculating the Jacobian matrix, PEST++ provides the composite parameter sensitivity for each parameter with and without regularization, where regularization is the ability to limit parameter changes in PEST++ by linking that parameter to a specific value or to other parameters. During the calibration process, changes in parameters with the greatest composite sensitivity generally have the greatest effect on numerical model outputs. Specifically, the most sensitive parameters or parameter groups have the greatest effect on results at calibration targets used during calibration.

Composite sensitivities without regularization were calculated by PEST++ for the calibrated numerical model parameters and were averaged by parameter group. The parameter group with the highest mean composite sensitivity was the recharge multiplier parameter group, which was representative of the recharge multiplier applied to the model. The parameter groups with the next highest mean composite sensitivity were the evapotranspiration multiplier and specific yield parameter groups, which were representative of the evapotranspiration multiplier and specific yield parameters applied to the model. The lowest mean composite sensitivities were for parameter groups for specific storage, streambed hydraulic conductivity, horizontal hydraulic conductivity, and vertical hydraulic conductivity, which were representative of the specific storage, streambed hydraulic conductivity, horizontal hydraulic conductivity, and vertical hydraulic conductivity parameters applied to the model (fig. 32). The recharge multiplier parameter group was 5 times more sensitive than the evapotranspiration multiplier parameter group, 6 times more sensitive than the specific yield group, 18 times more sensitive than the specific storage group, 63 times more sensitive than the streambed hydraulic conductivity group, 89 times more sensitive than

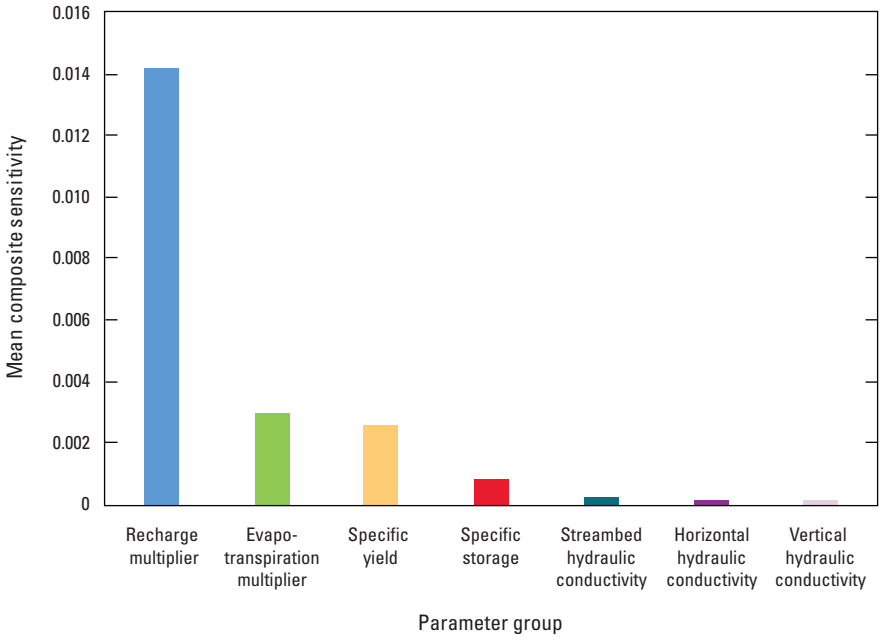

Figure 32. Mean numerical model parameter relative sensitivity by parameter group used in numerical model calibration.

the horizontal hydraulic conductivity group, and 120 times more sensitive than the vertical hydraulic conductivity group (fig. 32).

Model Simplifications, Assumptions, and Limitations

Numerical groundwater-flow models, by design, are simplified representations of complex natural systems and, as a result, rely on assumptions made during numerical model construction that lead to limitations in use and uncertainty in numerical model results. Simplifications, assumptions, and limitations for the numerical model affected discretization, aquifer representation, stream and stream flux representation, groundwater withdrawals, calibration processes, and sensitivity analysis.

Discretization of the model area into a uniform grid of 200 by 200 ft square cells resulted in a simplified representation of the aquifer and created inaccuracies in the total aquifer volume and the location of some aquifer boundaries represented in the numerical model. Aquifer properties were averaged and uniform in each model cell; however, actual aquifer material could be highly variable in each cell. The numerical model may misrepresent the effect of localized stresses, such as additional groundwater withdrawal, resulting from the spatial simplification of hydraulic properties. The numerical model was temporally discretized into monthly periods and required scaling daily rates into representative monthly rates for numerical model input and calibration targets. Daily streamflow, groundwater withdrawal, and precipitation recharge were scaled to representative monthly rates and resulted in the smoothing of maximum daily rates. The simplified temporal discretization, and to some extent spatial discretization, limited the ability of the numerical model to represent maximum water levels and streamflow.

Conceptually and numerically, the model was simplified in aquifer representation. The Split Rock Creek aquifer was included in the bedrock layer of the model based on the assumption that the connection between the Split Rock Creek and Big Sioux aquifers is negligible. Additionally, the Big Sioux aquifer was simplified by truncating its northern and southern boundaries where highs in the Sioux Quartzite have been observed near Dell Rapids and Sioux Falls, respectively, although the aquifer continues adjacent to the Big Sioux River. Both simplifications were assumed to have negligible effect on the numerical model results for the Big Sioux aquifer in the study area.

Boundary fluxes for the glacial till confining unit and bedrock layers were not included in numerical model construction because of the lack of water levels for these layers and their assumed small contribution to the overall water budget. Numerical model boundaries were determined by the drainage basin boundary between USGS streamgages 06481000 and 06482020 based on the assumption that inflows and outflows to adjacent areas along the drainage basin boundary were nearly equal, resulting in negligible effect on the water budget. Additionally, water inflow to the model area was assumed to be dominated by recharge from precipitation and streamflow, and inflows from the glacial till confining unit and bedrock aquifers adjacent to the model area were assumed to be negligible in comparison. Similarly, outflows for evapotranspiration and streamflow were assumed to greatly exceed outflows along the numerical model boundaries to adjacent areas so that localized fluxes also would have a negligible contribution to the overall numerical model water budget.

Stream cells also were simplified based on the spatial discretization of the numerical model using uniform square cells that were 200 ft on each side. Stream widths were interpolated between the uppermost upstream and lowermost downstream cells for each stream segment based on values estimated from areal imagery. Streambed bottom altitudes were manually adjusted to ensure that streams segments always flowed to lower elevations for connected cells. Additionally, stream channels were represented with rectangular cross sections with a uniform Manning's roughness coefficient for each segment. The ability of the numerical model to adequately calculate stream stage has not been evaluated based on the simplified stream representation, and the use of the numerical model to determine stream stage should be avoided. An additional model limitation was the use of measured monthly mean streamflow, instead of estimated stream base flow, for input, calibration targets, and assessment. Base flow commonly is used in numerical groundwater-flow models because base flow represents the portion of streamflow that is directly from groundwater discharge and does not include contributions to streamflow from direct overland runoff. However, total streamflow was used in the numerical model because the model area was relatively small compared to the total size of the Big Sioux River Basin, because the streamflow records were extensive and inclusive for the numerical model timeframe, and because of the assumption that overland runoff was a small contributor to total streamflow in the model area. Additionally, the discharge to the surface-water diversions in the model area is controlled by the city of Sioux Falls based on total streamflow at the streamgages in the model area; and, as a result, the estimates for the diversions used in the numerical model also were based on total streamflow.

Groundwater withdrawals from wells were simplified in the numerical model construction. Monthly mean rates for production wells within and about 6 miles north of the Sioux Falls Regional Airport area were based on available records for 1995–2017 and were used as input for that period; however, withdrawal before 1995 was estimated based on a regression relation of total withdrawals to population. Total withdrawals for production wells near Baltic and Dell Rapids were distributed proportionately to each well because rates for each individual well were not available. Additionally, simulated withdrawal at some wells was reduced using the auto-reduction setting in MODFLOW–6 that reduced withdrawal rates if the calculated water level in a numerical model cell was at or below 10 percent of the cell thickness. These

simplifications create localized inaccuracies in well withdrawal rates and in simulated absolute water-level drawdown estimates; however, the mean simulated reduction in well withdrawal was 2 percent and was considered to have a minimal effect on numerical model results. Relative water-level reductions, however, were reproduced in water-level hydrographs for observation wells in the model area (fig. 26).

The inability to characterize processes, properties, and hydrologic outputs in complex numeric groundwater systems can result in a nonuniqueness of the calibration process (Leaf and others, 2015); therefore, different combinations of hydraulic properties could be applied to the numerical model that could result in an acceptable comparison of observations and model-simulated values. The hydraulic properties determined through numerical model calibration minimized the difference between observations and model results, and these properties compared well with estimates from previous publications. Discrepancies between reported horizontal hydraulic conductivity values and calibrated horizontal hydraulic conductivity likely is because of the methods of estimation and the spatial scale used to represent the aquifer. The final distribution of numerical model parameters determined during calibration, in addition to the resulting groundwater levels and flow directions, was based on the spatial and temporal availability of hydrologic data. In parts of the model area (for example, in the glacial till confining unit and the bedrock aquifers), extensive hydrologic data were not available for use in numerical model calibration. Therefore, the results of the numerical model, determined through the calibration process, could be substantially different where little or no calibration information existed.

Numerical model calibration of hydraulic conductivity and storage parameters was simplified to optimize the time required for calibration. Horizontal and vertical hydraulic conductivity are spatially variable in the model area; however, the degree of heterogeneity that was represented in the numerical model was controlled by estimated values at pilot points distributed in the model area in each model layer. The hydraulic conductivity assigned to each model cell for each model layer was an interpolation of the calibrated values at pilot points. This simplification allowed for heterogeneity in the aquifer materials, but abrupt localized changes in heterogeneity were not represented because of interpolation. In contrast, uniform values for specific storage and specific yield were used for each model layer. Uniform values were used to reduce numerical model calibration time and because localized specific storage estimates were not available. Most of the simulated water-level changes were underestimated by the numerical model. The underestimate of water-level changes could indicate that aquifer storage was overestimated during numerical model calibration. A spatially variable representation of aquifer storage may have improved the comparison of observed and simulated water-level changes in the model area; however, calibrated values were within reasonable range of estimates from literature (table 3).

Composite scaled parameter sensitivities can provide insight into which parameters are important during the calibration process; however, other measures of model performance are available. Parameter sensitivity alone does not account for parameter covariance or correlation (Anderson and others, 2015). For example, parameters with high composite scaled sensitivities such as the recharge multiplier parameter, also may be correlated with other parameters such as those in the evapotranspiration multiplier and specific yield parameter groups. An analysis of parameter covariance and correlation is not included in this report.

Numerical model limitations include construction design for thin deposits, streamflow representation, and calibration data for the glacial till confining unit and bedrock aquifers. Thin model cells commonly are calculated as dry although those areas may be saturated in reality; for example, in many stress periods cells representing the Big Sioux aquifer in layer 1 were simulated as being dry. Dry cells were predominately calculated along the aquifer boundaries and in the southern part of the model area where the aquifer was thinnest. Although minimum thicknesses of 10 and 5 ft were applied to active cells in layers 1 and 2, respectively, areas where the aquifer thins may not be well represented by the numerical model.

Analysis of Groundwater and Surface-Water Interactions

Groundwater from an aquifer interacts with the surface waters of nearby streams and can flow into a stream when the water table altitude exceeds the altitude of the stream surface (Barlow and Leake, 2012). Conversely, stream water can flow into an aquifer if the stream surface altitude exceeds the water table altitude in the aquifer. Stream segments that receive groundwater from an aquifer are called gaining reaches, and stream segments that provide water to an aquifer are called losing reaches. A single stream could contain gaining and losing reaches depending on the hydraulic gradient of the reach, the hydraulic conductivity of its streambed material, the streambed thickness, and the effect of nearby withdrawal wells.

As a well withdraws water from an aquifer, a cone of depression can be observed in the water levels surrounding the well (Heath, 1983). The greatest water-level drawdown in the cone of depression is at the well, and drawdown decreases to zero as the distance from the well increases. The differences of water levels in the cone of depression create a hydraulic gradient that routes groundwater flow from the aquifer to the well. The cone of depression can grow out away from the well over time and at constant withdrawal rates.

Initially, the primary source of groundwater for a withdrawal well is supplied from aquifer storage, which is groundwater residing in the pores, fractures, and other voids in the sediments and rocks that constitute the aquifer (Barlow

and Leake, 2012). Aquifer storage supplies groundwater to the well, and other sources become available as the cone of depression grows enough to capture those sources. Therefore, as other water sources are captured, continued groundwater withdrawal either will increase inflow to the aquifer or decrease outflow from the aquifer. Sources of increased inflow may be nearby streams, other surface-water features, or adjacent aquifers.

Streamflow capture is the portion of water withdrawn by a well from an aquifer that is provided by a hydrologically connected stream or river. Sources of water other than streamflow can be captured by groundwater withdrawal. Groundwater that is available for evapotranspiration also can be captured. Additionally, capture can come from storage, spring flow, lakes, or other wells. Total capture is the sum of the fractions of changes in withdrawal-induced inflow to and outflow from the aquifer—from sources such as streamflow, evapotranspiration, storage, spring flow, lakes, and other wells (Barlow and Leake, 2012).

If the volume of captured groundwater from these sources is great enough, then groundwater supplies for these sources could be affected. For example, a well that withdraws enough water to reduce or eliminate the groundwater flow from an aquifer to a gaining stream could cause the stream reach to change from gaining to losing. Additionally, a well could capture a portion of groundwater withdrawn by another well.

The timing and magnitude of streamflow capture can be estimated using a numerical groundwater-flow model. A streamflow capture map consists of contours representing the amount of streamflow that is captured (shown as a percentage of the withdrawal rate) by a hypothetical well at a constant withdrawal rate for a given period (Leake and others, 2008). The numerical groundwater-flow model is used to calculate capture in three steps. First, the numerical model is run without withdrawal at a hypothetical well, and baseline groundwater flows are recorded. Second, the numerical model is run many times with each run moving the location of a single hypothetical well at a constant withdrawal rate. Third, the differences in groundwater distribution for the streams, storage, and evapotranspiration between the baseline numerical model run and the hypothetical well numerical model runs are calculated. These differences are expressed as a percentage of the hypothetical well withdrawal rates and then interpolated spatially.

The spatial distribution of simulated streamflow capture is useful for several reasons. Streamflow capture maps provide water managers insights on well field design and permit applications by providing estimates of the sources of groundwater that potentially supply a well. Additionally, streamflow capture maps show the effect of withdrawal on related water sources. For this analysis, two methods were used to map streamflow capture. First, streamflow capture was calculated and mapped using a steady-state numerical groundwater-flow model to determine the eventual or maximum capture in the model area (eventual capture analysis). Second, a transient numerical groundwater-flow model was used with all model stresses held constant to calculate the timing of capture from storage, streamflow, evapotranspiration, and existing wells for a period of 30 years at three hypothetical wells based on three different withdrawal rates (timing-of-capture analysis). Eventual and timing-of-capture analyses are described in the following sections.

Eventual Capture

Eventual capture was calculated in the model area using a steady-state numerical groundwater-flow model, hereafter referred to as the "eventual capture model," and was identical to the steady-state stress period in the transient numerical model, except that surface-water diversions to the Sioux Falls Diversion Dam and Weir and the wetlands pump were used in the SFR Package. The eventual capture analysis indicates the maximum or eventual extent and magnitude of capture derived from sources other than groundwater storage that could be incurred for wells completed in the Big Sioux aquifer in the model area if groundwater withdrawal continued indefinitely. Water supplied to groundwater withdrawals from aquifer storage is not included in the eventual capture analysis because the analysis was completed using a steady-state numerical groundwater-flow model that does not include calculations of storage. In the eventual capture model, the diversion rate for the Sioux Falls Diversion Dam and Weir was equal to the mean daily diversion rate used in the transient numerical model from June 1961 through December 2017, and the diversion rate for the wetlands pump was equal to the mean daily diversion rate for 2017.

The following steps from Barlow and Leake (2012) were used for the eventual capture analysis to create the eventual streamflow capture map: (1) the steady-state model was run without hypothetical withdrawal, and numerical model-computed water budgets for groundwater discharge to streams and evapotranspiration were recorded; (2) the model was run again but with a single hypothetical well in a specified model cell at a constant withdrawal rate, and model-computed budgets were recorded again for streams and evapotranspiration; (3) the model-computed water budgets from step 2 were subtracted from the water budgets calculated in step 1 and divided by the hypothetical well withdrawal rate; and (4) steps 2 and 3 were repeated for every cell at which hypothetical withdrawal could exist. Hypothetical withdrawals were only applied to model layer 1 (Big Sioux aquifer). The results from step 4 provide a spatial estimate of the percentage of the hypothetical withdrawal rate that is provided by available sources of water (capture) and were either reduced groundwater discharge to streams (stream capture) or decreased evapotranspiration (evapotranspiration capture) in the model area. The change in all groundwater budget terms (step 2), resulting from increased hypothetical withdrawal must sum to the hypothetical withdrawal rate, and as a result, total capture for each hypothetical well will sum to 100 percent. For example, a cell with 80 percent streamflow capture will have 20 percent evapotranspiration capture.

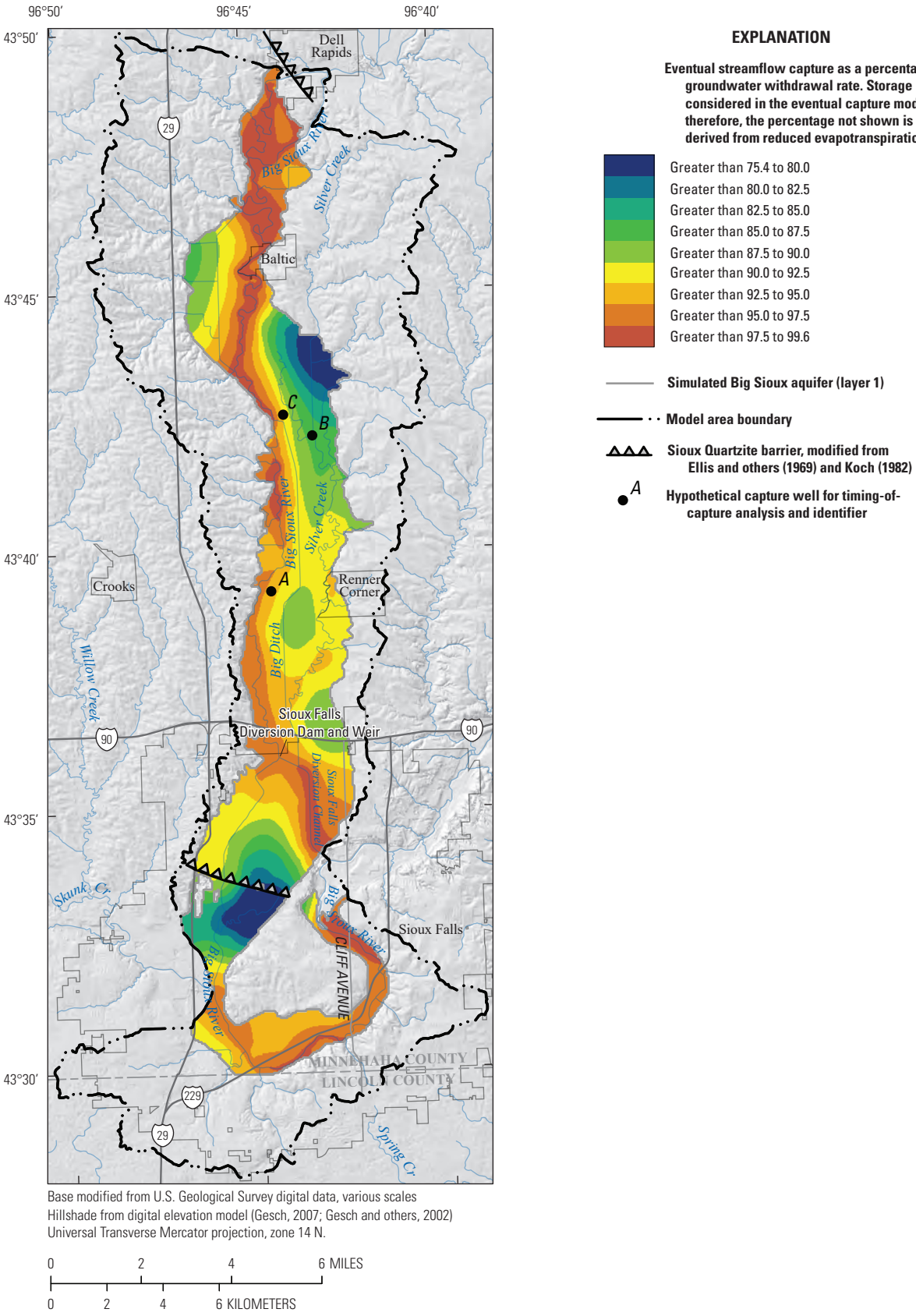

Figure 33. Spatial distribution of eventual streamflow capture and locations of hypothetical wells used for timing-of-capture analysis.

The steps defined in the previous paragraph were completed using the eventual capture model with a hypothetical well withdrawing water at 450.0 gal/min in all cells representing the Big Sioux aquifer (layer 1) in the model area (fig. 33). Calculated sources of groundwater to wells in the eventual capture model were from surface-water features (SFR, RIV, and DRN cells). The sum of water budget changes from these sources was used to calculate the total groundwater discharge to streams in the model area. The only other source of outflow available for capture in the eventual capture model was evapotranspiration. The results from step 4 were mapped for groundwater budget terms relating to groundwater discharge to streams (streamflow capture) and are expressed as the percentage of the hypothetical groundwater withdrawal rate (fig. 33). Storage is not considered in the eventual capture model; therefore, the remaining percentage not shown in figure 33 is the percentage of capture derived from reduced evapotranspiration.

Although the eventual streamflow capture map cannot provide information on the timing of the capture, the map can be used to indicate areas of high and low maximum streamflow capture. Additionally, the eventual capture map can be used to indicate areas of sustainable groundwater resources if streamflow is available for capture. The eventual capture map shows areas of higher streamflow capture (greater than 95 percent) adjacent to the Big Sioux River north of the city of Sioux Falls and along the lower part of the Sioux Falls Diversion Channel (fig. 33). Areas of lower streamflow capture were simulated along aquifer boundaries and near the southern Sioux Quartzite barrier (fig. 33). The eventual capture model results were consistent with previous studies and observations that the Big Sioux River is under strong hydraulic connection with the Big Sioux aquifer. The eventual capture analysis indicates that continuous groundwater withdrawal near the Big Sioux River likely includes a high fraction of surface water.

Timing of Capture

The timing of capture was determined using a transient numerical groundwater-flow model to determine the likely captured water sources for 30 years of groundwater withdrawal at three hypothetical wells using three different withdrawal rates and is hereafter referred to as the "timing-of-capture model." The timing-of-capture model was constructed by modifying the numerical model in the following ways: (1) the model was temporally discretized using an initial steady-state stress period followed by 30 annual stress periods with 12 time steps in the first 5 years; (2) recharge, evapotranspiration, and stream inflow for 1949 were used and held constant for the model timeframe; (3) surface-water diversions at the Sioux Falls Diversion Dam and Weir and the wetlands pump were the mean daily rates for 2017 and held constant for the model timeframe; (4) withdrawals from wells currently completed in the Big Sioux aquifer in the model area (background withdrawals) were included at the mean daily rate for 2017 and held constant during the steady-state and transient stress periods; and (5) withdrawals from hypothetical wells were only during the transient stress periods. At each of the three hypothetical wells, three constant withdrawal rates were simulated for the timing-of-capture analysis. Simulated background withdrawals from existing wells were allowed to reduce if the withdrawal reduced the saturated thickness of the Big Sioux aquifer at existing wells to 10 percent of the aquifer thickness. The rate of withdrawal at the hypothetical well was not allowed to reduce.

A four-step process, similar to the process used to create the eventual capture map, was used to generate capture curves. Capture curves can be used to estimate the timing and source of water to the hypothetical wells throughout the period represented in the timing-of-capture model. Only three hypothetical wells were selected for the timing-of-capture analysis. The three hypothetical well locations were selected based on the following criteria: within a publicly-owned land parcel, greater than 0.25 mile from another production well, and in an area with high calibrated values of hydraulic conductivity and transmissivity (figs. 13, 21, and 33). The timing-of-capture model was run without the hypothetical well and then run at three different withdrawal rates for each of the hypothetical wells.

The three withdrawal rates for the hypothetical wells used in the timing-of-capture analysis were 112.5, 450.0, and 900.0 gal/min. The resulting groundwater budget terms were subtracted from the budget terms calculated by the model run without the hypothetical well for each stress period and then divided by the well withdrawal rate. This process was used to calculate capture percentages and generate capture curves. Capture curves represent the simulated groundwater-flow model budget component without a hypothetical well, subtracted from corresponding simulated groundwater-flow model budget component from the model with the hypothetical well, divided by the hypothetical well withdrawal rate, and converted to a percentage. The capture percentages were plotted for every model stress period and time step (fig. 34).

The resulting capture curves can be used to determine the timing and magnitude of capture compared to the eventual capture analysis, which can only provide the magnitude and extent of maximum capture. Withdrawal from each hypothetical well initially is provided by reductions in storage in the model area (storage change; fig. 34). With time, the source of water to each hypothetical well transitions from predominantly storage-dominated supply to capture-dominated supply (indicated by the intersection of the storage depletion curves and stream capture curves in figure 34). This transition indicates that the primary source of water to the hypothetical wells after a period of time is from either reduced streamflow (stream capture), reduced background withdrawal (well capture), or reduced evapotranspiration (evapotranspiration capture). Capture calculated at hypothetical well A was dependent on the applied withdrawal rate and is indicated by the differences in capture curves derived from different withdrawal rates for similar terms in figure 34. Capture calculated at hypothetical

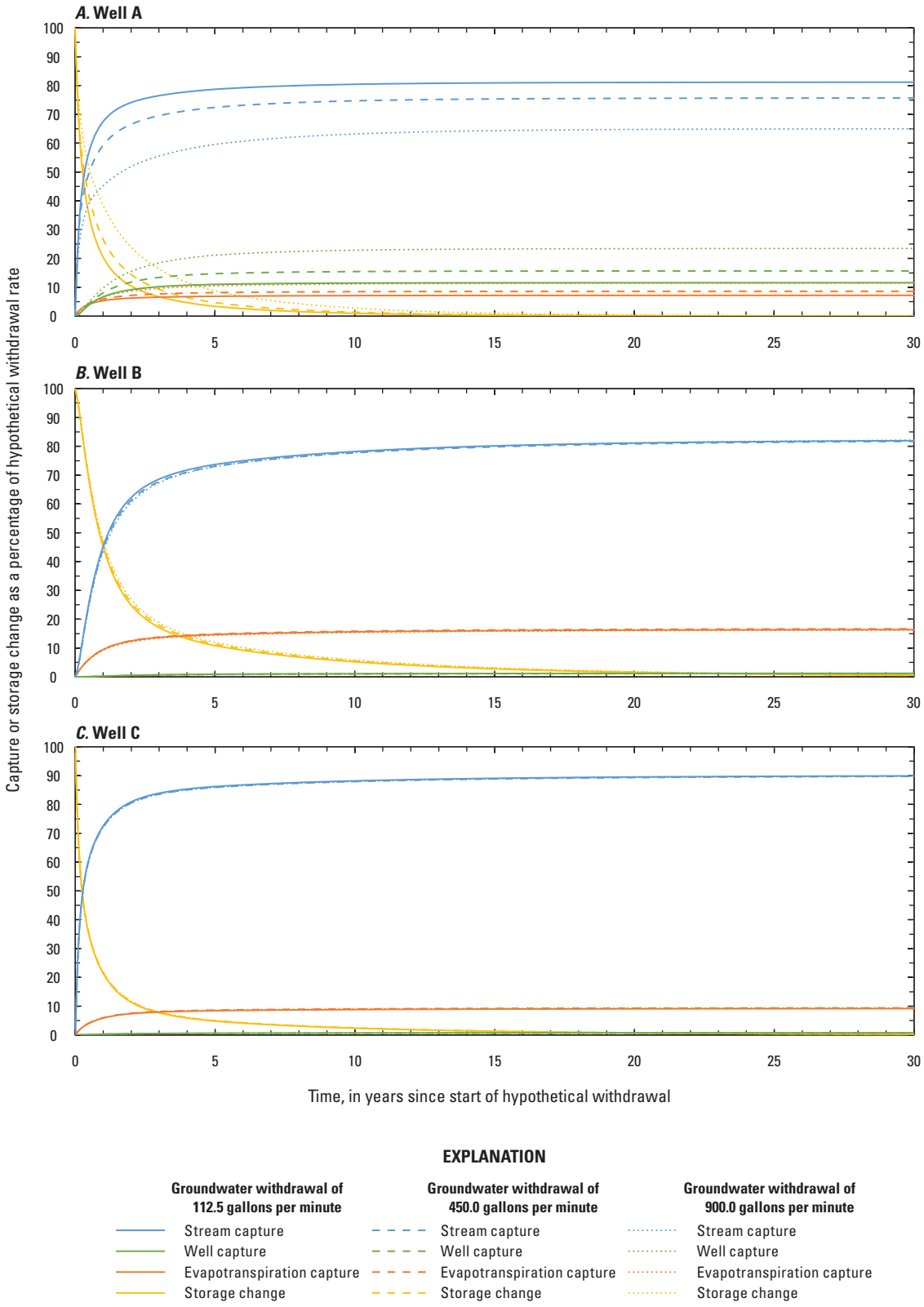

Figure 34. Curves for streamflow capture, evapotranspiration capture, well capture, and storage change for hypothetical well withdraws of 112.5, 450.0, and 900.0 gallons per minute for a 30-year period at *A*, well A; *B*, well B; and *C*, well C.

wells B and C was independent of the withdrawal rate and is indicated by the small differences in capture curves derived from different withdrawal rates for similar terms in figure 34.

Supply for all three hypothetical wells became capture-dominated after only a short period of continuous withdrawal. Hypothetical well A transitions from storage-dominated supply to streamflow capture dominated supply after about 0.3 year at a withdrawal of 112.5 gal/min and after about 0.8 year at a withdrawal of 900.0 gal/min. Hypothetical wells B and C transition to streamflow capture dominated supply after about 1.1 and 0.3 years, respectively, regardless of the withdrawal rate. Capture stabilized for well A after about 10–15 years, and streamflow capture was between about 65 and 81 percent, dependent on the applied withdrawal rate. Evapotranspiration capture stabilized at about 9–11 percent, and well capture stabilized at about 11–23 percent. Capture stabilized for hypothetical well B after 20–25 years of withdrawal, and capture stabilized for hypothetical well C after about 10–15 years. Capture for well B stabilized at about 82 percent for streamflow capture, about 17 percent for evapotranspiration capture, and about 1 percent for well capture. Capture for well C stabilized at about 90 percent for streamflow capture, 9 percent for evapotranspiration capture, and 1 percent for well capture. Capture for wells B and C stabilized at similar percentages regardless of the applied withdrawal rate.

Withdrawal at hypothetical wells A, B, and C also affected background withdrawal to various degrees. Hypothetical well A had the greatest reduction in background withdrawal compared to wells B and C. Withdrawals from well A reduced background withdrawal between 12.4 and 190.3 gal/min after 5 years of withdrawal at 112.5 and 900.0 gal/min, respectively, and between 13.1 and 211.2 gal/min after 30 years of withdrawal at 112.5 and 900.0 gal/min, respectively. Withdrawals from well B reduced background withdrawal between 1.0 and 7.2 gal/min after 5 years of withdrawal at 112.5 and 900.0 gal/min, respectively, and between 1.4 and 10.2 gal/min after 30 years of withdrawal at 112.5 and 900.0 gal/min, respectively. Withdrawals from well C reduced background withdrawal between 0.7 and 4.8 gal/min after 5 years of withdrawal at 112.5 and 900.0 gal/min, respectively, and between 0.9 and 6.0 gal/min after 30 years of withdrawal at 112.5 and 900.0 gal/min, respectively.

Capture Analysis Limitations

Capture analysis has limitations from mathematical biases and from assumptions in the methods. Most mathematical biases are from the reliance of capture calculations on the principle of superposition and its application to linear groundwater systems; however, the principle of superposition can be applied to mildly nonlinear groundwater systems (Reilly and others, 1987), such as those that simulate evapotranspiration in an unconfined aquifer. Other computational biases in capture analyses arise from the applied hypothetical withdrawal rate in nonlinear numerical groundwater-flow models. Nadler and others (2018) tested and quantified capture bias, the overestimation and underestimation of capture, using capture maps derived from nonlinear numerical groundwater-flow models. Capture bias was determined to be larger for hypothetical wells placed farther from streams compared to those placed closer to the same stream and larger in areas of low hydraulic conductivity. Capture bias was most sensitive to the extinction depth of evapotranspiration, model representation of stream incision, withdrawal rates, and stream continuity (Nadler and others, 2018). Capture bias was determined to be least sensitive to specific yield, streambed hydraulic conductivity, the maximum rate of PET, horizontal grid discretization, representation of a stream as a specified head boundary (SFR Package or other MODFLOW Packages), and number of model layers (Nadler and others, 2018).

Bias was minimized in the timing-of-capture analysis for this study by placing the hypothetical wells close to the streams and in areas with higher hydraulic conductivity and transmissivity. Additionally, bias was considered and shown in the timing-of-capture analysis by using three withdrawal rates for each of the three hypothetical wells (fig. 34). Well A showed a higher capture bias, indicated by the differences in capture curves for the three withdrawal rates, compared to the curves from wells B and C. The bias differences among the three wells indicate that the aquifer response to stress is more nonlinear near well A compared to the aquifer response at wells B and C. Additionally, the capture calculated at well A could be affected because well A is closer to several production wells in the model area than wells B and C (figs. 13 and 33).

Several assumptions used for constructing the capture analysis models also affected results. Primarily, model stresses, including the withdrawal rates from the hypothetical wells, were assumed to be constant, and this assumption is necessary for computational simplicity. Capture analyses also assumes accurate characterization and representation of hydraulic properties (Nadler and others, 2018). Hydraulic properties used for the capture analyses in this report were determined through numerical model calibration. A different distribution of hydraulic properties could produce the same calibration result but also substantially different capture results. The stresses applied to the capture analyses primarily were based on recharge, PET, and streamflow from 1949, but based on surface-water withdrawal from 2017 for the eventual capture analysis and based on surface-water and groundwater withdrawal from 2017 for the timing-of-capture analysis. A different selection of stresses could produce substantially different initial conditions and distributions of recharge and discharge calculated by the model and could affect the capture results derived from these initial conditions and stresses.

Summary and Conclusions

The city of Sioux Falls, in southeastern South Dakota, is the largest city in South Dakota. The U.S. Geological Survey (USGS), in cooperation with the city of Sioux Falls, completed a groundwater-flow model to use for improving the understanding of groundwater-flow processes, estimating hydrogeologic properties, and analyzing groundwater and surface-water interactions for the Big Sioux aquifer in the model area.

The model area includes the Big Sioux aquifer and the underlying hydrogeologic units from Dell Rapids, South Dakota, to the confluence of the Big Sioux River and the outlet of the Sioux Falls Diversion Channel in eastern Sioux Falls, S. Dak. The Big Sioux aquifer is the primary aquifer in the model area and the focus of the groundwater-flow model. In the model area, the Big Sioux aquifer extends from Dell Rapids in the north, to the center of the city of Sioux Falls in the south. Surface streams and aquifers provide the primary sources of water in the model area. The Big Sioux River is the largest stream in the model area and is in hydraulic connection with the Big Sioux aquifer.

A conceptual model for the area was constructed and includes a characterization of the hydrogeologic framework, analysis and construction of potentiometric surfaces, and summary of estimated water budget components in the model area. The primary hydrogeologic units in the model area consist of (1) the Big Sioux aquifer, (2) a glacial till confining unit, and (3) bedrock aquifers (Split Rock Creek and Sioux Quartzite aquifers). The three hydrogeologic units in the model area were conceptualized and represented as three layers in the groundwater-flow model. Sources of groundwater recharge included infiltration of precipitation, stream seepage, and groundwater exchanges among the hydraulically connected Big Sioux aquifer, glacial till confining unit, and bedrock aquifers. Groundwater losses included evapotranspiration, groundwater discharge to streams, and groundwater withdrawal to supply water-use needs.

A numerical groundwater-flow model (numerical model) was constructed and was used to simulate all aspects of the conceptual model for predevelopment (steady-state) and time-varying (transient) monthly conditions for 1950–2017. The numerical model was constructed using the USGS modular hydrologic simulation program, MODFLOW–6 and was calibrated using the Parameter ESTimation software, PEST++.

The model area was spatially discretized with a grid consisting of square cells of uniform size that measured 200 feet on each side. The numerical model was vertically discretized into three layers: layer 1 represented the Big Sioux aquifer, layer 2 represented the glacial till deposits (glacial till confining unit), and layer 3 represented underlying bedrock aquifers. Recharge from infiltration of precipitation on the land surface was simulated using the Recharge Package. Evaporation of groundwater and from plant transpiration was simulated using the Evapotranspiration Package. Estimates of recharge and potential evapotranspiration were determined using the Soil-Water-Balance model. Groundwater withdrawal for production wells in the model area was simulated using the Well Package. Routed streamflow for the Big Sioux River, its tributaries, and diversions between USGS streamgages 06481000 (Big Sioux River near Dell Rapids, S. Dak.) and 06482020 (Big Sioux River at North Cliff Avenue at Sioux Falls, S. Dak.) was simulated using the Streamflow Routing Package. The Big Sioux River and the tributaries upstream from USGS streamgage 06481000 were simulated as nonrouted streams using the River and Drain Packages, respectively. Initial values and distributions of hydrogeologic properties for the numerical model were determined from geophysical investigations, slug tests, and previously published estimates and consisted of horizontal and vertical hydraulic conductivity, specific yield, specific storage, and streambed hydraulic conductivity.

The transient numerical model was calibrated for steady-state and transient monthly conditions for 1950–2017. Calibration targets were observations of hydraulic head, changes in hydraulic head, monthly mean streamflow, and cumulative monthly stream discharge. Parameters adjusted during model calibration were horizontal and vertical hydraulic conductivity, specific storage, specific yield, recharge and evapotranspiration multipliers, and streambed hydraulic conductivity. Horizontal and vertical hydraulic conductivity were estimated at pilot points distributed within the model area; specific storage and specific yield were assigned to uniform values in each layer in the model area; recharge and evapotranspiration multipliers were assigned uniformly for every stress period in the numerical model; and streambed hydraulic conductivity values were assigned uniformly between stream confluences.

The final calibrated parameter values of horizontal and vertical hydraulic conductivity, specific yield, specific storage, streambed hydraulic conductivity, recharge, and evapotranspiration were considered reasonable for the hydrogeologic materials and conditions in the model area for 1950–2017. The mean horizontal hydraulic conductivity for the Big Sioux aquifer, estimated at pilot points during the calibration process, was about 158 feet per day (ft/d) and ranged from about 25 to 946 ft/d. Higher horizontal hydraulic conductivity values were typically in the northern part of the model area near Dell Rapids and Baltic and in the northern part of Sioux Falls near the Sioux Falls Regional Airport. Calibrated mean vertical hydraulic conductivity for the Big Sioux aquifer was about 15 ft/d and ranged from about 10 to 66 ft/d at pilot point locations. Calibrated vertical hydraulic conductivities were generally close to the initial values, and the areas with the highest vertical hydraulic conductivity corresponded to the areas of highest horizontal hydraulic conductivity. The calibrated specific storage and specific yield for the Big Sioux aquifer were lower than the initial values and lower than most literature values at 3.54×10^{-5} and 0.05, respectively. Calibrated streambed hydraulic conductivity ranged from about 0.02 to 0.65 ft/d with a mean of about 0.07 ft/d.

Observed hydraulic head altitudes were plotted with simulated hydraulic head altitudes and compared to a 1:1

perfect-fit line to assess the overall model-to-measurement fit. Overall, simulated hydraulic head altitudes had a linear regression coefficient of determination of 0.48. Hydraulic head altitude residuals for the glacial till confining unit and bedrock aquifers were typically greater in magnitude when compared to residuals in the Big Sioux aquifer, but simulated hydraulic head altitudes in the Big Sioux aquifer compared favorably with mean observed hydraulic head altitudes and had a linear regression R^2 of 0.93. Observed and simulated hydraulic head hydrographs were created for the Big Sioux aquifer and bedrock aquifer for observation wells with more than three water-level observations during the numerical model period. In general, the numerical model overestimated initial water levels in the Big Sioux aquifer, but subsequent water-level changes were underestimated.

Simulated streamflow hydrographs matched the general trends of observed increases and decreases in streamflow for USGS streamgages 06482000 (Big Sioux River at Sioux Falls, S. Dak.) and 06482020 (Big Sioux River at North Cliff Avenue at Sioux Falls, S. Dak.), but larger streamflows were overestimated at the first streamgage and underestimated at the second streamgage. The numerical model reasonably estimated cumulative monthly stream discharge for the first 10–15 years of available streamflow records at both USGS streamgages. After the first 10–15 years of available streamflow record, cumulative monthly stream discharge was closely estimated for USGS streamgage 06482000 and underestimated at USGS streamgage 06482020.

Composite sensitivities without regularization were calculated by PEST++ for the calibrated numerical model parameters and were averaged by parameter group. The parameter group with the highest mean composite sensitivity was the recharge multiplier parameter group.

Model simplifications, assumptions, and limitations were necessary for construction of the conceptual and numerical models and for calibration efficiency. Spatial simplification of hydraulic properties could cause the numerical model to misrepresent reactions to changes in localized stresses, such as additional demands for groundwater withdrawal. The numerical model was temporally discretized into monthly periods and required scaling daily rates into representative monthly rates for model input and calibration targets. Daily streamflow, groundwater withdrawal, and precipitation recharge were scaled to representative monthly rates and resulted in the smoothing of maximum daily rates. However, based on the comparison between the observed and simulated groundwater levels, monthly mean streamflow (as a rate) and cumulative monthly stream discharge (as a volume), and general groundwater distribution and flow, the numerical model favorably simulated the flow in the Big Sioux aquifer.

Eventual capture was calculated in the model area using a steady-state numerical groundwater-flow model. The eventual capture analysis indicates the maximum or eventual extent and magnitude of capture derived from sources other than groundwater storage that could be incurred for wells completed in the Big Sioux aquifer in the model area if groundwater withdrawal continued indefinitely. The eventual capture map shows areas of higher streamflow capture (greater than 95 percent) adjacent to the Big Sioux River north of the city of Sioux Falls and along the lower part of the Sioux Falls Diversion Channel, and areas of lower streamflow capture were simulated along aquifer boundaries and near the southern Sioux Quartzite barrier. The eventual capture analysis indicates that continuous groundwater withdrawal near the Big Sioux River likely includes a high fraction of surface water.

The timing of capture was determined using a transient numerical groundwater-flow model to determine the likely captured water sources for 30 years of groundwater withdrawal at three hypothetical wells using three continuous withdrawal rates (112.5, 450.0, and 900.0 gallons per minute). Supply for all three hypothetical wells became capture-dominated after only a short period of continuous withdrawal. Capture stabilized after about 10–15 years for well A, and streamflow capture was between 65 and 81 percent, dependent on the applied withdrawal rate. Capture stabilized after 20–25 for well B years, and capture stabilized for well C after about 10–15 years. Capture for well B stabilized at about 82 percent for streamflow capture and capture for well C stabilized at about 90 percent for streamflow capture.

The groundwater-flow model is a suitable tool to use for improving the understanding of groundwater-flow processes, estimating hydrogeologic properties, and analyzing groundwater and surface-water interactions for the Big Sioux aquifer near Sioux Falls, S. Dak. The numerical model can be used to simulate hydrologic scenarios, advance understanding of groundwater budgets, compute system response to stress, and determine likely sources of water supplied to wells. Additionally, the numerical model can be useful for assessing the timing and source of water to wells and the response of the aquifer to additional stresses, including increased well withdrawals.

References Cited

Anderson, M.P., Woessner, W.W., and Hunt, R.J., 2015, Applied groundwater modeling—Simulation of flow and advective transport: Academic Press, 564 p.

Barbosa, V.C.F., and Silva, J.B.C., 1994, Generalized compact gravity inversion: Geophysics, v. 59, no. 1, p. 57–68, https://doi.org/10.1190/1.1443534.

Barlow, P.M., and Leake, S.A., 2012, Streamflow depletion by wells—Understanding and managing the effects of groundwater pumping on streamflow: U.S. Geological Survey Circular 1376, 84 p., https://doi.org/10.3133/cir1376.

Bayless, E.R., Arihood, L.D., Reeves, H.W., Sperl, B.J.S., Qi, S.L., Stipe, V.E., and Bunch, A.R., 2017, Maps and grids of hydrogeologic information created from standardized water-well drillers' records of the glaciated United States: U.S. Geological Survey Scientific Investigations Report 2015–5105, 34 p., https://doi.org/10.3133/sir20155105.

Doherty, J.E., 2003, Ground water model calibration using pilot points and regularization: Ground Water, v. 41, no. 2, p. 170–177, https://doi.org/10.1111/j.1745-6584.2003.tb02580.x.

Doherty, J.E., 2018, PEST—Model-independent parameter estimation & uncertainty analysis—User manual (7th ed.): Brisbane, Australia, Watermark Numerical Computing, accessed January 24, 2019, at http://www.pesthomepage.org/Downloads.php.

Doherty, J.E., and Hunt, R.J., 2010, Approaches to highly parameterized inversion—A guide to using PEST for groundwater-model calibration: U.S. Geological Survey Scientific Investigations Report 2010–5169, 59 p., https://doi.org/10.3133/sir20105169.

Eldridge, W.G., and Davis, K.W., 2019, MODFLOW–6 model of the Big Sioux aquifer, Sioux Falls, South Dakota: U.S. Geological Survey data release, https://doi.org/10.5066/P9O59RO0.

Eldridge, W.G., and Medler, C.J., 2019, Hydraulic conductivity estimates from slug tests in the Big Sioux aquifer, near Sioux Falls, South Dakota: U.S. Geological Survey Scientific Investigations Report 2019–5013, 23 p., https://doi.org/10.3133/sir20195013.

Ellis, M.J., Adolphson, D.G., and West, R.E., 1969, Hydrology of a part of the Big Sioux drainage basin eastern South Dakota: U.S. Geological Survey Hydrologic Atlas HA–311, 5 p., https://doi.org/10.3133/ha311.

Esri, 2011, ArcGIS Desktop help—How Topo to Raster Works: Esri, ArcGIS Desktop, accessed December 6, 2018, at https://pro.arcgis.com/en/pro-app/tool-reference/3d-analyst/how-topo-to-raster-works.htm.

Esri, 2018, World imagery: Esri, scale not given, accessed August 31, 2018, at https://www.arcgis.com/home/item.html?id=10df2279f9684e4a9f6a7f08febac2a9.

Flint, R.F., 1955, Pleistocene geology of eastern South Dakota: U.S. Geological Survey Professional Paper 262, 181 p., https://doi.org/10.3133/pp262.

Gesch, D.B., 2007, The National Elevation Dataset, *in* Maune, D.F., ed., Digital elevation model technologies and applications—The DEM user's manual 2nd ed.: Bethesda, Md., American Society for Photogrammetry and Remote Sensing, p. 99–118.

Gesch, D.B., Oimoen, M.J., Greenlee, S.K., Nelson, C.A., Steuck, M.J., and Tyler, D.J., 2002, The national elevation dataset: Photogrammetric Engineering and Remote Sensing, v. 68, no. 1, p. 5–11.

Hansen, D.S., 1988, Appraisal of the water resources of the Big Sioux Aquifer, Moody County, South Dakota: U.S. Geological Survey Water-Resources Investigations Report 87–4057, 44 p., https://doi.org/10.3133/wri874057.

Hargreaves, G.H., and Samani, Z.A., 1985, Reference crop evapotranspiration from temperature: Applied Engineering in Agriculture, v. 1, no. 2, p. 96–99, https://doi.org/10.13031/2013.26773.

HDR Engineering, Inc., 1990, Big Sioux aquifer study: HDR Engineering, Inc., 364 p.

Heath, R.C., 1983, Basic ground-water hydrology: U.S. Geological Survey Water-Supply Paper 2220, 86 p., https://pubs.usgs.gov/wsp/2220/report.pdf.

Hendry, M.J., 1982, Hydraulic conductivity of a glacial till in Alberta: Ground Water, v. 20, no. 2, p. 162–169, https://doi.org/10.1111/j.1745-6584.1982.tb02744.x.

Homer, C.G., Dewitz, J.A., Yang, L., Jin, S., Danielson, P., Xian, G., Coulston, J., Herold, N.D., Wickham, J.D., and Megown, K., 2015, Completion of the 2011 National Land Cover Database for the conterminous United States—Representing a decade of land cover change information: Photogrammetric Engineering and Remote Sensing, v. 81, no. 5, p. 345–354, available at https://cfpub.epa.gov/si/si_public_record_report.cfm?dirEntryId=309950.

Jorgensen, D.G., and Ackroyd, E.A., 1973, Water resources of the Big Sioux River Valley near Sioux Falls, South Dakota: U.S. Geological Survey Water-Supply Paper 2024, 59 p., https://doi.org/10.3133/wsp2024.

Koch, N.C., 1970, A graphic presentation of stream gain or loss as an aid in understanding streamflow characteristics: Water Resources Research, v. 6, no. 1, p. 239–245, https://doi.org/10.1029/WR006i001p00239.

Koch, N.C., 1980, Appraisal of the water resources of the Big Sioux aquifer, Brookings, Deuel, and Hamlin Counties, South Dakota: U.S. Geological Survey Water-Resources Investigations Report 80–100, 46 p., https://doi.org/10.3133/wri80100.

Koch, N.C., 1982, A digital-computer model of the Big Sioux aquifer in Minnehaha County, South Dakota: U.S. Geological Survey Water-Resources Investigations Report 82–4064, 56 p., https://doi.org/10.3133/wri824064.

Koch, N.C., 1986, Post-Cretaceous uplift of the Sioux Quartzite ridge in southeastern South Dakota, U.S. Geological Survey Open-File Report, 86–419W, 10 p., https://doi.org/10.3133/ofr86419W.

Langevin, C.D., Hughes, J.D., Banta, E.R., Niswonger, R.G., Panday, Sorab, and Provost, A.M., 2017, Documentation for the MODFLOW 6 Groundwater Flow Model: U.S. Geological Survey Techniques and Methods, book 6, chap. A55, 197 p., https://doi.org/10.3133/tm6A55.

Langevin, C.D., Hughes, J.D., Banta, E.R., Provost, A.M., Niswonger, R.G., and Panday, Sorab, 2018, MODFLOW 6 Modular Hydrologic Model version 6.0.3: U.S. Geological Survey Software Release, accessed August 9, 2018, at https://doi.org/10.5066/F76Q1VQV.

Leaf, A.T., Fienen, M.N., Hunt, R.J., and Buchwald, C.A., 2015, Groundwater/surface-water interactions in the Bad River Watershed, Wisconsin: U.S. Geological Survey Scientific Investigations Report 2015–5162, 110 p., https://doi.org/10.3133/sir20155162.

Leake, S.A., Pool, D.R., and Leenhouts, J.M., 2008, Simulated effects of ground-water withdrawals and artificial recharge on discharge to streams, springs, and riparian vegetation in the Sierra Vista Subwatershed of the Upper San Pedro Basin, southeastern Arizona: U.S. Geological Survey Scientific Investigations Report 2008–5207, 14 p., https://pubs.usgs.gov/sir/2008/5207/.

Lebeda Consulting, 2016, Big Sioux River Watershed Strategic Plan: Lebeda Consulting, LLC, 149 p.

Lewis and Clark Regional Water System, 2018, About Lewis & Clark: Lewis and Clark Regional Water System, accessed August 23, 2018, at http://lcrws.org/about-lewis-clark/.

Lindgren, R.J., and Niehus, C.A., 1992, Water resources of Minnehaha County, South Dakota: U.S. Geological Survey Water-Resources Investigations Report 91–4101, 80 p., https://pubs.er.usgs.gov/publication/wri914101.

Nadler, C., Allander, K.K., Pohll, G., Morway, E.D., Naranjo, R.C., and Huntington, J., 2018, Evaluation of bias associated with capture maps derived from nonlinear groundwater flow models: Groundwater, v. 56, no. 3, p. 458–469, https://doi.org/10.1111/gwat.12597.

National Oceanic and Atmospheric Administration, 2018, Climate Data Online: National Centers for Environmental Information, accessed August 24, 2018, at https://www.ncdc.noaa.gov/cdo-web.

Neupane, R.P., Mehan, S., and Kumar, S., 2017, Use of geochemical tracers for estimating groundwater influxes to the Big Sioux River, eastern South Dakota, USA: Hydrogeology Journal, v. 25, no. 6, p. 1647–1660, https://doi.org/10.1007/s10040-017-1597-x.

Niehus, C.A., and Thompson, R.F., 1998, Appraisal of the water resources of the Big Sioux aquifer, Lincoln and Union Counties, South Dakota: U.S. Geological Survey Water-Resources Investigations Report 97–4161, 41 p., https://pubs.er.usgs.gov/publication/wri974161.

Niswonger, R.G., Panday, Sorab, and Ibaraki, Motomu, 2011, MODFLOW–NWT, A Newton formulation for MODFLOW–2005: U.S. Geological Survey Techniques and Methods 6–A37, 44 p., https://pubs.usgs.gov/tm/tm6a37/.

Pence, S.F., 1996, Hydrogeology and recharge of the Split Rock Creek aquifer, southeastern South Dakota: Grand Forks, N. Dak., University of North Dakota, M.S. Thesis, 150 p.

Putnam, L.D., 1998, Hydrogeology of the Split Rock Creek aquifer with emphasis on calibration of a numerical flow model, southeast Minnehaha County, South Dakota: U.S. Geological Survey Water-Resources Investigations Report 97–4102, 39 p., https://pubs.er.usgs.gov/publication/wri974102.

Putnam, L.D., and Thompson, R.C., 1996, Appraisal of the water resources of the Big Sioux Aquifer, Coddington and Grant Counties, South Dakota: U.S. Geological Survey Water-Resources Investigations Report 96–4275, 34 p., https://doi.org/10.3133/wri964275.

Reilly, T.E., Franke, O.L., and Bennett, G.D., 1987, The principle of superposition and its application in groundwater hydraulics: U.S. Geological Survey Open-File Report 84–459, 36 p., https://doi.org/10.3133/twri03B6.

Rossum, Guido van, and Drake, F.L., Jr., 2011, The Python language reference manual: United Kingdom, Network Theory Limited, 150 p.

Rothrock, E.P., and Newcomb, R.V., 1926, Sand and gravel deposits of Minnehaha County: South Dakota Geology and Natural History Survey Circular 26, 167 p.

Rothrock, E.P., and Otton, E.G., 1947, Ground water resources of the Sioux Falls area, South Dakota: South Dakota Geological Survey Report of Investigations No. 56, 70 p.

Shah, N., Nachabe, M., and Ross, M., 2007, Extinction depth and evapotranspiration from ground water under selected land covers: Ground Water, v. 45, no. 3, p. 329–338, https://doi.org/10.1111/j.1745-6584.2007.00302.x.

Soller, D.R., Packard, P.H., and Garrity, C.P., 2012, Database for USGS Map I–1970—Map showing the thickness and character of Quaternary sediments in the glaciated Unites States east of the Rocky Mountains: U.S. Geological Survey Data Series 656, scale 1:1,000,000, https://pubs.usgs.gov/ds/656/.

South Dakota Department of Environment and Natural Resources, 2018a, Observation wells available on the World Wide Web: South Dakota Department of Environment and Natural Resources web site, accessed July 30, 2019, at https://apps.sd.gov/nr69obswell/default.aspx.

South Dakota Department of Environment and Natural Resources, 2018b, Water well completion reports available on the World Wide Web: South Dakota Department of Environment and Natural Resources web site, accessed July 30, 2019, at https://apps.sd.gov/nr68welllogs/.

Stach, R.L., Mika, J., Tomhave, D.W., and Wittenhagen, D., 1981, Task I—Completion report Big Sioux aquifer study, eastern South Dakota: South Dakota Geological Survey Open File Report No. 1–BAS, 65 p., http://www.sdgs.usd.edu/pubs/pdf/BAS-01.pdf.

Steece, F.V., 1959a, Geology of the Hartford quadrangle: South Dakota Geological Survey, scale 1:62,500.

Steece, F.V., 1959b, Geology of the Sioux Falls quadrangle: South Dakota Geological Survey, scale 1:62,500.

Stoeser, D.B., Green, G.N., Morath, L.C., Heran, W.D., Wilson, A.B., Moore, D.W., and Van Gosen, B.S., 2005, Preliminary integrated geologic map databases for the United States—Central States—Montana, Wyoming, Colorado, New Mexico, North Dakota, South Dakota, Nebraska, Kansas, Oklahoma, Texas, Iowa, Missouri, Arkansas, and Louisiana: U.S. Geological Survey Open File Report 2005–1351, p. 44, https://pubs.usgs.gov/of/2005/1351/.

Thornthwaite, C.W., and Mather, J.R., 1957, The water balance: Centerton, N.J., Drexel Institute of Technology Laboratory of Climatology, 104 p.

Tikhonov, A.N., 1963a, Regularization of incorrectly posed problems: Soviet Mathematics, v. 4, no. 6, p. 1624–1637.

Tikhonov, A.N., 1963b, Solution of incorrectly formulated problems and the regularization method: Soviet Mathematics Doklady, v. 4, no. 4, p. 1035–1038.

Tipton, M.J., 1959a, Geology of the Chester quadrangle: South Dakota Geological Survey, scale 1:62,500.

Tipton, M.J., 1959b, Geology of the Dell Rapids quadrangle: South Dakota Geological Survey, scale 1:62,500.

Tomhave, D.W., 1994, Geology of Minnehaha County, South Dakota: South Dakota Department of Environment and Natural Resources, Bulletin 37, 53 p.

Tomhave, D.W., 2001, First occurrence of aquifer materials in Minnehaha County, South Dakota: South Dakota Geological Survey Aquifer Materials Map 9, scale 1:100,000.

Tomhave, D.W., 2006, First occurrence of aquifer material in the Sioux Falls, South Dakota, metropolitan growth area: South Dakota Geological Survey Aquifer Materials Map 23, scale 1:24,000.

Tonkin, M.J., and Doherty, John, 2005, A hybrid regularized inversion methodology for highly parameterized environmental models: Water Resources Research, v. 41, no. 10, paper W10412, 16 p., https://doi.org/10.1029/2005WR003995.

U.S. Army Corps of Engineers, 1990, Water Resource Development in South Dakota 1989: U.S. Army Corps of Engineers Missouri River Division, 32 p.

U.S. Census Bureau, 2018, QuickFacts: accessed July 19, 2017, at https://www.census.gov/quickfacts/fact/table/siouxfallscitysouthdakota/PST045216.

U.S. Geological Survey, 2017, About 3DEP products and services: U.S. Geological Survey The National Map—Data Delivery, 3D Elevation Program web page, accessed May 25, 2017, at https://nationalmap.gov/3DEP/3dep_prodserv.html.

U.S. Geological Survey, 2018, USGS water data for the Nation: U.S. Geological Survey National Water Information System database, accessed July 30, 2019, at https://dx.doi.org/10.5066/F7P55KJN.

U.S. Geological Survey and U.S. Department of Agriculture, Natural Resources Conservation Service, 2013, Federal standards and procedures for the National Watershed Boundary Dataset (WBD) (4 ed.): Techniques and Methods 11–A3, 63 p., https://pubs.usgs.gov/tm/11/a3/.

Valseth, K.J., Delzer, G.C., and Price, C.V., 2018, Delineation of the hydrogeologic framework of the Big Sioux aquifer near Sioux Falls, South Dakota, using airborne electromagnetic data: U.S. Geological Survey Scientific Investigations Map 3393, 2 sheets, accessed August 2018 at https://doi.org/10.3133/sim3393.

Welter, D.E., White, J.T., Hunt, R.J., and Doherty, J.E., 2015, Approaches in highly parameterized inversion— PEST++ Version 3, a Parameter ESTimation and uncertainty analysis software suite optimized for large environmental models: U.S. Geological Survey Techniques and Methods, book 7, chap. C12, 54 p., https://dx.doi.org/10.3133/tm7C12.

Westenbroek, S.M., Kelson, V.A., Dripps, W.R., Hunt, R.J., and Bradbury, K.R., 2010, SWB—A modified Thornthwaite-Mather soil-water-balance code for estimating groundwater recharge: U.S. Geological Survey Techniques and Methods 6–A31, 60 p., https://doi.org/10.3133/tm6A31.

Wilson, W.E., and Moore, J.E., eds., 1998, Glossary of hydrology: Alexandria, Va., American Geological Institute, 248 p.

Appendixes

Appendix 1. Hydraulic Conductivity Estimates with Small-Diameter Nuclear Magnetic Resonance Logging Tool

Hydraulic conductivity within the model area was estimated using the following two field-based techniques: (1) slug tests (Eldridge and Medler, 2019) and (2) nuclear magnetic resonance (NMR) data collection. The field-based measurements were necessary to augment aquifer characterization by airborne electromagnetic survey (Valseth and others, 2018) because electrical and magnetic interferences from utility infrastructure, such as power lines and water pipelines, created noise in the dataset and the data collected in these areas could not be processed. The slug tests and NMR provided supplemental hydrogeologic data for the areas with unusable data.

The NMR data collection was accomplished using a small-diameter NMR logging tool specifically developed for use in polyvinyl chloride (PVC)-cased boreholes with diameters as small as 2 inches (Walsh and others, 2013). Data were collected during June 13–15, 2017, at nine observation wells completed in the Big Sioux aquifer. Wells were selected based on several factors including casing material, casing diameter, availability of lithology and well construction information, ease of access, and distance from utility infrastructure to minimize electrical or magnetic interferences.

The wells were constructed in the 1980s and 1990s by the South Dakota Department of Environmental and Natural Resources-Water Rights (SDDENR–WR) Division and the South Dakota Geological Survey with 2-inch diameter PVC casings. Wells constructed by the SDDENR–WR have names with "MA" prefixes (South Dakota Department of Environment and Natural Resources, 2018), and wells constructed by the South Dakota Geological Survey have names with "R" prefixes (South Dakota Geological Survey, 2018). The latitude and longitude of each well were determined using a hand-held global positioning system unit with an inferred accuracy of about 10 feet (U.S. Geological Survey, 2018a). Well name, U.S. Geological Survey (USGS) site identifier, latitude and longitude, and additional selected information are available in the USGS National Water Information System database (U.S. Geological Survey, 2018b). Drillers' logs for South Dakota Geological Survey wells indicated that schedule 40 PVC casing was used. Although not specified in the SDDENR–WR drillers' logs, schedule 40 PVC casing also was assumed to be used. Well depth, casing stick-up, and water levels were measured in the field using USGS approved field methods and techniques (Cunningham and Schalk, 2011; Valder and others, 2018).

Three logging tool field runs were completed at each well. The first run (run 1) used a Mount Sopris Instruments (MSI) 2PIA–1000 (serial number 2337), calibrated in the field on the same day as the run, to measure bulk electrical conductivity. The second run (run 2) used an MSI 2PGA (serial number 2339), factory calibrated, to measure natural gamma. The third run (run 3) used a Vista Clara NMR JP175 (serial number 002), calibrated in May 2016, to measure total, mobile, and bound water content at 0.5-meter increments. Specific run information including location information, water level at the time of measurement, environmental data, run rates, and the geophysical data collected at each well are available in the accompanying data release (Eldridge and Davis, 2019).

The geophysical data collected by the Vista Clara NMR JP 175 borehole tool are based on the response of hydrogen nuclei to magnetic fields (Walsh and others, 2013). When hydrogen atoms in water are disturbed by the NMR and then return to their natural state, the atoms emit a measurable signal. If the NMR disturbances are pulsed, then the successive times and amplitudes of the signals emitted by the hydrogen atoms returning to their natural state also can be measured. The time and the decay of the signal amplitude from successive pulses provide information linked to the properties of the water-bearing aquifer material, such as permeability or hydraulic conductivity. The following two equations were used to estimate hydraulic conductivity from NMR data: (1) the Schlumberger-Doll Research (SDR) equation and (2) the sum of square echoes (SOE) equation. The SOE equation is a simpler equation that is less susceptible to data noise than the SDR equation (Walsh and others, 2013). Hydraulic conductivity can be estimated along the length of the borehole at various intervals using either or both equations.

The borehole geophysical data for the NMR in the accompanying data release (Eldridge and Davis, 2019) were multilevel decay time distributions with amplitudes, water content (mobile and immobile), estimates of hydraulic conductivity using SDR and SOE equations, and a signal noise percentage. Each geophysical data log shows (1) the multilevel decay time distributions with amplitude and the mean value for each interval, (2) the immobile water content followed by the total water content with the mobile and immobile fractions, (3) the hydraulic conductivity calculated at each measurement interval using the SDR and SOE equations, and (4) the relative noise ratio at each measurement interval.

The data collected by the MSI 2PGA gamma probe measured levels of natural gamma radiation at each well by converting gamma rays to measured and counted electronic pulses in counts per second (cps). Natural gamma sensors measure the total gamma radiation detected within a selected energy range emitted by rock near the borehole. In aquifers, the most important gamma-emitting radioisotopes are potassium-40 and uranium- and thorium-decay series, which are common in feldspar, micas, clays, and shales (Keys, 1990). Clays and shales typically emit relatively high levels of gamma radiation, compared to sands and gravels, because they generally consist of eroded feldspar, mica, and uranium and thorium ions.

The borehole geophysical logs for each well in the accompanying data release (Eldridge and Davis, 2019) include relative gamma radiation displayed as a color stretch. The data are provided in cps ranging from 0 to 120. Higher cps values indicate aquifer material more likely to be clays or shales, which also should have lower hydraulic conductivities. Zones of higher cps values would be expected in the Big Sioux aquifer because of its lithology that includes clay lenses and layers. Most of the gamma logs in the model area contain areas of high gamma cps corresponding to silt or clay layers recorded in the well lithology from drillers' logs. For example, the gamma log for well R20–89–120, indicates a high gamma cps from 7 to 9 feet below the top of casing, which corresponds to a pebbly clay layer specified in the lithology.

Data collected by the MSI 2PIA–1000 sensor measured bulk electrical conductivity in millisiemens per meter at various water temperatures, which can be converted to resistivity in ohm-meters by mathematical inversion. The sensor creates a magnetic field to induce an electrical field, which produces an electric current in the surrounding aquifer materials (Mount Sopris Instrument Co., Inc., 2001). The magnitude of the electrical current is proportional to the conductivity of the material, and changes in the conductivity can be measured continuously as the sensor moves through the borehole.

The geophysical logs for calibrated conductivity (millisiemens per meter) and resistivity (ohm-meter) are available in the accompanying data release (Eldridge and Davis, 2019). The measurements are inversions of each other, so that high conductivity corresponds to low resistivity. Resistivity and conductivity are measures of water quality (Keys, 1990). Water with high concentrations of salts is characterized by higher conductivity and lower resistivity. Lithology containing clay layers generally has waters with low resistivity, whereas sand layers with freshwater tend to have higher resistivity (Heath, 1983). In addition to resistivity and conductivity, the geophysical logs include fluid specific conductance in microsiemens per centimeter at 25 degrees Celsius at measured intervals, temperature (degrees Celsius), measured water level, and the date the water level was recorded in month, day, and year format. The specific conductance and temperature were measured with a multiparameter water-quality sonde at the specified intervals, and the water level was measured with an electric tape (Cunningham and Schalk, 2011). Lastly, lithology and well construction information from well logs (South Dakota Department of Environment and Natural Resources, 2018; South Dakota Geological Survey, 2018) are presented.

Borehole geophysical data were compiled and are presented in table 1.1. The number of NMR measurements used to calculate the mean hydraulic conductivity for a well ranged from 5 to 26 depending on total well depth. Hydraulic conductivity calculated by the SDR equation ranged from 43.2 to 286.5 feet per day (wells MA–80J and R20–89–120, respectively), and hydraulic conductivity calculated by the SOE equation ranged from 45.0 to 177.9 feet per day (wells

Table 1.1. Summary of borehole geophysical data collected June 13–15, 2017, in the Big Sioux aquifer near Sioux Falls, South Dakota.

[NMR, nuclear magnetic resonance; Ksdr, hydraulic conductivity determined using the Schlumberger-Doll Research equation; ft/d, foot per day; Ksoe, hydraulic conductivity determined using the sum of squared echoes equation; µS/cm, microsiemens per centimeter at 25 degrees Celsius; °C, degrees Celsius; LMP, log measurement point; m, meter]

Type of data	Observation well[a]								
	MA–80D	MA–80DA	MA–80H	MA–80J	R20–90–119	R20–89–120	R20–90–02	R20–92–86	R20–92–104
Measurement date	6/15/2017	6/14/2017	6/15/2017	6/15/2017	6/13/2017	6/13/2017	6/13/2017	6/14/2017	6/14/2017
Number of NMR measurements	26	11	14	11	7	5	8	15	19
Mean Ksdr (ft/d)	168.6	272.2	141.7	43.2	137.6	286.5	131.6	70.9	268.6
Mean Ksoe (ft/d)	97.1	177.9	125.0	51.3	45.0	116.1	78.7	57.2	129.3
Total water content range (proportion)	0.22–0.35	0.20–0.45	0.15–0.35	0.18–0.35	0.05–0.25	0.05–0.34	0.06–0.36	0.05–0.31	0.20–0.30
Noise range (percent)	2.5–7.5	5.0–11.0	4.0–10.0	2.5–9.0	7.5–17.5	15.0–29.0	17.0–22.0	4.0–7.0	3.0–7.0
Fluid specific conductance range (µS/cm)	925–975	930–955	620–975	812–822	1,060–1,075	800–1,250	1,745–1,785	1,065–1,088	840–860
Fluid temperature range (°C)	9–10	8.5–9.5	9.5–10.5	9.3–9.7	9.5–11.3	10.5–11.5	10.5–12.5	10.3–11.2	11.7–12.8
Water level below LMP (m)	3	2.24	2.2	2.07	4.82	4.61	4.45	3.81	2.71

[a]Well locations are available in figure 20 of the main text of this report.

R20–90–119 and MA–80DA, respectively). The total water content, a unitless volumetric ratio, at all wells ranged from 0.05 to 0.45. The NMR signal noise ranged from 2.5 to 29 percent with measurements at well R20–89–120 recording the highest noise ratio of 29 percent. Fluid specific conductance ranged from 620 to 1,785 microsiemens per centimeter at 25 degrees Celsius (wells MA–80H and R20–90–02, respectively) at fluid temperatures ranging from 8.5 to 12.8 degrees Celsius (wells MA–80DA and R20–92–104, respectively). Water levels ranged from 2.07 to 4.82 meters below the log measurement point (wells MA–80J and R20–90–119, respectively).

References Cited

Cunningham, W.L., and Schalk, C.W., comps., 2011, Groundwater technical procedures of the U.S. Geological Survey: U.S. Geological Survey Techniques and Methods, book 1, chap. A1, 151 p., https://pubs.usgs.gov/tm/1a1/.

Eldridge, W.G., and Davis, K.W., 2019, MODFLOW–6 model of the Big Sioux aquifer, Sioux Falls, South Dakota: U.S. Geological Survey data release, https://doi.org/10.5066/P9O59O0.

Eldridge, W.G., and Medler, C.J., 2019, Hydraulic conductivity estimates from slug tests in the Big Sioux aquifer, near Sioux Falls, South Dakota: U.S. Geological Survey Scientific Investigations Report 2019–5013, 23 p., https://doi.org/10.3133/sir20195013.

Heath, R.C., 1983, Basic ground-water hydrology: U.S. Geological Survey Water-Supply Paper 2220, 86 p., https://doi.org/10.3133/wsp2220.

Keys, W.S., 1990, Borehole geophysics applied to groundwater investigations: U.S. Geological Survey Techniques of Water-Resources Investigations 02–E2, 150 p.

Mount Sopris Instrument Co., Inc., 2001, 2PIA–1000 Poly Induction Probe, 2EMA–1000 Conductivity Probe (2EMB–000 and 2EMC–1000) EMP–2493 and EMP–4493: Golden, Colo., Mount Sopris Instrument Co., Inc., 19 p., accessed February 21, 2019, at ftp://ftpmusette.cr.usgs.gov/tmp/MT_SOPRIS/Docs/PDF/2PIA_2EMA_2EMC_2EMD_EMP_Induction_opman.pdf.

South Dakota Department of Environment and Natural Resources, 2018, Observation wells: South Dakota Department of Environment and Natural Resources database, accessed November 26, 2018, at http://apps.sd.gov/nr69obswell/default.aspx.

South Dakota Geological Survey, 2018, Lithologic logs database: South Dakota Geological Survey, Department of Environment and Natural Resources web page, accessed September 11, 2018, at http://cf.sddenr.net/lithdb/.

U.S. Geological Survey, 2018a, USGS global positioning application and practice: U.S. Geological Survey web page, accessed November 26, 2018, at https://water.usgs.gov/osw/gps/.

U.S. Geological Survey, 2018b, USGS water data for the Nation: U.S. Geological Survey National Water Information System database, accessed September 13, 2018, at https://doi.org/10.5066/F7P55KJN.

Valder, J.F., Carter, J.M., Robinson, S.M., Laveau, C.D., and Petersen, J.A., 2018, Quality-assurance plan for groundwater activities, U.S. Geological Survey Dakota Water Science Center: U.S. Geological Survey Open-File Report 2018–1103, 28 p., https://doi.org/10.3133/ofr20181103.

Valseth, K.J., Delzer, G.C., and Price, C.V., 2018, Delineation of the hydrogeologic framework of the Big Sioux aquifer near Sioux Falls, South Dakota, using airborne electromagnetic data: U.S. Geological Survey Scientific Investigations Map 3393, 2 sheets, accessed August 2018 at https://doi.org/10.3133/sim3393.

Walsh, D., Turner, P., Grunewald, E., Zhang, H., Butler, J., Reboulet, E., Knobbe, S., Christy, T., Lane, J.W., Johnson, C.D., Munday, T., and Fitzpatrick, A., 2013, A small-diameter NMR logging tool for groundwater investigations: Groundwater, v. 51, no. 6, 12 p., https://doi.org/10.1111/gwat.12024.

Appendix 2. Analysis of Recharge and Evapotranspiration using a Soil-Water-Balance Model

The spatial and temporal distribution of precipitation recharge and potential evapotranspiration in the model area was estimated using a Soil-Water-Balance (SWB) model (Westenbroek and others, 2010). In the model area, recharge to the Big Sioux aquifer is from infiltration of precipitation below the root zone, and evapotranspiration from groundwater is discharge from the aquifer directly from evaporation and plant transpiration. Evapotranspiration from groundwater typically happens where the water table is at or near the land surface. The SWB model uses a modified Thornthwaite-Mather soil-water-balance approach (Thornthwaite, 1948; Thornthwaite and Mather, 1957) on a daily time step. Required inputs for the SWB model include daily precipitation, daily minimum air temperature, and daily maximum air temperature. Additionally, cell-by-cell land cover classification, hydrologic soil group, available soil-water capacity, and general surface-water-flow direction are required SWB inputs. The SWB model can account for frozen ground, snowfall, snowmelt, and the dependency of recharge on the timing and spatial distribution of precipitation.

The SWB model was used to estimate precipitation recharge and potential evapotranspiration for calendar years 1949–2017 in the model area (Eldridge and Davis, 2019). Potential evapotranspiration is the amount of water that can be removed from the saturated groundwater regime by evapotranspiration if there never was a deficiency of water in the soil for use by vegetation (Wilson and Moore, 1998). A start-up period from January 1, 1945, through December 31, 1948, was simulated using the SWB model to provide the antecedent conditions for soil moisture and snow cover for estimates for 1949–2017.

The SWB model was discretized using 260 columns (oriented north-south) and 675 rows (oriented east-west) and had uniform cells that were 200 feet on each side. Daily climate data were provided using tabular text files. Gridded datasets in American Standard Code for Information Interchange (ASCII) format were provided for the remaining input. Land cover, hydrologic soil group, and available soil-water capacity were obtained from the U.S. Department of Agriculture Geospatial Data Gateway (U.S. Department of Agriculture, 2018), and the general surface-water-flow direction was developed from a digital elevation model obtained from the U.S. Geological Survey National Map (U.S. Geological Survey, 2017). Additional required inputs for the SWB model are control data variables that specify SWB model options and a lookup table that assigned curve number, infiltration rate, interception storage, and root zone depth to each land use and soil type combination.

Daily climate data for the SWB model were obtained for 1945–2017 from National Oceanic and Atmospheric Administration climate station USW00014944 (Sioux Falls Foss Field, South Dakota) at the Sioux Falls Regional Airport (National Oceanic and Atmospheric Administration, 2018) and were provided using annual tabular text files (Eldridge and Davis, 2019). Required daily climate data were minimum and maximum temperature (degrees Fahrenheit) and precipitation (inches). Other optional daily climate data that were not used in the SWB model are mean relative humidity (percent), mean temperature (degrees Fahrenheit), wind speed (meters per second), minimum relative humidity (percent), and possible sunshine (percent). Optional climate data or fields without data were assigned an arbitrary value of −99999. Missing daily climate data were replaced with data from the previous day, except for missing daily precipitation, which was assumed to be zero. Daily climate data and specific climate data replacements for missing data are available in the accompanying data release (Eldridge and Davis, 2019).

Land cover obtained for the SWB model was from the 2011 National Land Cover Database (Homer and others, 2015). Land cover was clipped to the model area and resampled to the model cell size and geographic projection using methods described by Tillman (2015). The land cover grid used by the SWB model is available in the accompanying data release (Eldridge and Davis, 2019).

The general surface-water-flow direction for the model area was generated for use in the SWB model to route surface-water flow (from rejected recharge) from model cells to adjacent model cells. A 30-meter digital elevation model for the model area (U.S. Geological Survey, 2017) was processed to obtain the ASCII surface-water-flow direction grid using methods described by Tillman (2015). The general surface-water-flow direction grid used by the SWB model is available in the accompanying data release (Eldridge and Davis, 2019).

Hydrologic soil group and available soil-water capacity were prepared with the Gridded Soil Survey Geographic (gSSURGO) soils data from the U.S. Department of Agriculture Natural Resources Conservation Service (U.S. Department of Agriculture, 2014). The Natural Resources Conservation Service defines four categories of hydrologic soil groups ranging from group A (high infiltration rate) to group D (low infiltration rate; U.S. Department of Agriculture, 2009). The 10-meter gSSURGO raster cells were linked by a map unit key to attribute tables using methods described by the gSSURGO User Guide (U.S. Department of Agriculture, 2014) and by Tillman (2015). Null (missing) data values (−99999) were replaced with soil type 5 (group C/D), which was the most

prevalent in the model area. The available soil-water capacity was prepared similarly using the gSSURGO raster by linking the raster map unit key to attributes for available water storage in the total soil profile from the surface to the depth of the soil profile (AWS0_999) and the thickness of soil components used in the total soil profile (tk0_999a). The available water content was calculated for each model cell by dividing AWS0_999 by tk0_999a and multiplying by a unit conversion factor of 1.19787 to convert from millimeters per centimeter to inches per foot. Values are required for every cell in the SWB model; therefore, cells with null (missing) data (−99999) were replaced with zero. The hydrologic soil group and available soil-water capacity grids used by the SWB model are available in the accompanying data release (Eldridge and Davis, 2019).

The SWB model requires control variables to specify several options, and the variables are provided in the accompanying data release (Eldridge and Davis, 2019). The growing season was set between the 122nd and 271st days of the year, corresponding to May 2 and September 28, based on the mean last spring frost and the mean first fall frost (South Dakota State University, 2014). Initial soil moisture was set to 50 percent saturation. Initial abstraction was set to the Hawkins method (Westenbroek and others, 2010). The initial frozen ground index was set to 83, assuming frozen ground at the SWB model start time of January 1. The upper and lower continuous frozen ground threshold values were set to 83 and 56, respectively, as recommended by Westenbroek and others (2010). Initial snow cover was set to 0.2 water equivalent (inches of water). The runoff method was set to downhill, which is a faster calculation method for routing surface-water flow (Westenbroek and others, 2010). The Hargreaves and Samani (1985) evaporation method was used between 43.46 and 43.83 degrees north latitude, which corresponded to the northern and southern SWB model boundaries.

Tabular information in the form of a lookup table is a required input for the SWB model. The lookup table is provided in the accompanying data release (Eldridge and Davis, 2019) and consists of runoff curve numbers, maximum daily infiltration rates, and root depths for each pair of the 5 hydrologic soil groups and 14 land cover types. Assumed impervious values and interception storage also are referenced in the lookup table, but those values are paired only with land cover types. Assumed impervious percentages were determined from Westenbroek and others (2010) and interception storage values were from Westenbroek and others (2010) and Tillman (2015). The curve numbers, which are indicators of relative runoff potential, for each hydrologic soil group were obtained from the Natural Resources Conservation Service Hydrology Handbook (U.S. Department of Agriculture, 2004), Westenbroek and others (2010), and Tillman (2015). Maximum daily infiltration rates, used by the SWB model to set a maximum recharge for each model cell, were assigned based on values also reported by Westenbroek and others (2010) and Tillman (2015). Root zone depth, used by the SWB model to determine a model cell maximum soil-water capacity, for each soil type were based on data from Canadell and others (1996), Westenbroek and others (2010), and Tillman (2015). In cases where runoff curve numbers, maximum daily infiltration rates, and root depths were not specified for a hydrologic soil group combination, such as B/D or C/D, the median values of the base hydrologic soil types were used.

The mean annual recharge for 1950–2017 was estimated and the spatial variation was plotted for the model area (fig. 2.1). The mean annual recharge matrix contained values ranging from 0 to 52 inches per year with a mean value of 2.1 inches per year. Higher recharge rates were estimated in the northern and eastern parts of the model area and near streams, and lower recharge rates were estimated in the central areas of the model area. Annual SWB-estimated potential evapotranspiration for 1950–2017 ranged from 29.1 to 40.3 inches, with a mean of 33.9 inches (Eldridge and Davis, 2019), and compared favorably with published estimates near the model area.

References Cited

Canadell, J., Jackson, R.B., Ehleringer, J.R., Mooney, H.A., Sala, O.E., and Schulze, E.D., 1996, Maximum rooting depth of vegetation types at the global scale: Oecologia, v. 108, no. 4, p. 583–595, https://doi.org/10.1007/BF00329030.

Eldridge, W.G. and Davis, K.W., 2019, MODFLOW–6 model of the Big Sioux aquifer, Sioux Falls, South Dakota: U.S. Geological Survey data release, https://doi.org/10.5066/P9O59O0.

Hargreaves, G.H., and Samani, Z.A., 1985, Reference crop evapotranspiration from temperature: Applied Engineering in Agriculture, v. 1, no. 2, p. 96–99, https://doi.org/10.13031/2013.26773.

Homer, C.G., Dewitz, J.A., Yang, L., Jin, S., Danielson, P., Xian, G., Coulston, J., Herold, N.D., Wickham, J.D., and Megown, K., 2015, Completion of the 2011 National Land Cover Database for the conterminous United States—Representing a decade of land cover change information: Photogrammetric Engineering and Remote Sensing, v. 81, no. 5, p. 345–354, available at https://cfpub.epa.gov/si/si_public_record_report.cfm?dirEntryId=309950.

National Oceanic and Atmospheric Administration, 2018, Climate Data Online: National Centers for Environmental information, accessed August 24, 2018, at https://www.ncdc.noaa.gov/cdo-web.

South Dakota State University, 2014, Vegetable gardening in South Dakota: Brookings, S. Dak., South Dakota State University iGrow, 18 p., accessed August 24, 2019, available at http://ashsmedia.org/hortim/files/original/cd7bfdaf509d938dd60de05d7cddb49d.pdf.

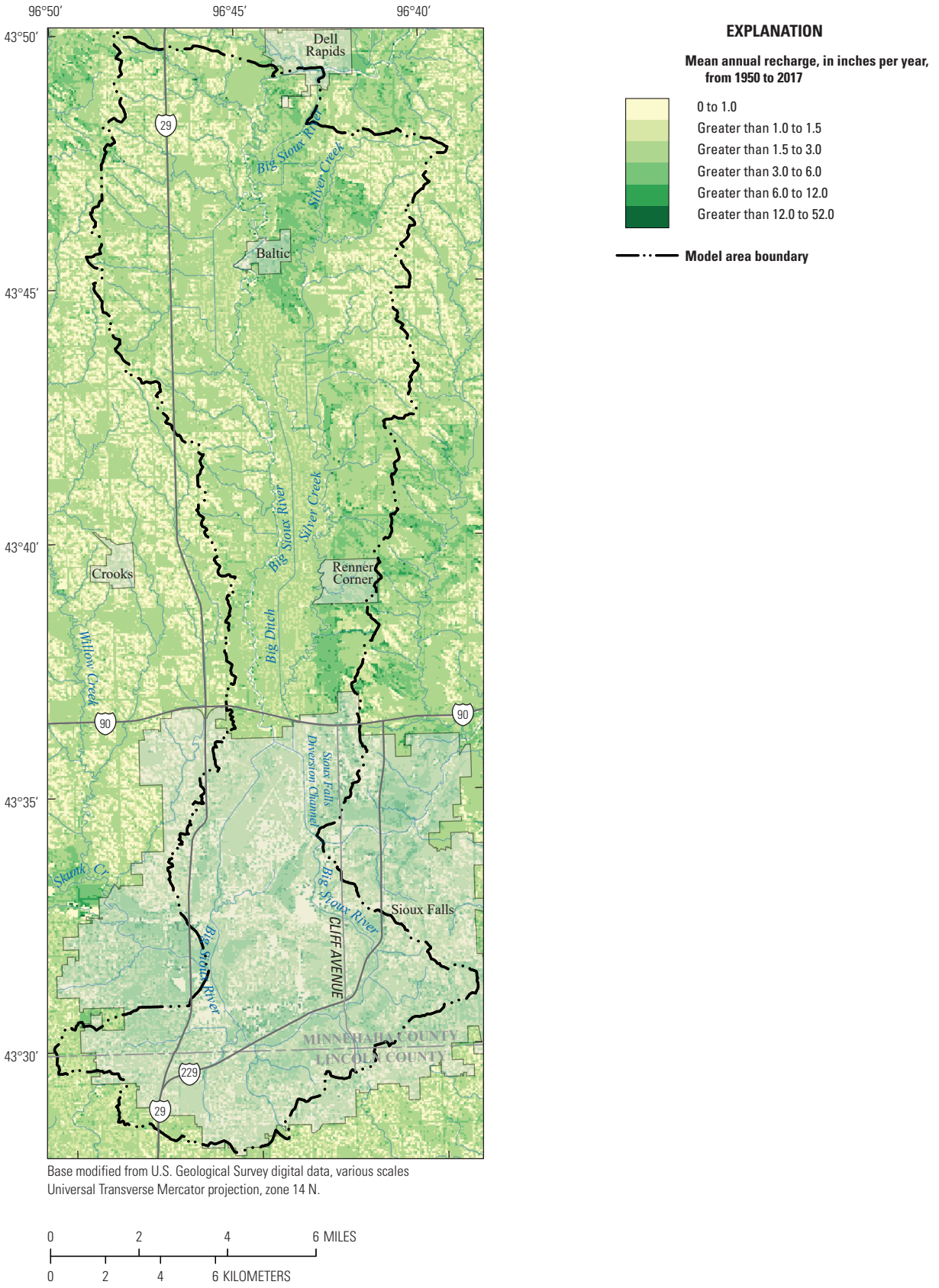

Figure 2.1. Soil-water balance calculated mean annual recharge 1950–2017 in inches per year for the model area.

Thornthwaite, C.W., 1948, An approach toward a rational classification of climate: Geographical Review, v. 38, no. 1, p. 55–94, https://doi.org/10.2307/210739.

Thornthwaite, C.W., and Mather, J.R., 1957, Instructions and tables for computing potential evapotranspiration and the water balance: Climatology, v. 10, no. 3, 311 p.

Tillman, F.D., 2015, Documentation of input datasets for the soil-water balance groundwater recharge model of the Upper Colorado River Basin: U.S. Geological Survey Open-File Report 2015–1160, 17 p., https://doi.org/10.3133/ofr20151160.

U.S. Department of Agriculture, 2004, Chapter 9, Hydrologic soil-cover complexes: Natural Resources Conservation Service, Part 630 Hydrology National Engineering Handbook, 210–VI–NEH, 20 p., accessed July 30, 2019, at https://directives.sc.egov.usda.gov/OpenNonWebContent.aspx?content=17758.wba.

U.S. Department of Agriculture, 2009, Chapter 7, Hydrologic soil groups: Natural Resources Conservation Service, Part 630 Hydrology National Engineering Handbook, 210–VI–NEH, 13 p., accessed January 2009 at https://www.wcc.nrcs.usda.gov/ftpref/wntsc/H&H/NEHhydrology/ch7.pdf.

U.S. Department of Agriculture, 2014, Gridded Soil Survey Geographic (gSSURGO) database user guide version 1.1: National Soil Survey Center National Geospatial Center of Excellence, 85 p.

U.S. Department of Agriculture, 2018, Geospatial Data Gateway: Natural Resources Conservation Service, accessed May 2018, at https://gdg.sc.egov.usda.gov/GDGOrder.aspx.

U.S. Geological Survey, 2017, About 3DEP products and services: U.S. Geological Survey The National Map—Data Delivery, 3D Elevation Program web page, accessed May 25, 2017, at https://nationalmap.gov/3DEP/3dep_prodserv.html.

Westenbroek, S.M., Kelson, V.A., Dripps, W.R., Hunt, R.J., and Bradbury, K.R., 2010, SWB—A modified Thornthwaite-Mather soil-water-balance code for estimating groundwater recharge: U.S. Geological Survey Techniques and Methods 6–A31, 60 p., https://doi.org/10.3133/tm6A31.

Wilson, W.E., and Moore, J.E., eds., 1998, Glossary of hydrology: Alexandria, Va., American Geological Institute, 248 p.

For more information about this publication, contact:
Director, USGS Dakota Water Science Center
821 East Interstate Avenue, Bismarck, ND 58503
1608 Mountain View Road, Rapid City, SD 57702
605–394–3200

For additional information, visit: https://www.usgs.gov/centers/dakota-water

Publishing support provided by the
Rolla Publishing Service Center

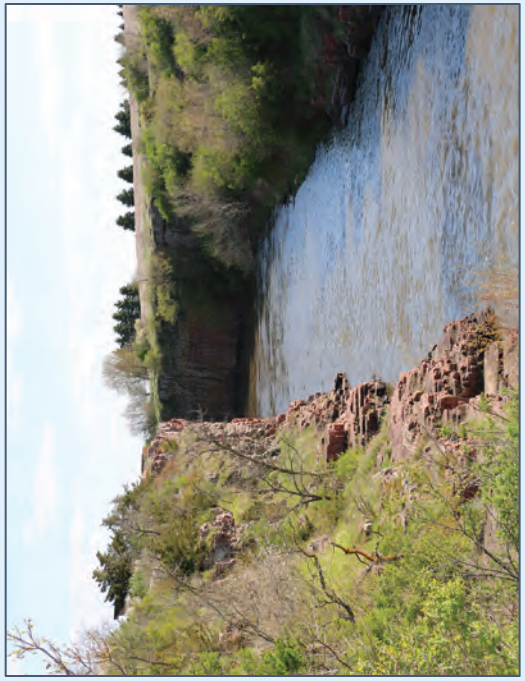

ISSN 2328-0328 (online)
https://doi.org/10.3133/sir20195117